

Physics and Engineering Laboratory  
D.S.I.R.  
Private Bag  
Lower Hutt  
New Zealand

INTERIM REPORT ON THE  
DETERMINATION OF ATMOSPHERIC TEMPERATURE PROFILES  
FROM SATELLITE RADIANCE MEASUREMENTS

M. J. Uddstrom

Physics Department,  
University of Canterbury,  
Christchurch,  
New Zealand.

June, 1979

BKS 551.52 INT

Interim report on the determination  
of atmospheric temperature profiles  
... / M.J. Uddstrom

ID: 367493  
BARCODE: 031996

Industrial Research Ltd



031996

## CONTENTS

Physics and Engineering Laboratory  
D.O.L.R.  
Private Bag  
Lower Hutt  
New Zealand

	Page
Abstract	
CHAPTER 1 : INTRODUCTION	1
CHAPTER 2 : THEORETICAL BACKGROUND FOR TEMPERATURE SENSING THROUGH A CLOUDLESS ATMOSPHERE	
2.1 Introduction	3
2.2 General Considerations	5
2.3 Instrumental Considerations	8
CHAPTER 3 : THE RETRIEVAL PROBLEM	
3.1 Introduction	12
3.2 The Linear Maximum a Posteriori (MAP) Estimator	14
3.3 Sequential MAP Estimation	23
3.4 Covariance Analysis and Interpretation	26
3.5 Vertical Resolution	37
CHAPTER 4 : SIMULATION RESULTS	
4.1 Introduction	44
4.2 Weighting Functions	45
4.3 The Atmospheric Covariance Matrices	48
4.4 The Backus and Gilbert Diagnostics	52
4.5 Retrieval Calculations	88
4.6 Covariance Analysis	108
4.7 Conclusions for Simulation Study	128

APPENDIX 1	:	Satellite Weighting Functions (NIMBUS IV)	131
APPENDIX 2	:	Matrix Identities	134
APPENDIX 3	:	Covariance Matrices	136
REFERENCES			152
ACKNOWLEDGEMENTS			155

## ABSTRACT

A Maximum A Posteriori (MAP) estimator is used for the purpose of retrieving atmospheric temperature profiles from Selective Chopper Radiometer (SCR) satellite measurements of emission from the  $15\mu\text{m}$  carbon dioxide absorption band of the Earth's atmosphere.

Diagnostic methods are derived so that confidence regions, vertical resolution and information content of all observations may be determined.

The theoretical aspects of the retrieval problem are illustrated by application to a realistic temperature profile.

## CHAPTER I

### INTRODUCTION

This is an interim report on work being carried out for a Ph.D thesis. It describes a technique for determining cloud free atmospheric temperature retrievals from measurements of radiance by a selective chopper radiometer type instrument as carried on Nimbus IV.

In finding a suitable estimator for the retrieval procedure, it has become obvious that suitable diagnostics for the estimator should be incorporated. Therefore the derivation and interpretation of some suitable estimator diagnostics are included in this work.

The work described in this report falls into the following categories :

- (a) General and instrumental considerations of the radiative transfer theory for this application.
- (b) A specification of the retrieval problem and the derivation of a linear Maximum A Posteriori (MAP) estimator, suitable for retrieval of temperature profiles from satellite radiance measurements.
- (c) An analysis and interpretation of the MAP estimator's covariance matrix involving determination of approximate confidence regions for the retrieval temperature profile.
- (d) A method for determining a measure of the

"information content" of the satellite measurements.

- (e) A description of some aspects of the Backus and Gilbert theory applicable to the present application, in order that the vertical resolution of the retrieved profiles may be measured.
- (f) A semi quantitative method for finding the "intrinsic information content" of the a priori data.
- (g) Presentation of realistic temperature profile retrievals (in a simulation study) in order that the MAP estimator and diagnostics may be applied in discovering the importance of
  - (i) the a priori data, and
  - (ii) the satellite noise variance.
- (h) A Summary of the important aspects of the retrieval problem, the MAP estimator and its diagnostics.

## CHAPTER 2

### THEORETICAL BACKGROUND FOR TEMPERATURE SENSING THROUGH A CLOUDLESS ATMOSPHERE

#### 2.1 INTRODUCTION

In remote sounding of the earth's atmosphere, measurements of radiation emitted to space by the atmosphere and some lower boundary, which may or may not be the earth's surface, are recorded by instruments (radiometers) on board a satellite. From appropriate measurements the vertical temperature structure of the atmosphere may be deduced.

The method was first proposed by Kaplan (1959). Kaplan suggested that a determination of the vertical temperature structure might be made by utilizing emission from the rotation vibration absorption band of carbon dioxide, centred at wavelength  $15\mu\text{m}$ , in the infrared. In this band the absorber (carbon dioxide) is approximately uniformly mixed over the height range of interest and no other major atmospheric constituent absorbs in this region of the spectrum.

Bishof and Bolin (1966) and Georgii and Jost (1969) have shown that carbon dioxide is uniformly mixed to within one or two percent, up to an altitude of approximately 100km (Hays and Olivero (1970)). Consequently, from radiative transfer theory, the emitted radiation

can be considered principally as a function of the temperature distribution of the absorber, at the given wavelength. However, this is only correct if the absorber is in local thermodynamic equilibrium. Houghton (1969) concludes that the  $15\mu\text{m}$  band for carbon dioxide is in local thermodynamic equilibrium to an altitude of approximately 90km. Thus recovery of temperature information from satellite observations of radiation is a particular solution of the radiative transfer equation with approximations pertaining to the earth's atmosphere for the  $15\mu\text{m}$  carbon dioxide absorption band.

Remote temperature sounding over a range of altitudes is therefore possible if a set of  $n$  frequency intervals can be chosen such that the corresponding radiances (from these  $n$  intervals) each originate from different levels within the atmosphere. This height resolution is possible since in any absorption band the absorption coefficient varies rapidly with frequency. Thus radiation from the wings of the absorption band will originate near the surface of the earth (or lower boundary), whereas radiation from the centre of the band will originate from near the top of the atmosphere.



## 2.2 GENERAL CONSIDERATIONS

Consider an infinitely deep atmosphere which is horizontally stratified, is free of scattering agents, and is in local thermodynamic equilibrium, then

$$dI(\nu, \phi, \phi') = \{-I(\nu, \phi, \phi') + B[\nu, T(u)]\}k(\nu, u)\rho(u)du \quad \dots(2.2.1)$$

where

$I$	is radiance,
$\phi, \phi'$	are spherical space coordinates (azimuth and elevation respectively),
$u$	is the geometrical path of the pencil of radiation,
$k$	is the mass absorption coefficient,
$\rho$	is the density of the absorbing gas,
$\nu$	is a spectral frequency,
$T$	is the temperature, and
$B$	is the Planck Radiance.

From the hydrostatic equation the variable "u" can be transformed to pressure so that

$$\rho du = - \frac{q}{g} \sec \theta dp \quad \dots(2.2.2)$$

where

$\theta$	is the angle between the path of the beam of radiation and the local vertical,
$p$	is the atmospheric pressure,
$q$	is the mass fraction of the absorbing gas, and
$g$	is the acceleration of gravity.

Thus equation (2.2.1) can be written :-

$$dI(\nu, \theta) = \{I(\nu, \theta) - B[\nu, T(p)]\} k(\nu, p) \frac{q(p)}{g} \sec \theta dp \quad \dots (2.2.3)$$

If the surface of the earth (or some lower boundary) is assumed to be black, then the solution to equation (2.2.3.) is :-

$$\begin{aligned} I(\nu, \theta) = & B[\nu, T(p_o)] \exp \left[ - \frac{1}{g} \int_0^{p_o} k(\nu, p') q(p') \sec \theta dp' \right] \\ & + \frac{1}{g} \int_0^{p_o} B[\nu, T(p)] \exp \left[ - \frac{1}{g} \int_0^p k(\nu, p') q(p') \sec \theta dp' \right] \\ & \times k(\nu, p) q(p) \sec \theta dp \quad \dots (2.2.4) \end{aligned}$$

by Chandrasekhar (1950). The subscript o refers to the lower boundary. Equation (2.2.4) breaks the radiance observed above the atmosphere into two components :-

- (i) that arising from the boundary and attenuated by the atmosphere, and
- (ii) that arising from the atmosphere itself.

By definition the fractional transmittance of the pencil of radiation between level p and the top of the atmosphere is :-

$$\tau(\nu, p, \theta) = \exp \left[ - \frac{1}{g} \int_0^p k(\nu, p') q(p') \sec \theta dp' \right] \quad \dots (2.2.5)$$

Therefore, substituting equation (2.2.5) into equation (2.2.4) gives the following form for the radiative transfer equation :-

$$I(\nu, \theta) = B[\nu, T(p_o)] \tau(\nu, p_o, \theta) - \int_1^{\tau(\nu, p_o, \theta)} B[\nu, T(p)] d\tau(\nu, p, \theta) \quad \dots (2.2.6)$$

Consequently for the stated assumptions of :-

- (i) a plane parallel stratified atmosphere,
- (ii) local thermodynamic equilibrium,
- (iii) a "black" lower boundary, and
- (iv) no scattering agents,

the radiance at the top of the atmosphere depends only on the temperature variation of the absorber with altitude, given that the atmospheric transmittance is known for the given absorber, and the angle  $\theta$  is constant.

### 2.3 INSTRUMENT CONSIDERATIONS

The characteristics of the satellite radiometer will now be incorporated into the radiative transfer equation, that is, equation (2.2.6). The relationship between the satellite measurements and the radiance at the top of the atmosphere may then be determined.

Assuming that the satellite radiometer measures radiation from a narrow cone in the local vertical, then  $\sec\theta$  varies only slightly over the field of view. Consequently its value at the centre of the field may be used to represent the entire field. Thus, for nadir observations,  $\sec\theta = 1$ .

Equation (2.2.6) gives the radiance at the top of the atmosphere for a particular wavelength of radiation. However, for any realistic instrument, the finite width of the spectral interval being observed requires an appropriate integration over the response of the instrument. Thus for the Selective Chopper (filter type) Radiometer instrument (henceforth referred to as the "SCR"), the measurable radiance for the  $i$ th filter is :-

$$\begin{aligned}
I(\nu_i, 0) &= \int_0^\infty I(\nu, 0) f_i(\nu) d\nu / \int_0^\infty f_i(\nu) d\nu \\
&= \left[ \int_0^\infty B[\nu, T(p_0)] \tau(\nu, p_0, 0) f_i(\nu) d\nu \right. \\
&\quad \left. - \int_0^\infty \int_i^{\tau(\nu, p_0, 0)} B[\nu, T(p)] f_i(\nu) d\tau(\nu, p, 0) d\nu \right] \\
&\quad \div \int_0^\infty f_i(\nu) d\nu \quad \dots (2.3.1)
\end{aligned}$$

where

$f_i(\nu)$  is the frequency dependent part of the optical transmission characterising the response of the  $i^{\text{th}}$  radiometer channel.

If the spectral interval over which  $f_i(\nu)$  is non zero, is small, then  $B[\nu, T(p)]$  varies little and is nearly linear in the interval (Elsasser (1938)). Hence  $B[\nu, T(p)]$  can be factored out of the  $\nu$  integral for a suitably chosen mean frequency  $\bar{\nu}_i$ .

In order that the transmittance may be more nearly independent of temperature, the height variable is changed from pressure,  $p$  to  $y \equiv -\ln p$ , (see Houghton and Taylor (1973)). Further, this change of variable gives the altitude in terms of scale heights. Thus equation (2.3.1) will have the form :-

$$\begin{aligned}
I(\bar{\nu}_i, 0) &= B[\bar{\nu}_i, T(p_0)] \tau(\bar{\nu}_i, p_0, 0) \\
&\quad - \int_{\infty}^{-\ln p_0} B[\bar{\nu}_i, T(y)] \frac{d\tau(\bar{\nu}_i, y, 0)}{dy} dy \quad \dots (2.3.2)
\end{aligned}$$

where

$$y = -\ln p, \quad \dots (2.3.3)$$

$$\tau(\bar{v}_i, p, 0) = \frac{\int_0^\infty \tau(v, p, 0) f_i(v) dv}{\int_0^\infty f_i(v) dv} \quad \dots (2.3.4)$$

and

$$\frac{d\tau}{dy}(\bar{v}_i, y, 0) = \frac{\int_0^\infty \left( \frac{d\tau(v, y, 0)}{dy} \right) f_i(v) dv}{\int_0^\infty f_i(v) dv} \quad \dots (2.3.5)$$

$$\equiv K_i,$$

where  $K_i$  is termed the "weighting function" for the  $i^{\text{th}}$  radiometer (or  $i^{\text{th}}$  channel). Further define the equivalent square bandwidth of the  $i^{\text{th}}$  radiometer to be  $\Delta v_i$  where

$$\Delta v_i = \int_0^\infty f_i(v) dv. \quad \dots (2.3.6)$$

Consequently for a radiometer with an entrance aperture area  $A$  (metres squared), and an angular field of view  $\Omega$  (steradians), and finally, if all other frequency independent constants combine to form the single constant  $\alpha_i$ , then the quantity recorded by the  $i^{\text{th}}$  radiometer will be:-

$$F(\bar{v}_i, 0) = A_i \Omega_i \alpha_i (\Delta v_i) \left\{ B[\bar{v}_i, T(p_0)] \tau(\bar{v}_i, p_0, 0) - \int_0^{-\ln p_0} B[\bar{v}_i, T(y)] K(y) dy \right\} \quad \dots (2.3.7)$$

or equivalently

$$F(\bar{v}_i, 0) = A_i \Omega_i \alpha_i (\Delta v_i) I(\bar{v}_i, 0) \quad \dots (2.3.8)$$

One further implicit assumption is present in the preceding work. And this is that the ground (or boundary) emissivity is equal to unity. This is probably correct for observations over the sea surfaces, but not, for those over land (see Houghton and Taylor 1973 pg.843).

Consequently, from the foregoing work, it is clear that the radiance (plus instrumental noise) may be measured by an orbiting spacecraft.

The radiometers (SCR) used for this work are mounted on the Nimbus IV satellite. The principle by which the SCR actually measures the radiation in a given number of frequency intervals and the data collection procedure are given in Abel et al (1970).

## CHAPTER 3

THE RETRIEVAL PROBLEM3.1 INTRODUCTION

The retrieval problem can be specified in the following way :- given a set of measurements of thermal radiation emitted by the atmosphere and some boundary, for which the intensity and spectral distribution depend on the vertical temperature structure of the atmosphere (as in equ(2.3.2), deduce the best estimate of the atmospheric vertical temperature structure.

There are two separate aspects to this problem :-

- (i) inversion of the known integral equation of radiative transfer (equation (2.3.2), and
- (ii) an estimation problem, since (i) is an ill-conditioned problem giving no mathematically unique solution.

Clearly then it is not sufficient to find just any solution which satisfies the observations. The solution must be meteorologically reasonable, and must be the "best" solution in some sense.

There are two fundamental uniqueness problems associated with the solution. First, there is noise in the radiometer measurements and therefore a non-uniqueness in the original observations. Therefore, it is important, to determine how the error bars of the measurements map onto the error bars of the solution. Second, the problem is ill-conditioned, for there are components of the atmospheric profile which make no contribution to the



quantities measured by the radiometers on board the satellite.

Further problems occur due to the overlap of the weighting functions since this implies a lack of vertical independence of the weighting functions, and consequently, a lack of vertical resolution in the measurements.

### 3.2 THE LINEAR MAXIMUM A POSTERIORI (MAP) ESTIMATOR

As noted above, there are components in the atmospheric profile which may not contribute to the quantities measured by the radiometers. For example, in the case of a linearized radiative transfer equation, it is possible to add any function which is orthogonal to the weighting functions to the atmospheric temperature profile, without changing the measured radiances. Such components are unmeasurable, and must therefore be estimated from additional information contained within some linear a priori constraints on the solution.

Maximum a posteriori estimation utilizes prior information, called a priori data (or virtual observations) regarding the atmospheric temperature profile, in addition to the information contained in satellite measurements and the statistics of the measurement errors.

Since the radiative transfer equation (2.3.2) will be linearized so that the problem may be solved analytically, it is necessary also to have the a priori information in the form of linear constraints. A linear constraint takes the same mathematical form as a linear direct measurement, i.e. it gives a value for a known linear function of the profile together with an error covariance matrix for this value. For this case, both the constraints and the measurements are

linear, therefore the problem is linear and consequently a linear MAP estimator may be used.

The continuous functions, such as the unknown profile and the weighting functions, will be expressed in a discrete form so that the algebra of matrices may be used in place of the algebra for Hilbert space. Thus, the a priori information is expressed and incorporated into the estimator in a discretized form.

Therefore, in order to remove some of the ill-conditioning and to make the problem well-posed, the two sets of data will be combined. One set, the satellite measurements, is small but relatively noise free. The second set, the a priori data, is large but very "noisy". The method is by the MAP estimator first proposed in this context, by Rodgers (1970).

The equation of radiative transfer (equation 2.3.2) is not a linear equation, so must first be linearized. If the  $\bar{\nu}_i$  for each channel of the radiometer are close together (in wave-number) then the problem may be linearized by selecting a suitable mean wavenumber  $\bar{\nu}$  of the  $\bar{\nu}_i$ . Thus :-

$$B[T(y)] \equiv B[\bar{\nu}, T(y)]. \quad \dots (3.2.1)$$

Equation (2.3.2) can now be written in a linear form since the wavenumber dependence of the Planck function has been removed. Thus :-

$$I(\bar{v}_i, 0) = B[\bar{v}_i, T(p_0)]\tau(\bar{v}_i, p_0, 0) - \int_{\infty}^{-\ln p_0} B[T(y)]K_i(y)dy. \quad \dots(3.2.2)$$

However, the first term on the right hand side of equation (3.2.2) is a constant for each channel for any retrieval, consequently, in the following analysis this term will be neglected. Therefore, let

$$I(\bar{v}_i, 0) = - \int_{\infty}^{-\ln p_0} B[T(y)]K_i(y)dy \quad \dots(3.2.3)$$

The equation may be discretized thus :-

$$\underline{y} = K\underline{x} \quad \dots(3.2.4)$$

where

$\underline{y}$  is a vector of the quantities measured  
for one observation<sub>2</sub> (the  $I(\bar{v}_i, 0)$ ),

$\underline{x}$  is the unknown profile ( $B[T(y)]$ ) and

matrix  $K$  is a discrete form of the weighting  
functions.

Therefore the integral has been made equivalent to a matrix multiplication for a suitable tabulation interval, that is :-

$$K_{ij} = hK_i(jh) \quad \dots(3.2.5)$$

where

$h$  is the tabulation interval in  $y$ ,

$i$  refers to the  $i^{\text{th}}$  weighting function, and

$j$  refers to the  $j^{\text{th}}$  height of the  
discretization in  $y$ .

Since  $\underline{y}$  is one observation whose vector components are the measurements from the radiometer channels, there is an implied measurement error, that is :-

$$\underline{y} = \underline{y'} + \underline{\varepsilon} \quad \dots (3.2.6)$$

where

$\underline{\varepsilon}$  the vector of the measurement errors  
is a random variable, with assumed  
known variance, and

$\underline{y'}$  is the vector of exact radiances for a  
given atmospheric state.

For MAP estimation, the estimated atmospheric temperature profile vector (henceforth, called simply the "profile vector"), is the one that maximises the conditional probability density  $f(\underline{y}|\underline{x})$ . This density is related to  $f(\underline{x}|\underline{y})$  and that for the random vector,  $f(\underline{x})$  by Bayes' Theorem :-

$$f(\underline{x}|\underline{y}) = \frac{f(\underline{y}|\underline{x})f(\underline{x})}{f(\underline{y})} \quad \dots (3.2.7)$$

where

$f(\underline{x}|\underline{y})$  is the conditional probability  
density function of  $\underline{x}$  given  $\underline{y}$ ,

$f(\underline{y}|\underline{x})$  is the conditional probability density  
function of  $\underline{y}$  given  $\underline{x}$ .

$f(\underline{x})$  is the probability density function  
of the atmospheric profiles, and

$f(\underline{y})$  is the probability density function  
of the measurements.

As the measurement errors  $\epsilon_i$  are assumed to be additive, with zero mean and normal distribution and known covariance, then  $f(\underline{y}|\underline{x})$  is a gaussian distribution and can be expressed in the following way (Beck and Arnold (1977)) :-

$$f(\underline{y}|\underline{x}) = (2\pi)^{-\frac{n}{2}} |\psi|^{-\frac{1}{2}} \exp[-\frac{1}{2}(\underline{y}-\underline{y}')^T \psi^{-1} (\underline{y}-\underline{y}')] \quad \dots (3.2.8)$$

where

- $n$  is the number of measurements in each observation, i.e. the dimension of the vectors  $\underline{y}$  and  $\underline{\epsilon}$ , and
- $\psi$  is the covariance matrix of the measurement errors, expressed  $\text{cov}(\underline{\epsilon})$ .

It is necessary to assume some algebraic form for the probability density functions. The function  $f(\underline{x})$  may be estimated from available radiosonde and rocketsonde temperature measurements. However, it is necessary to assume some algebraic form for the probability density functions. The most convenient form is gaussian.

Rodgers (1970) reports that examination of the available data indicates that the statistics are by no means gaussian, if the whole earth and all seasons are considered altogether. However, smaller regions of space and time give distributions which are nearly gaussian. Further, non-gaussian distributions give rise to non-linear estimators which make the problem much more difficult to solve. Therefore,  $f(\underline{x})$  will be expressed in the following multidimensional gaussian form :-

$$f(\underline{x}) = (2\pi)^{-\frac{p}{2}} |\underline{S}_x|^{-\frac{1}{2}} \exp[-\frac{1}{2}(\underline{x} - \bar{\underline{x}})^T \underline{S}_x^{-1} (\underline{x} - \bar{\underline{x}})] \quad \dots(3.2.9)$$

where

$\underline{S}_x$  is the covariance matrix of a set of atmospheric temperature profiles,

$\bar{\underline{x}}$  is the mean profile of the set,

$\underline{x}$  is any given profile, and

$p$  is the dimension of the profile vector.

An element of the covariance matrix of a set  $\{S\}$  of atmospheric temperature profiles is :-

$$S_{x_{ij}} = \frac{1}{S} \sum_{s=1}^S (x_{is} - \bar{x}_i)(x_{js} - \bar{x}_j) \quad \dots(3.2.10)$$

where  $i, j$  belong to  $(1, 2, \dots, p)$  and refer to the height discretization. The sample size of the set is  $S$ .

The probability density  $f(\underline{y})$  need not be known explicitly. It is a constant in the maximisation of the equation (3.2.7) since it is not a function of the profile  $\underline{x}$ .

The maximum of  $f(\underline{x}|\underline{y})$  given by equation (3.2.7) occurs at the same profile vector component values as does the maximum of its natural logarithm,

Therefore

$$\max(\ln[f(\underline{x}|\underline{y})]) = \max(\ln[f(\underline{y}|\underline{x}) f(\underline{x})])$$

and

$$\ln[f(\underline{x}|\underline{y})] = -\frac{1}{2}[(n+p)\ln 2\pi + \ln|\psi| + \ln|\underline{S}_x| + S_{MAP}] \quad \dots(3.2.11)$$

where

$$S_{\text{MAP}} \equiv (\underline{y} - \underline{y}')^T \psi^{-1} (\underline{y} - \underline{y}') + (\underline{x} - \underline{\bar{x}})^T S_x^{-1} (\underline{x} - \underline{\bar{x}}). \quad \dots (3.2.12)$$

However the only component values of interest occur in the profile vector  $\underline{x}$ , therefore, maximising  $f(\underline{x}|\underline{y})$  with respect to  $\underline{x}$  can be accomplished by minimizing  $S_{\text{MAP}}$ , i.e. the logarithm of  $f(\underline{x}|\underline{y})$ . Let  $\hat{\underline{x}}$  be the MAP estimator for the temperature profile  $\underline{x}$ . By differentiating equation (3.2.12) with respect to  $\underline{x}$ , given equation (3.2.4), it is found (Beck and Arnold (1977)) that :-

$$\nabla_{\underline{x}} S_{\text{MAP}} \Big|_{\hat{\underline{x}}} = 2[-K^T \psi^{-1} \underline{y} + K^T \psi^{-1} K \hat{\underline{x}} - S_x^{-1} \underline{\bar{x}} + S_x^{-1} \hat{\underline{x}}] = 0 \quad \dots (3.2.13)$$

Solving for the estimator  $\hat{\underline{x}}$  gives :-

$$\hat{\underline{x}} = \hat{S}_{\text{MAP}} [K^T \psi^{-1} \underline{y} + S_x^{-1} \underline{\bar{x}}] \quad \dots (3.2.14)$$

where

$$\hat{S}_{\text{MAP}}^{-1} \equiv K^T \psi^{-1} K + S_x^{-1}. \quad \dots (3.2.15)$$

By adding and subtracting  $2K^T \psi^{-1} K \underline{\bar{x}}$  in equation (3.2.13) the following expression of

$$\hat{\underline{x}} = \underline{\bar{x}} + \hat{S}_{\text{MAP}} K^T \psi^{-1} (\underline{y} - K \underline{\bar{x}}) \quad \dots (3.2.16)$$

can be given for  $\hat{\underline{x}}$ . Equation (3.2.16) is the MAP estimator for the atmospheric temperature profile, given the satellite measurements  $\underline{y}$  and  $\underline{\varepsilon}$  and a priori data  $\underline{\bar{x}}$  and  $S_x$  the atmospheric covariance matrix. Clearly, from equation (3.2.16) the term on the right hand side can be understood



as a correction to the a priori "first guess" atmospheric profile  $\bar{\underline{x}}$ , as a result of the satellite observation.

The covariance matrix for the MAP estimated profile, is just the covariance of  $\hat{\underline{x}} - \underline{x}$  i.e.  $\text{cov}(\hat{\underline{x}} - \underline{x})$ , which is the covariance of the difference between the estimated profile vector and the actual profile vector. This covariance matrix may therefore be derived as follows-

From equation (3.2.14),

$$\hat{\underline{x}} - \underline{x} = \hat{S}_{\text{MAP}} K^T \psi^{-1} (K \underline{x} + \underline{\epsilon}) - \underline{x} + \hat{S}_{\text{MAP}} S_{\underline{x}}^{-1} \bar{\underline{x}}$$

(since  $\underline{y} = K \underline{x} + \underline{\epsilon}$ ) ... (3.2.17)

$$= (\hat{S}_{\text{MAP}} K^T \psi^{-1} K - I) \underline{x} + \hat{S}_{\text{MAP}} K^T \psi^{-1} \underline{\epsilon} + \hat{S}_{\text{MAP}} S_{\underline{x}}^{-1} \bar{\underline{x}} .$$

... (3.2.18)

Take the covariance of  $\hat{\underline{x}} - \underline{x}$  :-

$$\begin{aligned} \text{cov}(\hat{\underline{x}} - \underline{x}) &= (\hat{S}_{\text{MAP}} K^T \psi^{-1} K - I) S_{\underline{x}} (\hat{S}_{\text{MAP}} K^T \psi^{-1} K - I)^T \\ &+ (\hat{S}_{\text{MAP}} K^T \psi^{-1}) \psi (\psi^{-1} K \hat{S}_{\text{MAP}}) \end{aligned}$$

... (3.2.19)

$$\text{Since } \text{cov}(\hat{\underline{x}} - \underline{x}) = E[(\hat{\underline{x}} - \underline{x})(\hat{\underline{x}} - \underline{x})^T] .$$

$\text{Cov}(\hat{\underline{x}} - \underline{x})$  is therefore the covariance of the estimator  $\hat{\underline{x}}$ .

Expanding the right hand side of equation (3.2.19) yields:-

$$\begin{aligned}
\text{cov}(\hat{\underline{x}} - \underline{x}) &= \hat{\underline{S}}_{\text{MAP}} K^T \psi^{-1} K S_x K^T \psi^{-1} K \hat{\underline{S}}_{\text{MAP}} - \hat{\underline{S}}_{\text{MAP}} K^T \psi^{-1} K S_x \\
&\quad - S_x K^T \psi^{-1} K \hat{\underline{S}}_{\text{MAP}} + S_x + \hat{\underline{S}}_{\text{MAP}} K^T \psi^{-1} K \hat{\underline{S}}_{\text{MAP}} \\
&= - S_x K^T \psi^{-1} K \hat{\underline{S}}_{\text{MAP}} + S_x \\
&= - S_x K^T \psi^{-1} K \hat{\underline{S}}_{\text{MAP}} + S_x \hat{\underline{S}}_{\text{MAP}}^{-1} \hat{\underline{S}}_{\text{MAP}} \\
&= S_x [-K^T \psi^{-1} K + \hat{\underline{S}}_{\text{MAP}}^{-1}] \hat{\underline{S}}_{\text{MAP}} \\
&= S_x [-K^T \psi^{-1} K + K^T \psi^{-1} K + S_x^{-1}] \hat{\underline{S}}_{\text{MAP}}
\end{aligned}$$

and therefore the covariance of  $\hat{\underline{x}} - \underline{x}$  is just

$$\text{cov}(\hat{\underline{x}} - \underline{x}) = \hat{\underline{S}}_{\text{MAP}} = [K^T \psi^{-1} K + S_x^{-1}]^{-1} \quad (3.2.20)$$

Hence, the two necessary equations for a MAP estimation of a temperature profile have been derived. These are, the MAP estimator,  $\hat{\underline{x}}$ , and its covariance,  $\text{cov}(\hat{\underline{x}} - \underline{x})$  :-

$$\hat{\underline{x}} = \bar{\underline{x}} + \hat{\underline{S}}_{\text{MAP}} K^T \psi^{-1} (\underline{y} - K \bar{\underline{x}}) \quad \dots (3.2.16)$$

$$\text{cov}(\hat{\underline{x}} - \underline{x}) = \hat{\underline{S}}_{\text{MAP}} = [K^T \psi^{-1} K + S_x^{-1}]^{-1} \quad \dots (3.2.20)$$

The equation (3.2.16) will therefore find the most likely solution consistent with the satellite measurements and the atmospheric statistics, as contained in the a priori data covariance matrix  $S_x$ .

An analysis of the covariance matrix,  $\text{cov}(\hat{\underline{x}} - \underline{x})$  will be given in section 3.4 of this chapter.

### 3.3 SEQUENTIAL MAP ESTIMATION

The equation (3.2.16) developed in the previous section would require that matrices of dimension  $p \times p$  be inverted for a solution to be found. This is expensive in computer time, and roundoff errors may produce further problems in a system of equations that are "almost" ill-conditioned. A sequential method of finding the solutions generated by equation (3.2.16) and (3.2.20) will therefore be used for the inversion estimation procedure.

In this section the "mechanics" of sequential estimation for the MAP estimator are developed. The development follows that of Beck and Arnold (1977).

In using a sequential estimator for nadir satellite observations, only scalar inverses will occur in the profile estimation procedure since each component of the observation vector is one dimensional. A further advantage of the method is the property of seeing clearly how additional measurements affect the solution profile as it is updated.

It is assumed that the satellite measurements of radiance are independent in time and that the instrumental error covariance matrix,  $\psi$ , is diagonal only. Neither of these assumptions will introduce errors into the solution since this is the case for filter radiometers.

A MAP sequential estimator can be derived by letting

$$\begin{aligned}
\underline{\hat{x}} &\rightarrow \underline{\hat{x}}_{i+1} \quad , \quad \underline{\bar{x}} \rightarrow \underline{\hat{x}}_i \quad , \quad y_i \rightarrow y_{i+1} \\
\psi_{ii} &\rightarrow \sigma_{i+1}^2 \quad , \quad K_i \rightarrow K_{i+1} = (k_{i+1,1} k_{i+1,2} \dots k_{i+1,p}) \\
\hat{S}_{\text{MAP}} &\rightarrow \hat{S}_{i+1} \quad , \quad S_x \rightarrow \hat{S}_i \quad \dots (3.3.1)
\end{aligned}$$

where

$$\underline{y}^T = (y_1 y_2 \dots y_n) \quad ,$$

$\sigma_{i+1}^2$  is the variance of  $y_{i+1}$  ,

$i$  refers to the  $i^{\text{th}}$  channel of the radiometer ,

... the arrowed ( $\rightarrow$ )  $i+1$  quantities refer to the modified  $i^{\text{th}}$  quantity after the  $i^{\text{th}}$  piece of information (satellite measurement) has been added to the solution via the MAP estimator, and

$i = 0$  implies the a priori data.

Further, it is necessary to use the following matrix identities which are derived in Appendix 2.

$$\begin{aligned}
\hat{S}_{i+1} &= \left[ \underline{k}_{i+1}^T (\sigma_{i+1}^2)^{-1} \underline{k}_{i+1} + \hat{S}_i^{-1} \right]^{-1} \\
&= \hat{S}_i - \hat{S}_i \underline{k}_{i+1}^T (\underline{k}_{i+1} \hat{S}_i \underline{k}_{i+1}^T + \sigma_{i+1}^2)^{-1} \underline{k}_{i+1} \hat{S}_i \quad \dots (3.3.2)
\end{aligned}$$

and

$$\hat{S}_{i+1} \underline{k}_{i+1}^T (\sigma_{i+1}^2)^{-1} = \hat{S}_i \underline{k}_{i+1}^T (\underline{k}_{i+1} \hat{S}_i \underline{k}_{i+1}^T + \sigma_{i+1}^2)^{-1} \quad \dots (3.3.3)$$

Equation (3.3.2) is known as the matrix inversion lemma.

Substitute equation (3.3.1) into equation (3.2.16)

$$\hat{\underline{x}}_{i+1} = \hat{\underline{x}}_i + \hat{S}_{i+1} \underline{k}_{i+1}^T (\sigma_{i+1}^2)^{-1} (y_{i+1} - \underline{k}_{i+1} \hat{\underline{x}}_i) \quad \dots (3.3.4)$$

further, substitute equation (3.3.3) into equation (3.3.4) :-

$$\hat{\underline{x}}_{i+1} = \hat{\underline{x}}_i + \hat{S}_{i+1} \underline{k}_{i+1}^T (\underline{k}_{i+1} \hat{S}_{i+1} \underline{k}_{i+1}^T + \sigma_{i+1}^2)^{-1} (y_{i+1} - \underline{k}_{i+1} \hat{\underline{x}}_i)$$

therefore

$$\hat{\underline{x}}_{i+1} = \hat{\underline{x}}_i + \hat{S}_{i+1} \underline{k}_{i+1}^T (y_{i+1} - \underline{k}_{i+1} \hat{\underline{x}}_i) / (\underline{k}_{i+1} \hat{S}_{i+1} \underline{k}_{i+1}^T + \sigma_{i+1}^2) \quad \dots (3.3.5)$$

In order to determine the sequential form for the solution covariance of the previous section, substitute equations (3.3.1) into equation (3.2.20), then

$$\hat{S}_{i+1} = [\underline{k}_{i+1}^T (\sigma_{i+1}^2)^{-1} \underline{k}_{i+1} + \hat{S}_i^{-1}]^{-1}$$

Applying equation (3.3.2) to this result produces

$$\hat{S}_{i+1} = \hat{S}_i - \hat{S}_i \underline{k}_{i+1}^T \underline{k}_{i+1} \hat{S}_i / (\underline{k}_{i+1} \hat{S}_i \underline{k}_{i+1}^T + \sigma_{i+1}^2) \quad \dots (3.3.6)$$

Therefore, the sequential equivalent solutions for equations (3.2.16) and (3.2.20) are

$$\hat{\underline{x}}_{i+1} = \hat{\underline{x}}_i + \hat{S}_{i+1} \underline{k}_{i+1}^T (y_{i+1} - \underline{k}_{i+1} \hat{\underline{x}}_i) / (\underline{k}_{i+1} \hat{S}_{i+1} \underline{k}_{i+1}^T + \sigma_{i+1}^2) \quad \dots (3.3.5)$$

and

$$\hat{S}_{i+1} = \hat{S}_i - \hat{S}_i \underline{k}_{i+1}^T \underline{k}_{i+1} \hat{S}_i / (\underline{k}_{i+1} \hat{S}_i \underline{k}_{i+1}^T + \sigma_{i+1}^2) \quad \dots (3.3.6)$$

where

$$i = 0, 1, 2, \dots, n,$$

$$\hat{\underline{x}}_0 \text{ is } \bar{\underline{x}}, \text{ and}$$

$$\hat{S}_0 = S_x.$$

Clearly, no matrices need be inverted, only simple scalar reciprocals occur for this formulation of the estimator and the estimated solution covariance matrix.

### 3.4 COVARIANCE ANALYSIS AND INTERPRETATION

Uncertainty in the solution profile is a consequence of uncertainty in the satellite measurements and the near ill-conditioning of the equations used in the retrieval procedure. Other uncertainties arise owing to the overlap of the weighting functions and consequent lack of independence of the satellite measurements. These uncertainties are formally expressed in terms of the solution covariance matrix which has the form of equation (3.2.20). To understand this equation it is necessary to interpret it in terms of possible deviations from the true value of the unknown profile. This section will attach confidence regions to the temperatures estimated for each level of discretization. The development is similar to that of Beck and Arnold (1977).

The diagonal of the solution covariance matrix contains the variances of the individual components of the estimated profile  $\hat{\underline{x}}$ . However, if the covariance matrix  $\hat{S}_{MAP}$  has no zero entries, then all temperature levels within the atmosphere are correlated to some degree. Consequently it is not adequate to use the variances as a measure of confidence in the solution profile since this is not using all information available and therefore the magnitude of the confidence regions would be underestimated.

It is necessary, therefore, to find a way of expressing the error estimate (or an estimate of the errors) as a sum of individual components such that the components are independent of each other.

For additive, zero mean and normal measurement errors, the joint probability density function for the estimated profile vector,  $\hat{\underline{x}}$ , may be written thus :-

$$f(\hat{\underline{x}}) = (2\pi)^{-\frac{P}{2}} |\hat{S}_{MAP}|^{-\frac{1}{2}} \exp\left(-\frac{1}{2}(\hat{\underline{x}} - \underline{x})^T \hat{S}_{MAP}^{-1} (\hat{\underline{x}} - \underline{x})\right) \quad \dots (3.4.1)$$

where  $\hat{S}_{MAP}$  and  $\hat{\underline{x}}$  are as defined by equations (3.2.16) and (3.2.20). Given equation (3.4.1) and the inherent assumptions as stated, (which seem reasonable), it is possible to determine approximate confidence regions for the estimated profile.

Let the matrix product of the exponential of equation (3.4.1) equal  $r^2$  since it is a non-negative scalar

$$(\hat{\underline{x}} - \underline{x})^T \hat{S}_{MAP}^{-1} (\hat{\underline{x}} - \underline{x}) = r^2 \quad \dots (3.4.2)$$

where

$\hat{\underline{x}}$  is the estimated profile, and  
 $\underline{x}$  is the true profile.

Equation (3.4.2) is that of an hyperellipsoid of  $p$  dimensions (since  $\hat{S}_{MAP}^{-1}$  is symmetric), centred at the origin with coordinates  $\hat{x}_1 - x_1, \hat{x}_2 - x_2, \dots, \hat{x}_p - x_p$ .

If  $\ell^2$  is some specific value, then for  $r^2 \leq \ell^2$ , equation (3.4.2) represents the interior of the hyperellipsoid.

At  $r = \ell$  equation (3.4.2) produces hypersurfaces of constant probability density.

The determination of the value of  $\ell$ , which specifies the confidence in the estimation of the errors, a description of the orientation of the hyperellipsoid in profile space and the lengths of the axes of the hyperellipsoid, is the aim of this section. The latter two properties of  $\hat{S}_{MAP}$  may be found directly by eigenanalysis of the covariance matrix. It can be shown that the principal axes of the ellipse are the eigenvectors of  $\hat{S}_{MAP}^{-1}$  and the corresponding eigenvalues of  $\hat{S}_{MAP}^{-1}$  are equal to the reciprocal squares of the length of the corresponding axes. (See Franklin (1968)). (The eigenvalues of  $\hat{S}_{MAP}$  are simply the reciprocals of those of  $\hat{S}_{MAP}^{-1}$ ).

Let

$$\hat{S}_{MAP}^{-1} = \Sigma \quad \dots (3.4.3)$$

The eigenvalues of  $\Sigma$  are found by solving the determinant equation:-

$$\det|\Sigma - \Lambda I| = 0 \quad \dots (3.4.4)$$

then the eigenvalues of  $\Sigma$  are the  $\lambda_i, i = 1, 2, \dots, p$  where  $\Lambda = \text{diag}[\lambda_1 \lambda_2 \dots \lambda_p]$ . The  $\lambda$ 's may be ordered such that  $\lambda_i \leq \lambda_j$  for  $i < j$ . Then :-

$$\Sigma = L \Lambda L^T \quad \dots (3.4.5)$$

thus  $L$  is a  $p \times p$  matrix of the form:-



$$L = \begin{bmatrix} \ell_{11} & \ell_{12} & \ell_{1p} \\ \ell_{21} & \ell_{22} & \ell_{2p} \\ \ell_{31} & \ell_{32} & \ell_{3p} \\ \vdots & \vdots & \vdots \\ \vdots & \vdots & \vdots \\ \ell_{p1} & \ell_{p2} & \ell_{pp} \end{bmatrix} = [\underline{\ell}_1 \ \underline{\ell}_2 \ \dots \ \underline{\ell}_p] \quad \dots (3.4.6)$$

and the  $\underline{\ell}_i$  are the eigenvectors of  $\Sigma$ . The eigenvectors,  $\underline{\ell}_i$  are orthogonal and of unit length, therefore

$$L^T L = I \quad \text{or} \quad \underline{\ell}_i^T \underline{\ell}_i = 1 \quad \dots (3.4.7)$$

which implies that

$$L^T = L^{-1} \quad \dots (3.4.8)$$

From equation (3.4.5) then

$$\Sigma L = L \Lambda L^T L = L \Lambda \quad \dots (3.4.9)$$

thus

$$\Sigma \underline{\ell}_i = \lambda_i \underline{\ell}_i \quad \dots (3.4.10)$$

Defining a new coordinate vector  $\underline{g}$ , such that

$$\underline{g} \equiv L^T (\hat{\underline{x}} - \underline{x}) \quad \text{or} \quad g_i = \underline{\ell}_i^T (\hat{\underline{x}} - \underline{x}) \quad \dots (3.4.11)$$

produces on substituting equations (3.4.5) and (3.4.11) into (3.4.2)

$$\begin{aligned} r^2 &= (\hat{\underline{x}} - \underline{x})^T L \Lambda L^T (\hat{\underline{x}} - \underline{x}) \\ &= \underline{g}^T \Lambda \underline{g} \\ &= \sum_{i=1}^p \lambda_i g_i^2 \quad \dots (3.4.12) \end{aligned}$$

Further, let

$$z_i^2 = \lambda_i g_i^2 \quad \dots (3.4.13)$$

therefore, it follows that equation (3.4.2) may be rewritten as :-

$$r^2 = \underline{z}^T \underline{z} \quad \dots (3.4.14)$$

$$= z_1^2 + z_2^2 + z_3^2 + \dots + z_p^2 \quad \dots (3.4.15)$$

where all the  $z_i$  are independent since the  $\underline{\ell}_i$  are independent, as are the  $g_i$ .

The probability of a vector  $\underline{z}$  (or  $\hat{\underline{x}} - \underline{x}$ ) lying inside the hypersphere  $\ell^2 \geq r^2$ , where  $\ell$  is some fixed value, can be found using equation (3.4.14) (the equation of a hypersphere) in equation (3.4.1) for the joint probability density function. Thus, by Beck and Arnold (1977):-

$$P(r^2 \leq \ell^2) = \iiint \dots \int (2\pi)^{-p/2} \exp\left(-\frac{r^2}{2}\right) dz_1 dz_2 dz_3 \dots dz_p$$

$$\text{since } |\Sigma|^{1/2} = |\hat{S}_{\text{MAP}}|^{-1/2} = (\lambda_1 \lambda_2 \dots \lambda_p)^{+1/2}.$$

The integration is performed over the interior of the hypersphere described by equation (3.4.14). Now a volume element inside the hyperellipse can be described by

$$dV = \frac{\pi^{p/2} r^{p-1} dr}{\Gamma\left(\frac{p}{2} + 1\right)} \quad \dots (3.4.18)$$

where  $\Gamma(\cdot)$  is the gamma function. Substituting equation (3.4.18) into equation (3.4.16) then yields

$$P(r^2 \leq \ell^2) = \frac{p 2^{-\frac{p}{2}}}{\Gamma\left(\frac{p}{2} + 1\right)} \int_0^{\ell^2} \exp\left(-\frac{r^2}{2}\right) r^{p-1} dr \quad \dots (3.4.19)$$

This integral therefore, gives the probability that the error vector  $\underline{z}$ , lies within an error ellipsoid corresponding to  $r^2 \leq \ell^2$ . It is also the integral of the chi-squared probability density function with  $p$  degrees of freedom. The value of  $\ell$  can therefore be chosen in such a way that the desired level of confidence in the solution profile vector error envelope may be achieved. The values of  $\ell_{1-\alpha}(p)$  can be obtained by using  $\chi^2$  tables, since

$$\ell_{1-\alpha}(p) = [\chi^2(p)]^{\frac{1}{2}} \quad \dots (3.4.20)$$

Thus the confidence regions of the solution covariance,  $\hat{S}_{MAP}$ , is the interior of the hyperellipsoid

$$(\hat{\underline{x}} - \underline{x})^T S_{MAP}^{-1} (\hat{\underline{x}} - \underline{x}) = \ell_{1-\alpha}^2(p) \quad \dots (3.4.21)$$

where

$\ell_{1-\alpha}(p)$  is the  $\ell$  value associated with the 100(1- $\alpha$ )% confidence region for the solution profile.

In order to find the values of the confidence region envelope at each level of discretization, the error envelope will be defined in profile space by locating the principal axes of the hyperellipsoid described above. The extremes of these axes, (the "lengths") are expressed in terms of the set of coordinates  $g_1, g_2, \dots, g_p$  given by equation (3.4.11). The  $g_i$ ,  $i = 1, 2, \dots, p$ , are the

projections of the errors in the solution profile  $\hat{\underline{x}}$ , as expressed by the covariance matrix  $\hat{S}_{MAP}$ , onto the principal axes of the hyperellipsoid of equation (3.4.21). The maximum coordinate values along the new axes are however given by the following set of equations :-

$$\begin{aligned}
 g_1 &= \pm \ell_{1-\alpha}(p) \lambda_1^{-\frac{1}{2}}, \quad g_2 = 0, \quad g_3 = 0, \quad \dots, \quad g_p = 0 \\
 g_1 &= 0, \quad g_2 = \pm \ell_{1-\alpha}(p) \lambda_2^{-\frac{1}{2}}, \quad g_3 = 0, \quad \dots, \quad g_p = 0 \\
 &\cdot \\
 &\cdot \\
 &\cdot \\
 &\cdot \\
 &\cdot \\
 g_1 &= 0, \quad g_2 = 0, \quad g_3 = 0 \dots \dots \dots, \quad g_p = \pm \ell_{1-\alpha}(p) \lambda_p^{-\frac{1}{2}}.
 \end{aligned}$$

... (3.4.22)

This is so since the lengths of the principal axes are given by the reciprocal square roots of the  $\lambda_i$ , where the  $\lambda_i$  are the eigenvalues of the covariance matrix  $\hat{S}_{MAP}^{-1}$ , and  $r^2 = \ell_{1-\alpha}^2(p)$ . The  $g_i$  values can therefore be related to points in the  $(\hat{\underline{x}} - \underline{x})$  coordinates, which are the errors required. Equation (3.4.22) can be rewritten :-

$$G = \pm \ell_{1-\alpha}(p) \text{diag}[\lambda_1^{-\frac{1}{2}} \lambda_2^{-\frac{1}{2}} \dots \lambda_p^{-\frac{1}{2}}]$$

... (3.4.23a)

but from equation (3.4.11)

$$G = L^T X'$$

... (3.4.23b)

where

$$X' = [\underline{x}'_1 \quad \underline{x}'_2 \quad \dots \quad \underline{x}'_p]$$

... (3.4.24)

and the

$\underline{x}'_i$  are the coordinates of  $(\hat{\underline{x}} - \underline{x})$  for the  $i^{\text{th}}$  axis.

Therefore, from equations (3.4.23a, b) and equation (3.4.24)

$$\underline{x}' = +\underline{l}_{1-\alpha}(p) \text{ L diag}[\lambda_1^{-\frac{1}{2}} \lambda_2^{-\frac{1}{2}} \dots \lambda_p^{-\frac{1}{2}}] \dots (3.4.25)$$

$$= +\underline{l}_{1-\alpha}(p) \begin{bmatrix} l_{11} & l_{12} & l_{1p} \\ l_{21} & l_{22} & l_{2p} \\ \cdot & \cdot & \cdot \\ \cdot & \cdot & \cdot \\ \cdot & \cdot & \cdot \\ l_{p1} & l_{p2} & l_{pp} \end{bmatrix} \begin{bmatrix} \lambda_1^{-\frac{1}{2}} \\ \lambda_2^{-\frac{1}{2}} \\ \cdot \\ \cdot \\ \cdot \\ \lambda_p^{-\frac{1}{2}} \end{bmatrix}$$

$$= +\underline{l}_{1-\alpha}(p) \begin{bmatrix} l_{11}\lambda_1^{-\frac{1}{2}} & l_{12}\lambda_2^{-\frac{1}{2}} & \dots & l_{1p}\lambda_p^{-\frac{1}{2}} \\ l_{21}\lambda_1^{-\frac{1}{2}} & l_{22}\lambda_2^{-\frac{1}{2}} & \dots & l_{2p}\lambda_p^{-\frac{1}{2}} \\ \cdot & \cdot & \cdot & \cdot \\ \cdot & \cdot & \cdot & \cdot \\ l_{p1}\lambda_1^{-\frac{1}{2}} & l_{p2}\lambda_2^{-\frac{1}{2}} & \dots & l_{pp}\lambda_p^{-\frac{1}{2}} \end{bmatrix}$$

... (3.4.26)

Therefore in order to find the magnitude of the confidence region at each level,  $j$ , of discretization, it is necessary to project  $\underline{x}'_{ji}$   $i = 1, 2, 3, \dots, p$  onto the  $p$  dimensional orthonormal solution profile basis  $(1 \ 0 \ 0 \dots 0), (0 \ 1 \ 0 \ 0 \dots 0), \dots, (00 \dots 001)$ , where 1 is the  $j^{\text{th}}$  component of the basis vector. Then, for the  $j^{\text{th}}$  level of discretization the magnitude of the  $(1-\alpha)$  confidence region will equal the largest projection onto the  $j^{\text{th}}$  new basis vector. The

percentage level of confidence in this error estimate is given by the value of  $100(1-\alpha)$  and the estimates of the errors will be independent.

### 3.4.1 Analysis Problems Due to Near Ill-Conditioning

The analysis above is, however, deficient if the covariance matrix  $\hat{S}_{MAP}$  is singular, that is,  $\hat{S}_{MAP}$  has one or more zero eigenvalues. The matrix  $\hat{S}_{MAP}$  is symmetric, and therefore is always non-negative definite. Should zero eigenvalues occur for  $\hat{S}_{MAP}$ , then the integral of equation (3.4.16) will not be defined since one or more of the eigenvalues of  $\hat{S}_{MAP}^{-1}$  will be infinite and  $\ell_{1-\alpha}(p)$  cannot be found since the magnitude of all confidence regions will be infinite.

Clearly, the equation

$$(\hat{\underline{x}} - \underline{x})^T \hat{S}_{MAP}^{-1} (\hat{\underline{x}} - \underline{x}) = r^2$$

does not define a closed surface, if  $S_{MAP}$  is not positive definite. The surface will then be hyper-hyperboloid or hyper-paraboloid in shape and therefore no confidence regions may be assigned to the estimated profile.

Near ill conditioning tends to "stretch" the error hyperellipsoid. Therefore eigenvectors with small eigenvalues will produce large confidence region estimates since the "length" of the principal axis described by an eigenvector is just the reciprocal of the square root of the corresponding eigenvalue (see equation (3.4.23a)).

In order to examine this "stretching" of the hyper-ellipsoid due to near ill-conditioning, the following product may be examined :- If  $\lambda_1$  is the smallest eigenvalue, and  $\lambda_p$  is the largest eigenvalue, then the solution estimate will exhibit problems of ill-conditioning if,

$$\frac{\lambda_1}{\lambda_p} \ll 1 \quad \dots (3.4.1.1)$$

This is so since, if this condition holds, then the hyperellipse is very elongated in one or more of the  $p$  dimensions. If, for a given covariance matrix, the relation (3.4.1.1) applies, then the magnitude of the confidence regions at some levels of discretization will be large due to the non hyper-sphericity of the hyper-ellipsoid associated with this covariance matrix.

However, the magnitude of the confidence region of the MAP estimator covariance may not be a good measure of the accuracy of the retrieved profile. This is so, since a large part of the confidence regions of the solution profile may be attributed to the noise in the a priori data, if there are few independent satellite measurements input to the MAP estimator.

For atmospheric statistics the effects of near ill conditioning will occur due to the high correlations between temperatures at different levels in the atmosphere. For ill conditioning occurs if :-

- (i) one or more rows of  $\hat{S}_{MAP}$  is filled with zeros,  
or if
- (ii) all elements of one row are identical with or  
multiples of the corresponding elements of  
another row.

So, by the very nature of the atmosphere and the way the covariance matrix is constructed near ill-conditioning problems will occur, and therefore the solution profile will have large confidence regions at some heights. Consequently absolute accuracy of the retrieval profile may be difficult to determine.



### 3.5 VERTICAL RESOLUTION

#### 3.5.1 Introduction

It has been difficult to assess the value of using a priori statistics to improve the vertical resolution of the MAP estimator retrieved profiles. However, the theory of Backus and Gilbert (1967, 1968, 1970) may be applied to this problem. Consequently in this section the diagnostic properties of the Backus and Gilbert theory will be given, in order that they may be applied to the MAP estimator derived atmospheric temperature profiles. These diagnostics will also be used to determine the "quality" of the a priori data and to interpret correlations within the a priori covariance matrices.

#### 3.5.2 The Method of Backus and Gilbert

The linearized MAP estimator, equation (3.2.16), may be rearranged in the following way :-

$$\hat{\underline{x}} - \underline{\bar{x}} = S_x K^T (K S_x K^T + S_e)^{-1} (\underline{y} - \underline{\bar{y}}) \quad \dots (3.5.2.1)$$

where

$$\psi = S_e \quad \text{and,}$$

$$\underline{\bar{y}} = K \underline{\bar{x}} \quad \dots (3.5.2.2)$$

Clearly  $S_x, K$  and  $S_e$  are constants for a given set of a priori statistics and fixed instrumental noise matrix, so that equation (3.5.2.1) may be further simplified, to yield,

$$\hat{\underline{x}} - \underline{\bar{x}} = G(\underline{y} - \underline{\bar{y}}) , \quad \dots (3.5.2.3)$$

where

$$G = S_X K^T (K S_X K^T + S_\epsilon)^{-1} \quad \dots (3.5.2.4)$$

The matrix  $G$  is  $p \times n$  and is the essential term in the MAP estimation retrieval procedure. Further, let

$$\begin{aligned} \Delta \underline{\hat{x}} &\equiv \underline{\hat{x}} - \underline{\bar{x}} \quad \text{and} \\ \Delta \underline{y} &\equiv \underline{y} - \underline{\bar{y}}, \end{aligned} \quad \dots (3.5.2.5)$$

where  $\Delta \underline{\hat{x}}$  is the vector of the differences between the estimated profile and the first guess profile.

Hence

$$\Delta \underline{\hat{x}} = G \Delta \underline{y} \quad \dots (3.5.2.6)$$

Further, let the equation of radiative transfer, equation (2.3.2), (neglecting the ground term), be expressed in terms of the present variables. It may be written as follows :-

$$y_j = \int_{z=0}^{z_t} x(z) K_j(z) dz \quad \dots (3.5.2.7)$$

where

- $y_j$  is the radiance for the  $j^{\text{th}}$  channel,
- $x(z)$  is the temperature profile,
- $K_j(z)$  is the satellite weighting function for the  $j^{\text{th}}$  channel,
- $z$  is the height variable, and
- $z_t$  is the effective top of the atmosphere.

In matrix form, equation (3.5.2.7) may be written in an equivalent form to equation (3.5.2.2). Thus

$$y_j = \sum_{i=1}^p K_{ji} x_i \quad \dots (3.5.2.8)$$

and therefore

$$y_j - \bar{y}_j = \sum_{i=1}^P K_{ji} (x_i - \bar{x}_i) \quad \dots (3.5.2.9)$$

$$\text{or} \quad \Delta y_j = \sum_{i=1}^P K_{ji} \Delta x_i$$

where

$i$  refers to the level of discretization,

$\Delta x_i = x_i - \bar{x}_i$ , and

$j$  refers to the  $j^{\text{th}}$  channel of the radiometer.

Therefore, in terms of  $\Delta y$  and  $\Delta x$ , equation (3.5.2.7) may be written in the form

$$\Delta y_j = \int_{Z=0}^{Z_t} \Delta x(Z) K_j(Z) dZ \quad \dots (3.5.2.11)$$

However, equation (3.5.2.6) expressed in component form yields:-

$$\hat{\Delta x}_i = \sum_{j=1}^n G_{ij} \Delta y_j \quad \dots (3.5.2.12)$$

Therefore, on substituting equation (3.5.2.11) into equation (3.5.2.12), yields

$$\hat{\Delta x}_i = \int_{Z=0}^{Z_t} \sum_{j=1}^n G_{ij} K_j(Z) \Delta x(Z) dZ \quad \dots (3.5.2.13)$$

or

$$\hat{\Delta x}_i = \int_{Z=0}^{Z_t} A_i(Z) \Delta x(Z) dZ \quad \dots (3.5.2.14)$$

where

$$A_i(Z) = \sum_{j=1}^n G_{ij} K_j(Z) \quad \dots (3.5.2.15)$$

and  $i$ ,  $j$  and  $Z$  refer to the same quantities as above, with  $Z$  being discretized by the tabulation interval.

Thus, from equation (3.5.2.14) it can be seen that the estimate of the profile  $\Delta\hat{x}_i$ , at a given level  $i$  can be regarded as a weighted average of the true profile (strictly, difference),  $\Delta x(Z)$ , with the weighting being determined by the "averaging kernel"  $A_i(Z)$ .

Consequently the vertical resolution of the estimated profile at height (level of discretization)  $i$  is determined by the behaviour of the averaging kernel  $A_i(Z)$ , for that height. In the ideal case,  $A_i(Z)$  would be a Dirac delta function, but since equation (3.5.2.15) only has a finite number of terms, there will be some spread about level  $i$ . A measure for this "spread" has been given by Backus and Gilbert (1970).

$$S_i = 12 \int_{Z=0}^{Z_t} (Z_i - Z)^2 A_i^2(Z) dZ \quad \dots (3.5.2.16)$$

where

$S_i$  is the Backus and Gilbert spread at level  $i$ , and

$Z_i$  refers to the height at level  $i$ .

The normalizing factor 12 is chosen such that, when  $A_i(Z)$  is a rectangular function of width  $\ell$  centred on  $Z_i$  and satisfying

$$\int_{Z=0}^{Z_t} A_i(Z) dZ = 1 \quad \dots (3.5.2.17)$$

then  $S_i = 1$ .

For any averaging kernel,  $A_i(Z)$ ,  $S_i$  is a quadratic polynomial in  $Z$  with a minimum value at  $Z = C_i$ ,

where

$$C_i = \int_{Z=0}^{Z_t} Z A_i^2(Z) dZ / \int_0^{Z_t} A_i^2(Z) dZ \quad \dots (3.5.2.18)$$

and  $C_i$  by definition is called the centre of the averaging kernel  $A_i(Z)$ . The spread of  $A_i(Z)$  about  $C_i$  is termed the resolving length of  $A_i(Z)$ , written  $W_i$  where,

$$\begin{aligned} W_i &= S_{C_i} \\ \text{or } W_i &= 12 \int_{Z=0}^{Z_t} [C_i - Z]^2 A_i^2(Z) dZ \quad \dots (3.5.2.19) \end{aligned}$$

Thus, the length of the interval around  $C_i$  that contains the heavily weighted values of  $x_i$  can be thought of as the resolving length of the data near  $C_i$ .

Further, equation (3.5.2.16) may be expressed in terms of  $C_i$  and  $W_i$  as

$$S_i = W_i + 12 [Z_i - C_i]^2 \int_{Z=0}^{Z_t} A_i^2(Z) dZ \quad \dots (3.5.2.20)$$

Therefore, the spread of  $A_i(Z)$  about  $Z_i$  can be large either because the resolving length of  $A_i(Z)$  is large or because the centre of  $A_i(Z)$  is far from  $Z_i$ .

In summary then, if  $A_i(Z)$  resembles a dirac delta function, then the estimated temperature  $\Delta \hat{x}_i$ , at level  $i$  (corresponding to height  $Z_i$ ) is an estimate of the true

temperature  $\hat{\Delta x}_i$  with resolving power given by the width of the peak of  $A_i(Z)$ , that is  $W_i$ . Clearly then,  $\hat{\Delta x}_i$  is just an average over a height interval given by  $W_i$ .

The precision to which the component  $x_i$  can be known is found by examination of equation (3.5.2.6).

$$\hat{\Delta \underline{x}} = G \Delta \underline{y} \quad \dots (3.5.2.6)$$

If the errors in  $\underline{y}$  are given by the instrumental noise covariance matrix  $S_\epsilon$ , then clearly the variance,  $\sigma^2_{\hat{\underline{x}}}(Z_i)$ , in the estimated profile,  $\hat{\underline{x}}$  at height  $Z_i$  (expressed as a radiance at the linearization wavenumber) is given by the relation;

$$\sigma^2_{\hat{\underline{x}}}(Z_i) = \sum_{j,k=1}^n G_{ij} S_{\epsilon jk} G_{ik}^T \quad \dots (3.5.2.21)$$

If the noise matrix  $S_\epsilon$  has only nonzero diagonal terms, then no correlation exists between the noise generated in different channels of the radiometer and further, if the measurement noise in each spectral interval is the same, then

$$S_\epsilon = \sigma_\epsilon^2 I \quad \dots (3.5.2.22)$$

Where  $I$  is the identity matrix and

$\sigma_\epsilon^2$  is the variance of the measurement noise. For these assumptions then, equation (3.5.2.21) may be expressed thus :-

$$\sigma_{\hat{\underline{x}}}(Z_i) = \sigma_\epsilon \left[ \sum_{j=1}^n G_{ij} G_{ij}^T \right]^{1/2} \quad \dots (3.5.2.23)$$

The quantity  $\sigma_{\underline{x}}^{\wedge}(Z_i)$  will be termed the "noise radiance" in the estimated profile at height  $Z_i$ . This quantity can easily be given on the Kelvin scale for temperature by inverting the Planck blackbody relation at the given wavenumber of linearization.

#### Intrinsic Information in the a priori data

If the averaging kernel,  $A_i(Z)$ , has large weight at altitudes not near level  $i$ , then a portion of the information for a retrieval of temperature at level  $i$  is determined from other levels, not near  $i$ . Hence, there is a lack of intrinsic information in the a priori covariance matrix and satellite weighting functions, for this level.

Therefore the term "lack of intrinsic information" shall be used in the sense, that if the averaging kernel's centre for level  $i$  differs greatly from the altitude of level  $i$ , then this implies that there is a lack of "intrinsic information" in the a priori covariance matrix and satellite weighting functions at that particular height.

## CHAPTER 4

SIMULATION RESULTS4.1 INTRODUCTION

In this chapter the procedures and radiometric modelling techniques developed in chapters two and three will be implemented for the retrieval and analysis of a realistic atmospheric temperature profile.

The application is for a Nimbus IV Selective Chopper Radiometer (or SCR) type sounding system. The weighting functions of equation (2.3.5) will consequently be those for the SCR instruments mounted on this satellite.

The ensuing results at various phases of the calculations will be presented and discussed in order to demonstrate the main features of the MAP estimator and the use of the retrieval diagnostics developed in chapter 3. For the purpose of this demonstration, a description is presented of the calculations for the Wallops Island rocketsonde and radiosonde derived temperature profile of the 10th June, 1970. The satellite weighting functions will be used to derive satellite radiances (via equation (2.3.8) for input to the MAP estimator.



## 4.2 THE WEIGHTING FUNCTIONS

The selective chopper radiometer on board Nimbus IV consists of six independent filter radiometers. The lower four channels utilize absorbing paths of CO<sub>2</sub> in order that these channels will not be sensitive to radiation originating near the centres of the absorption lines. The upper two channels are obtained by optically chopping the incoming radiation between two cells, one containing CO<sub>2</sub>, the other being empty.

The weighting functions may be measured in the laboratory by measuring with the satellite radiometer, the transmission through a synthetic atmosphere. A correction factor may be deduced which can then be applied to calculations of transmission under atmospheric conditions (see Barnett et al 1972).

The Nimbus 4 satellite weighting function curves used for this work are those given by Barnett et al (1972) and are illustrated in fig.4.1.

A full description of the SCR instruments is given by Houghton and Smith (1970) and by Abel et al (1970); however, the essential (for this simulation work) details of the radiometer channels are given in table 4.1.

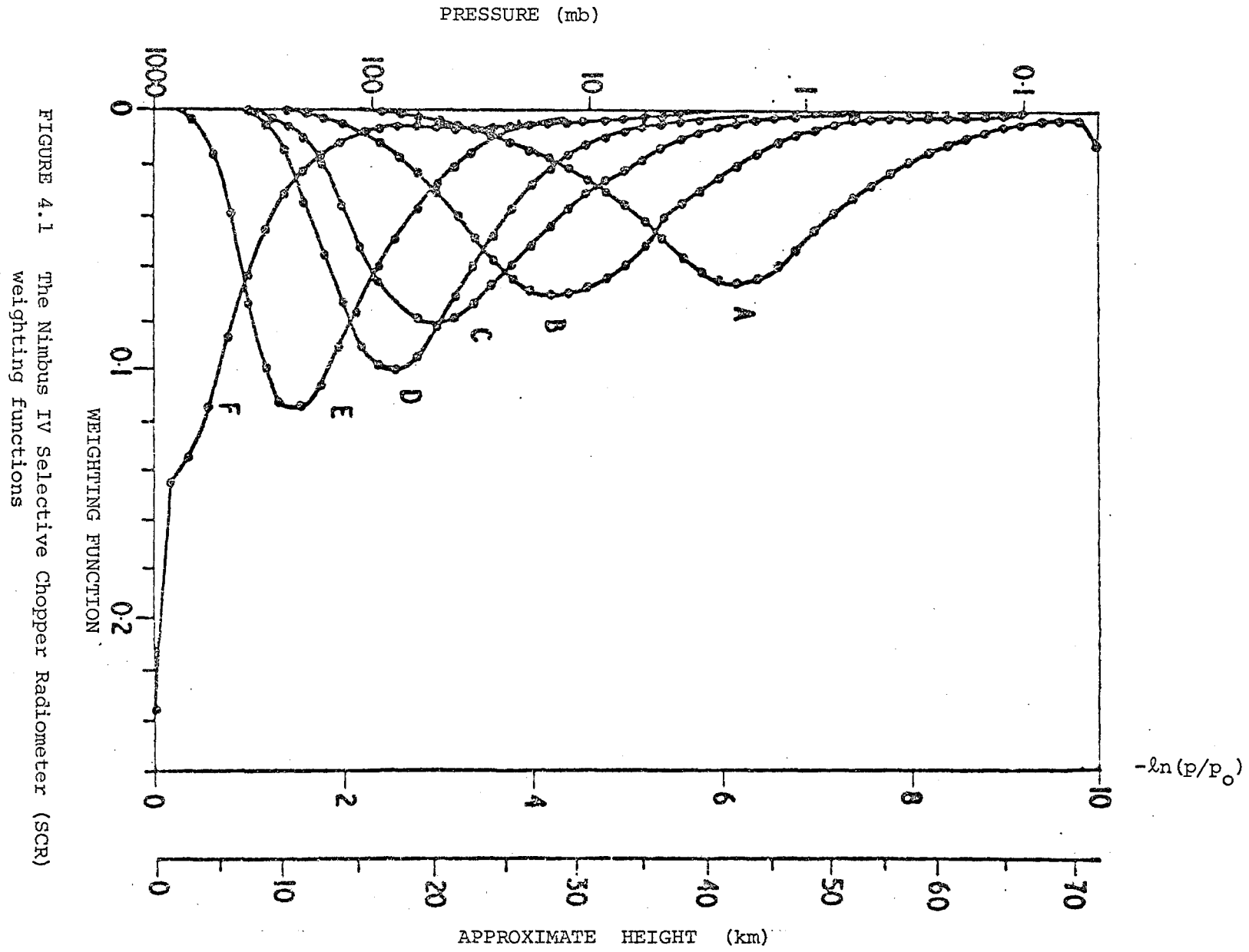


FIGURE 4.1 The Nimbus IV selective Chopper Radiometer (SCR) weighting functions

TABLE 4.1. . . . . DETAILS OF THE SCR CHANNELS

Channel	Centre, $\bar{\nu}_i$ ( $\text{cm}^{-1}$ )	Equivalent square bandwidth (after filter and selective absorption) $\text{cm}^{-1}$
1	668	1.35
2	668	1.3
3	668	3.9
4	673	3.2
5	695	3.2
6	728	5

In the absence of analytic functions for the weighting function curves of figure 4.1, a photographic print of the curves was made. The individual channel weighting function values were then digitized from this print, at the Geophysical Observatory of the N.Z. Department of Scientific and Industrial Research. Analytic functions for the weighting functions were then generated from this digitised data by a non linear gradient expansion least squares function fitting program. The precision of the generated analytic functions is equal to that of the digitization, that is,  $\pm 0.001$  units on the abscissa scale of fig. 4.1.

The analytic fitting functions are presented in appendix 1.

### 4.3 THE ATMOSPHERIC COVARIANCE MATRICES

The a priori atmospheric covariance matrices have been constructed from a sample of forty nine conjunctive Wallops Island rocketsonde and radiosonde determined temperature profiles. All temperature profiles in the sample arise from June flights in the years 1969 to 1972 inclusive. Further, only flights in this period that reached an altitude of  $7.1(-\ln(p/p_0))$  have been included in this sample.

The procedure for reduction of the raw temperature data is as follows: Each pair (rocketsonde and radiosonde) of temperature profiles are transformed in the following way :-

- (i) All temperature profiles are transformed into Planck Black Body radiances profiles at the given linearization wavenumber.
- (ii) The altitude is calculated in terms of the variable  $-\ln(p/p_0)$  (henceforth referred to as a scale height or sh), as measured by the rocketsonde and radiosonde.
- (iii) The profiles are discretized at seventy two intervals from 0 sh's to 7.1 sh's. All interpolations are linear between the nearest two points on either side of the discretization level.
- (iv) For each pair of radiosonde and rocketsonde temperature profiles, a single profile is calculated by linear interpolation of the radiosonde and rocketsonde profiles where altitude overlap of the

two profiles occurs.

The covariance matrix may then be calculated from the relation:-

$$S_x = \sum_{ij}^p \frac{1}{M} \sum_{m=1}^M (b_{im} - \bar{b}_i)(b_{jm} - \bar{b}_j) \quad \dots (4.3.1)$$

where:-

- M is the size of the sample
- p is the number of levels of discretization
- $b_{im}$  is the radiance "temperature" (calculated in (i) above) for level i and profile m of the sample
- $\bar{b}_i$  is the mean radiance "temperature" at level i for the sample of M profiles
- $S_x$  is the resultant covariance matrix of dimension p x p.

This matrix, so determined, will be referred to as the non ground corrected (henceforth NGC) covariance matrix. The NGC matrix includes a component for ground temperature variation. However, should the ground radiation be accurately known from other measurements, then the ground information in  $S_x$ , the NGC matrix, may be subtracted in the following way (see Peckham (1974)).

The row and column of  $S_x$  referring to ground values must be deleted to obtain the modified matrix.

$$S'_{x_{ij}} = S_{x_{ij}} - S_{x_{oi}} S_{x_{oj}} / S_{x_{oo}} \quad \dots (4.3.2)$$

where :-

$s'_{x_{ij}}$  is an element of the modified matrix referred to as the ground corrected (or GC) covariance matrix.

$i, j$  refer to levels of discretization and hence  $ij = 1, 2, \dots, p$ .

$S_x$  is the NGC matrix and the suffix o refers to ground values.

It is to be noted that no temperature corrections have been applied to the rocketsonde temperature profiles. The only corrections inherent in this data are those already applied by the World Data Centre A.

For the NGC and GC covariance matrices there are regions showing high correlations between the temperatures at many different heights. The evidence for this situation is expressed in these matrices by high covariance to variance ratios for many levels. This effect is especially noticeable in the stratosphere. Consequently, in order to investigate the effect on any MAP estimated temperature profile, a new covariance matrix has been developed. This matrix shall be referred to as the experimental or EXPT covariance matrix.

The EXPT matrix has been derived from the NGC covariance matrix in the following way :-

$$s'_{x_{ij}} = s_{x_{ij}} + 10 \delta_{ij} \quad \dots(4.3.3)$$

where

$$\delta_{ij} = 0 \text{ if } i \neq j ,$$

$s'_x$  is the derived EXPT matrix, and

$s_x$  is the NGC matrix.

The value  $10 \delta_{ij}$  has been chosen, so that in regions where the variance is already large compared to the relevant covariances the change in variance is relatively small. However, at heights where the situation is reversed, and high correlations occur, the variances are increased by as much as a factor of six so reducing the correlation between these levels and all other heights.

The covariance matrices NGC and GC are given in appendix 3.

#### 4.4 THE BACKUS AND GILBERT DIAGNOSTICS

The formulation of the Backus and Gilbert theory given in section 3.5 is here applied for an analysis of the vertical resolution in the estimated temperature profile inferred from measurements by the Nimbus IV SCR. Some characteristics of the SCR's weighting functions have been given in table 4.1 of section 4.2.

A series of numerical experiments have been carried out in an attempt to determine:-

- (i) How the vertical resolution of the retrieved profile will depend on the input atmospheric covariance matrix and the satellite weighting functions.
- (ii) If it is possible to determine, a priori, the effect of an input covariance matrix with large covariances relative to the variance for any particular level of discretization.
- (iii) What effect does ground correction of the input covariance have.
- (iv) What is the "intrinsic information" content of the covariance matrices and satellite weighting functions, and what is the maximum height for which a retrieval may reliably be made.
- (v) What is the precision of the retrieval profile.
- (vi) What is the effect of changing the SCR noise variance for the measured radiances.



- (vii) What is the interpretation of "sidebands" that are evident in the averaging kernels.
- (viii) Is the vertical resolution improved by using a priori atmospheric statistics (covariances) in the retrieval procedure.
- (ix) Can deviations in the retrieved profiles, from the actual profile, be predicted by examination of the given Backus and Gilbert diagnostics, a priori.

In sections 4.4.1 and 4.4.2, a presentation of results for some numerical experiments will be given. The questions above will be considered in section 4.4.3 on the understanding of the discussion of section 4.4.1 and 4.4.2. Question (ix) will be considered in section 4.7.

#### 4.4.1 The A Priori Covariance Matrices

The effect of three different a priori covariance matrices will be discussed here. These matrices are:-

- (i) the NGC covariance
- (ii) the GC covariance, and
- (iii) the EXPT covariance matrix.

Throughout this section the SCR noise variance,  $\sigma_{\epsilon}^2$  will be constant, at  $(0.01) \text{ mWm}^{-2} (\text{cm}^{-1})^{-1} \text{st}^{-1}$ .

##### 4.4.1.1 Presentation of Results

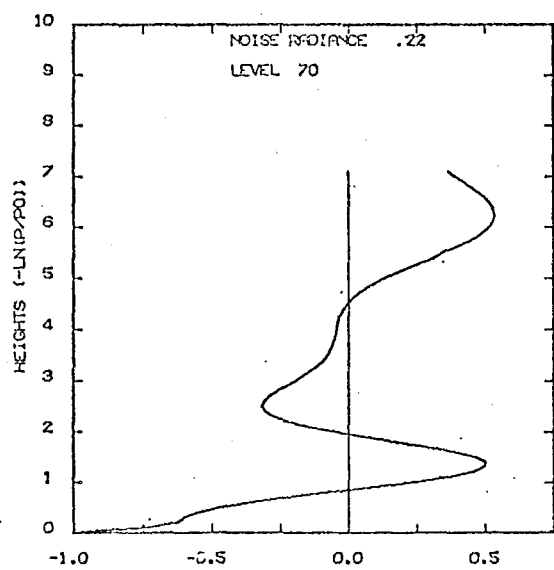
It will be instructive to consider the behaviour of the averaging kernels,  $A_i(Z)$ , for representative levels,  $i$ , and for the three covariance matrices. (By definition  $i$  refers to the level of discretization and consequently to obtain the altitude in sh's for this level, the value  $i$  must be divided by ten).

#### The Averaging Kernels

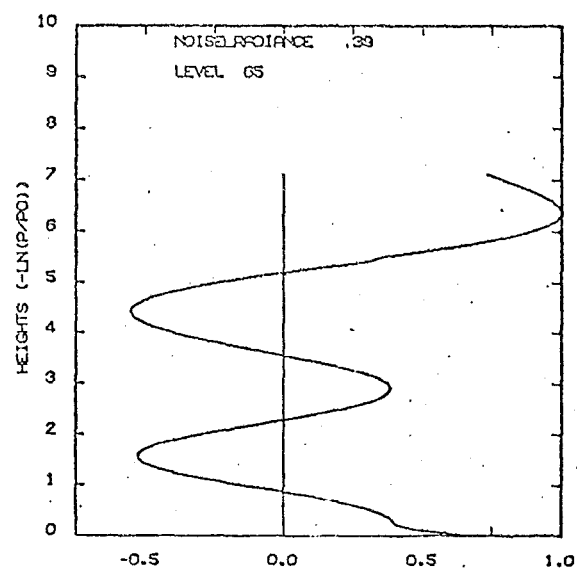
These are presented in figures 4.2, 4.3 and 4.4.

#### The Noise Radiance

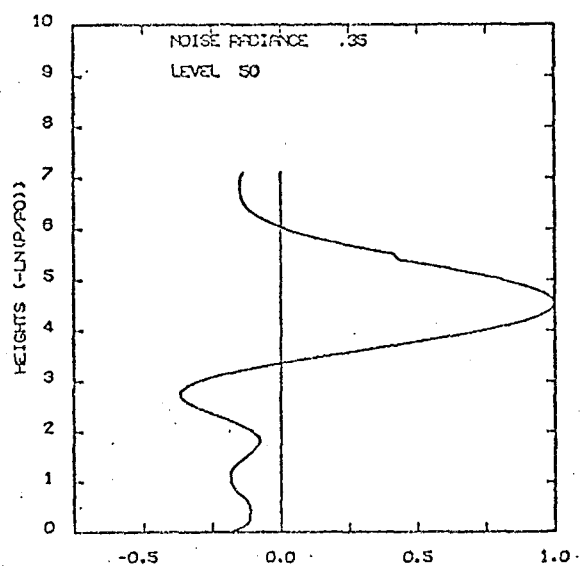
The random noise radiance indicated in figs 4.2, 4.3 and 4.4 is that determined from equation (3.5.2.23). This information is also presented in fig. 4.5. It is evident from fig. 4.5 that the precision in the retrieved radiance "temperature" profiles is approximately  $(0.3 \pm 0.2) \text{ mWm}^{-2} (\text{cm}^{-1})^{-1} \text{st}^{-1}$ . Although this implies a noise amplification of approximately three, that is



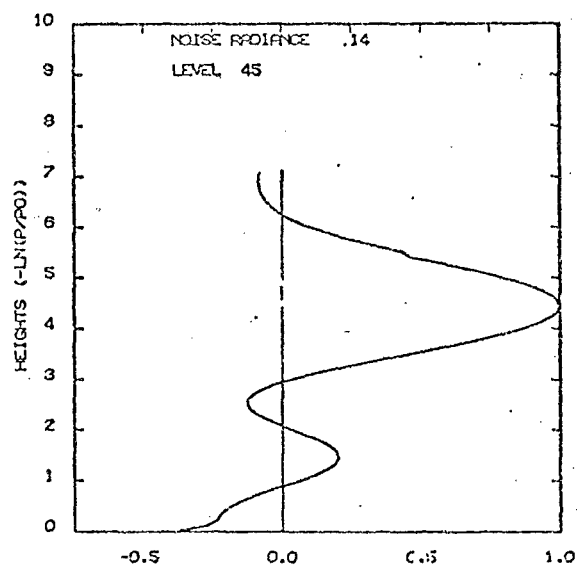
a



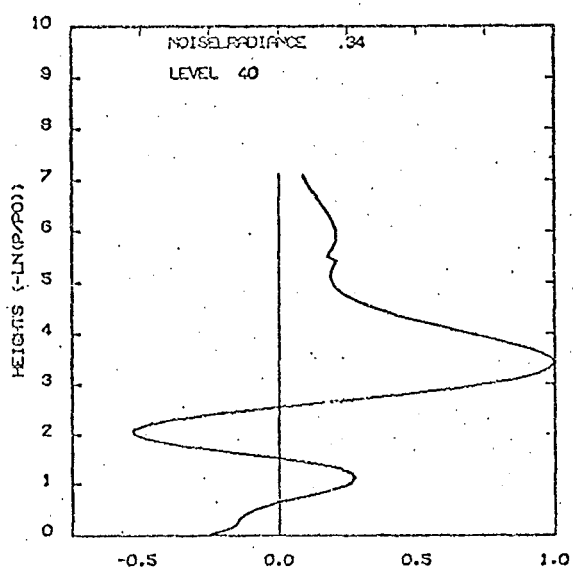
b



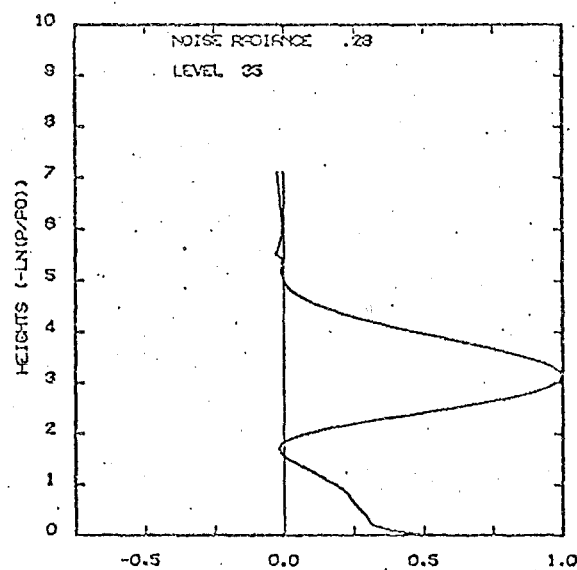
c



d



e



f

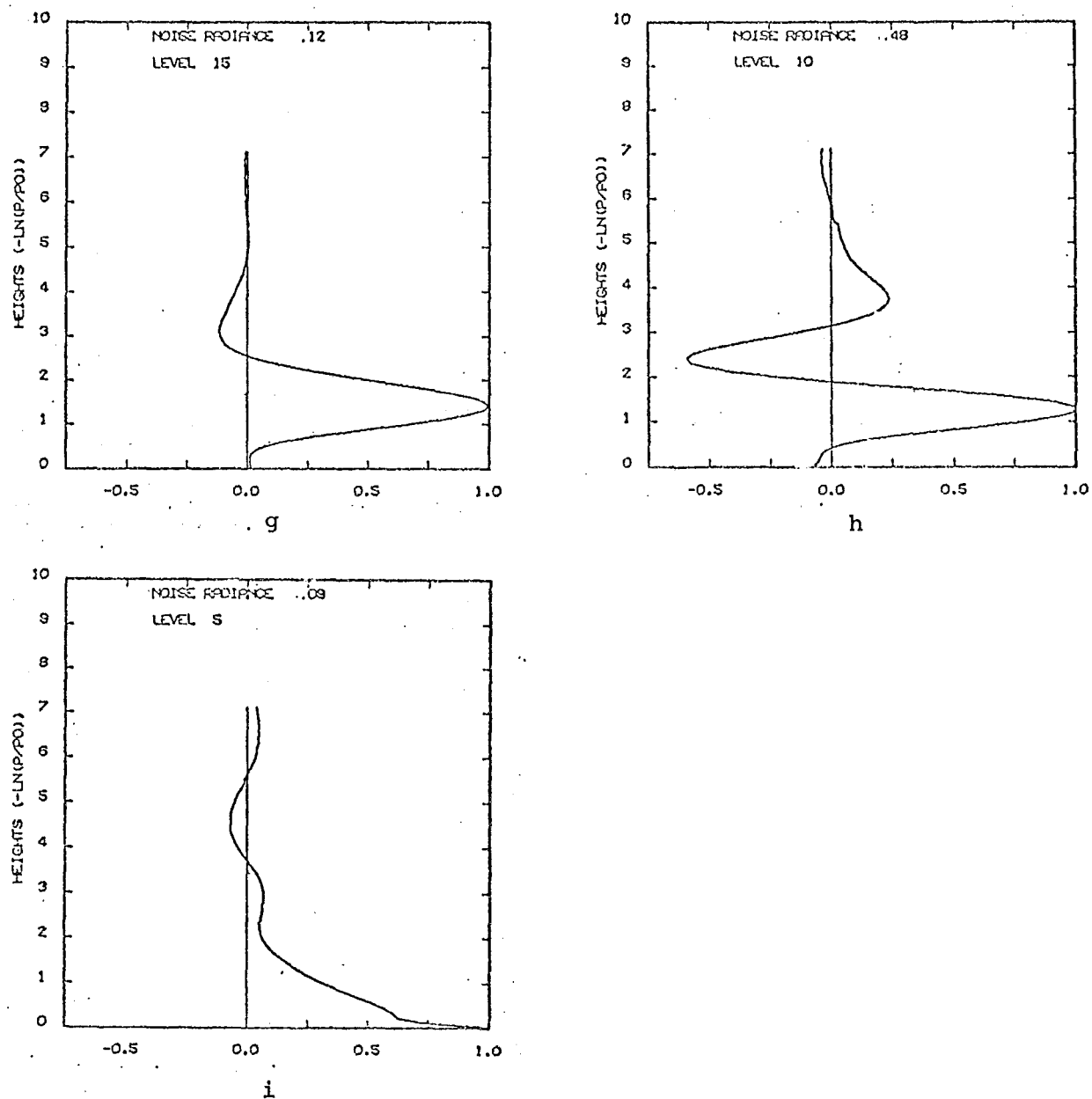
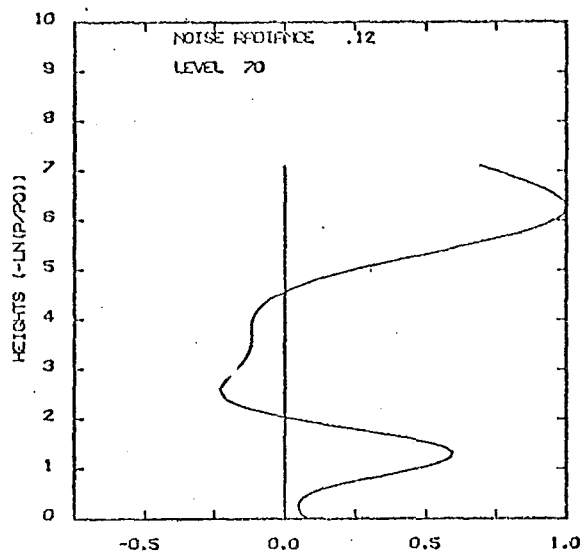
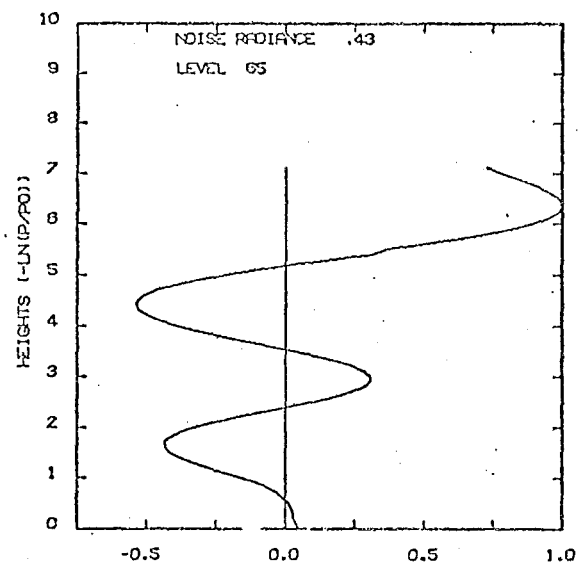


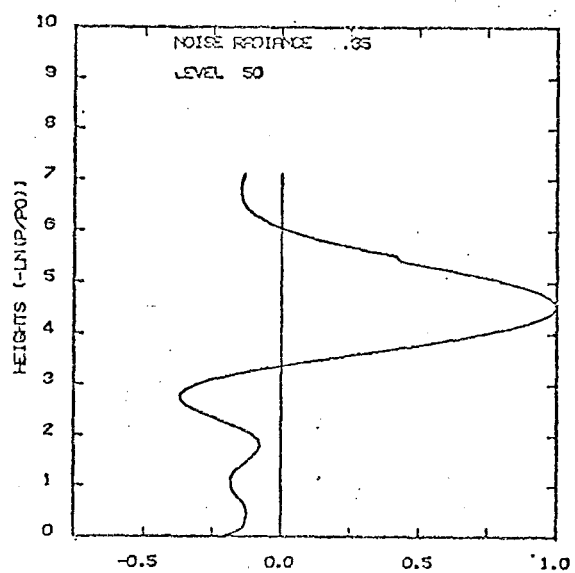
FIGURE 4.2 Averaging kernels of the MAP estimator derived using the NGC a priori matrix. Satellite noise variance  $0.01 \text{mWm}^{-2} (\text{cm}^{-1})^{-1} \text{s}^{-1}$ .



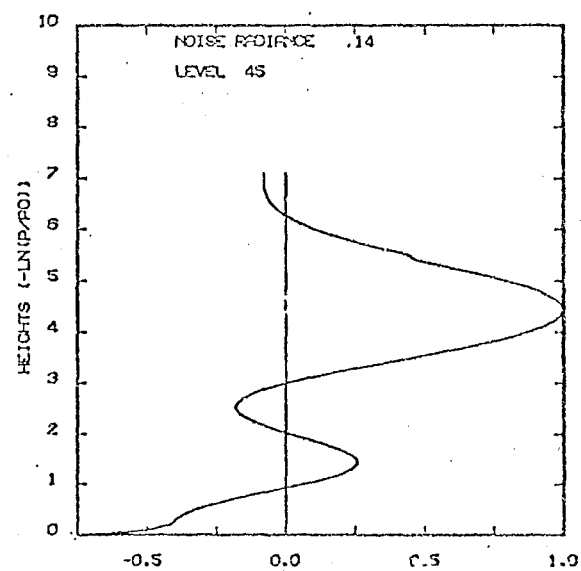
a



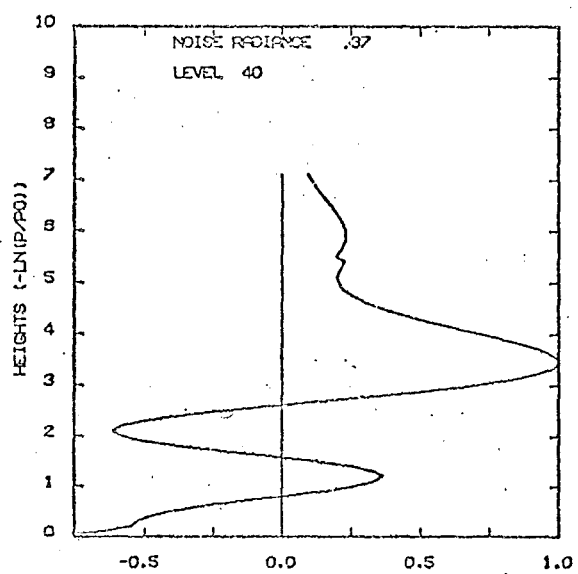
b



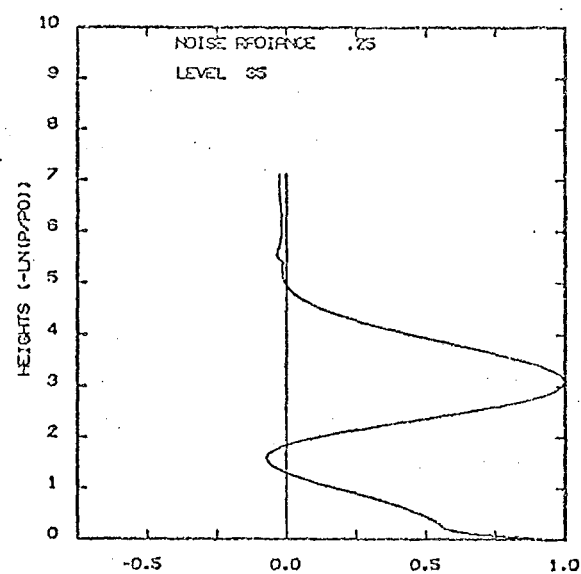
c



d



e



f

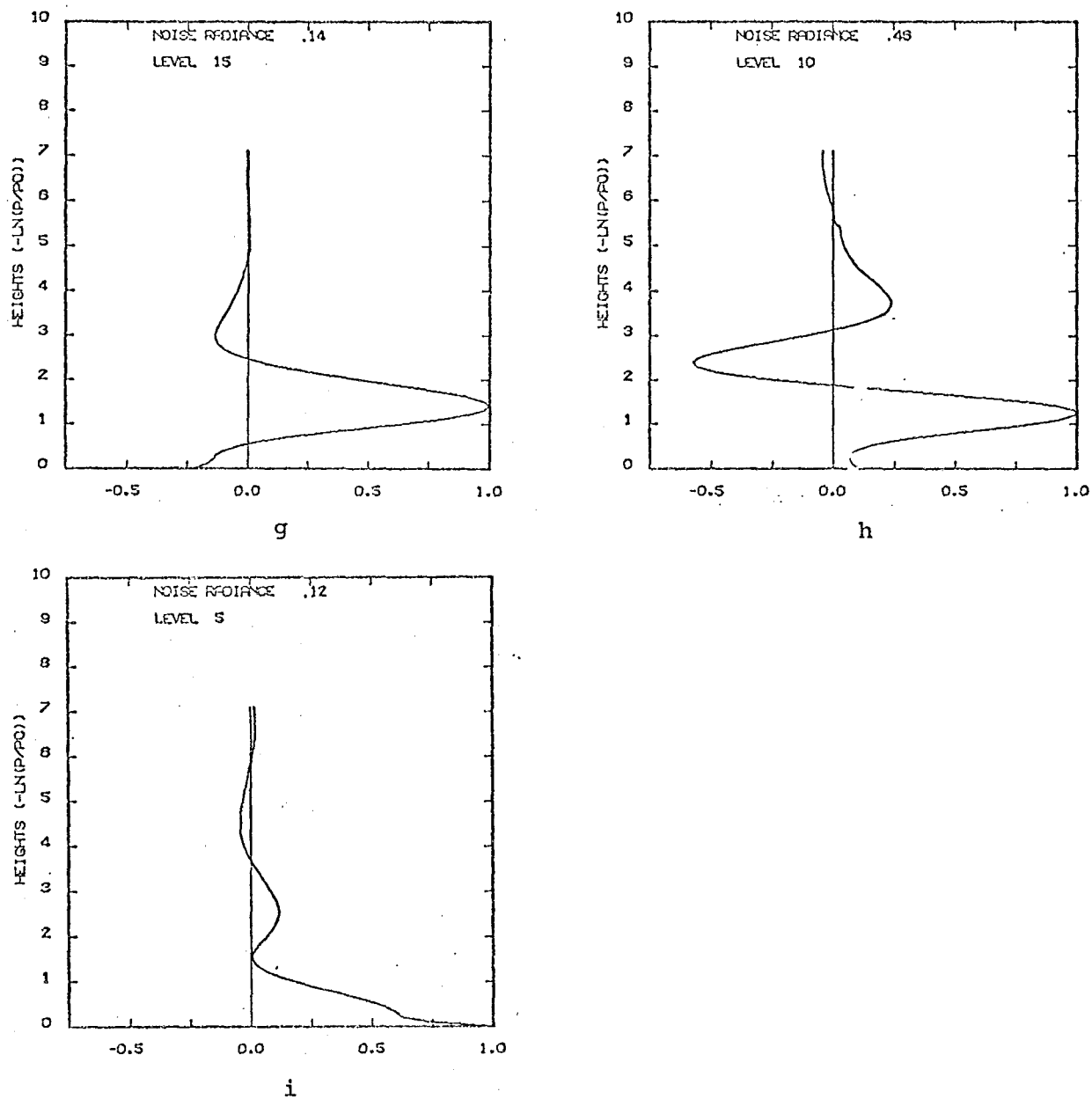
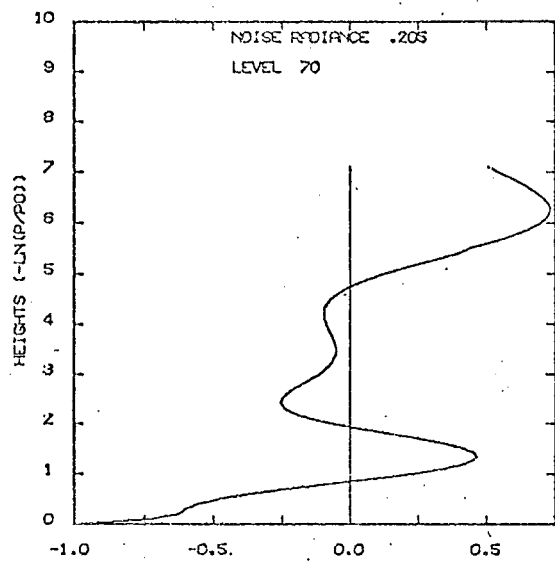
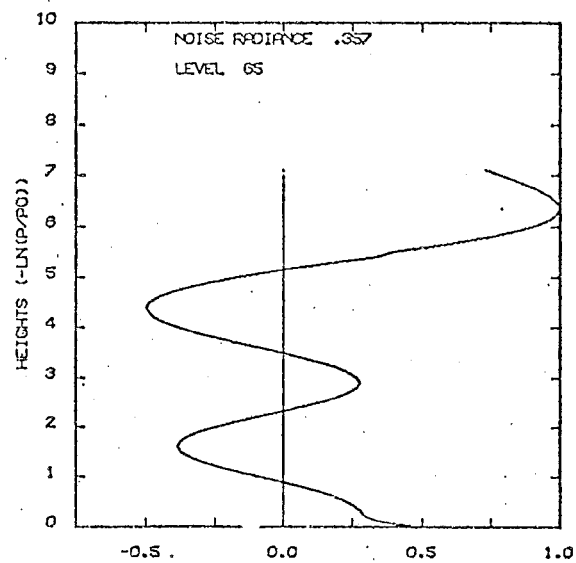


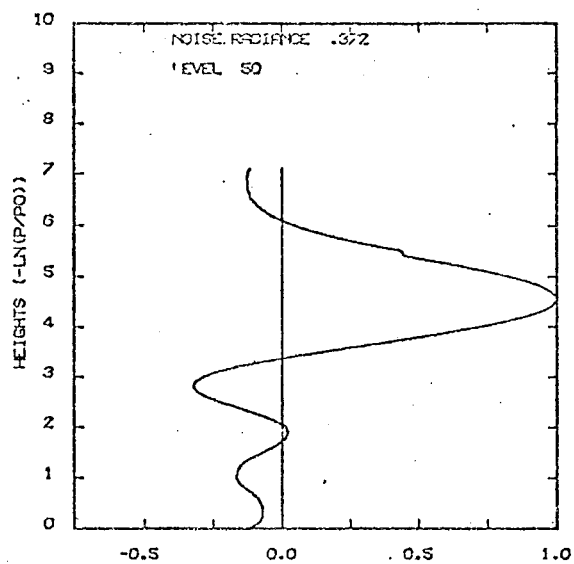
FIGURE 4.3 Averaging kernels of the MAP estimator derived using the GC a priori covariance matrix. Satellite noise variance  $0.01 \text{ mWm}^{-2} (\text{cm}^{-1})^{-1} \text{ s}^{-1}$ .



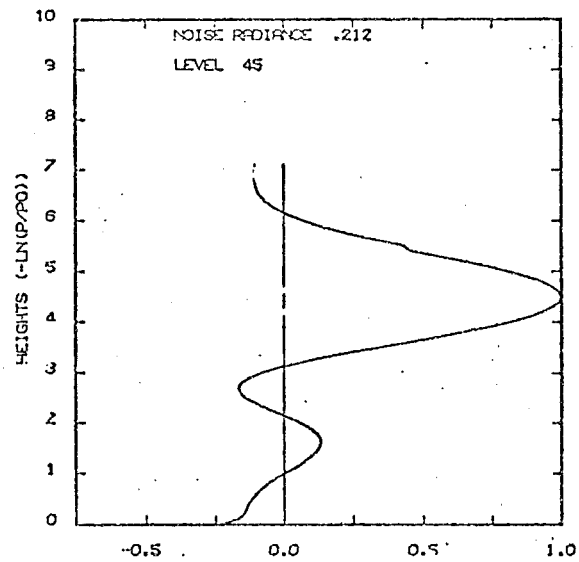
a



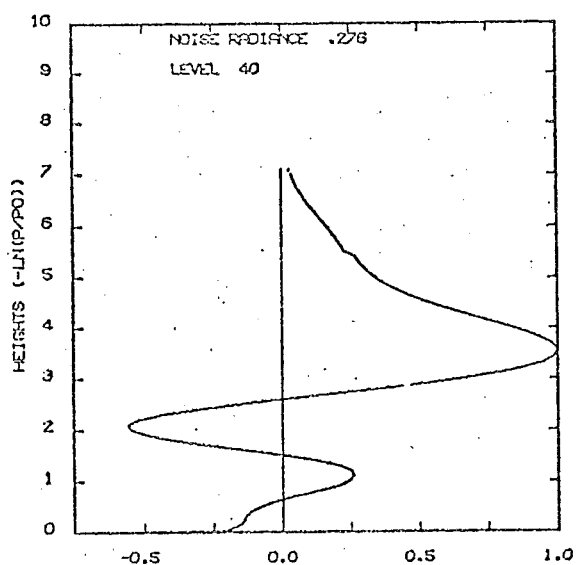
b



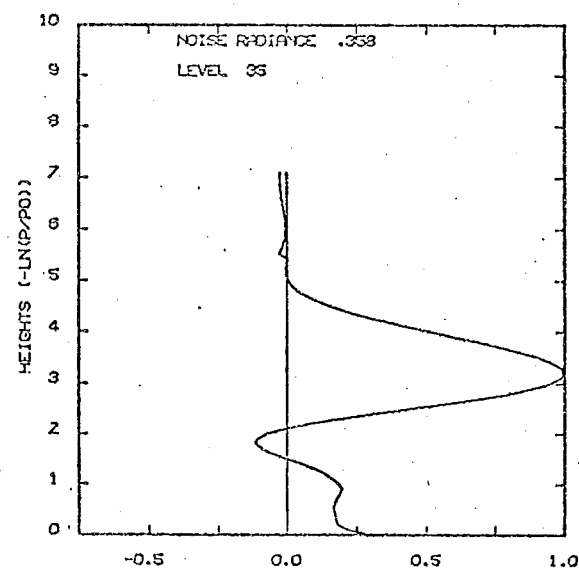
c



d



e



f

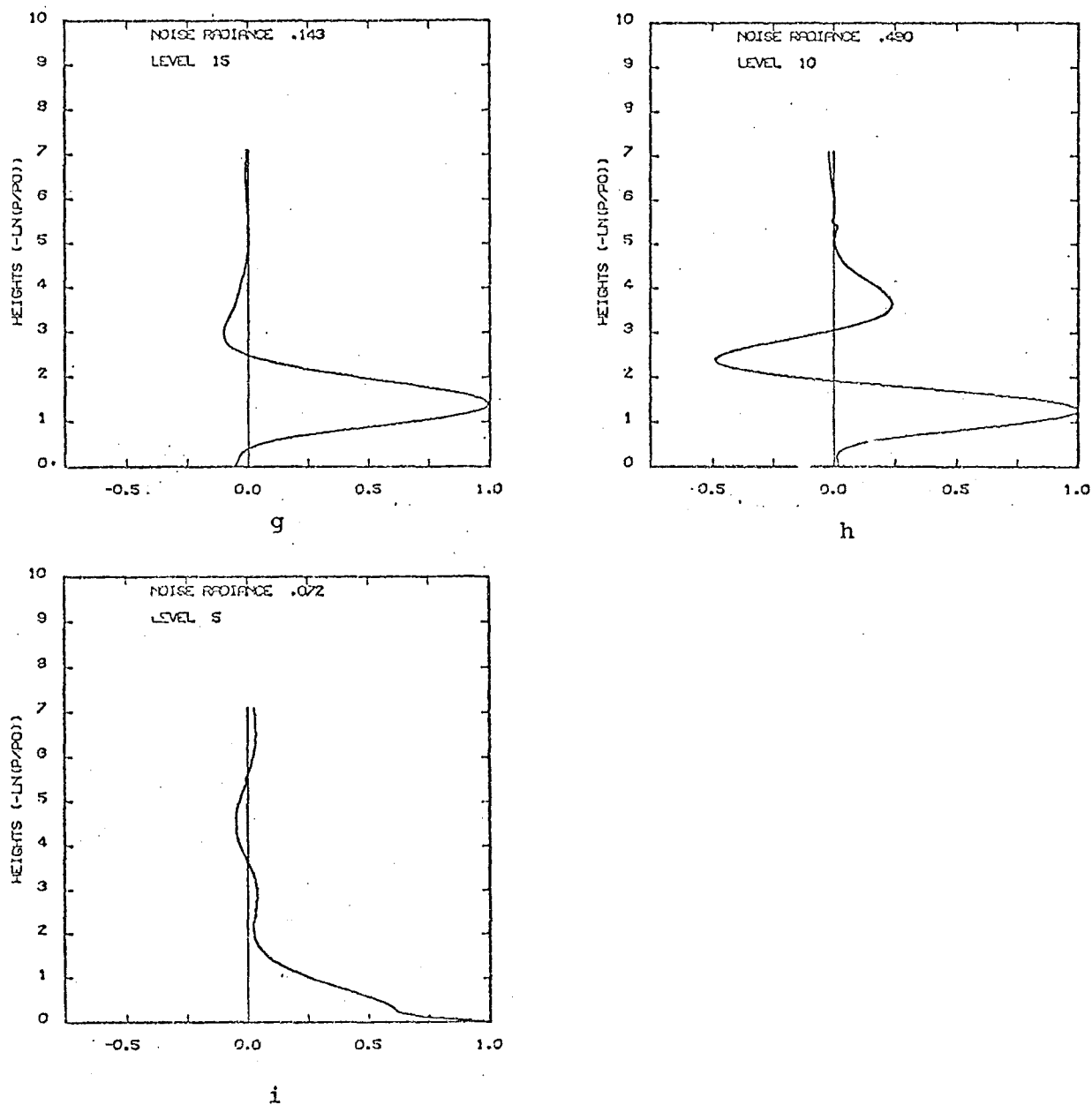


FIGURE 4.4 Averaging kernels of the MAP estimator derived using the EXPT a priori covariance matrix. Satellite noise variance  $0.01 \text{ mWm}^{-2} (\text{cm}^{-1})^{-1} \text{ st}^{-1}$ .



$$\frac{\hat{\sigma}_x}{\sigma_\epsilon} \approx 3+2$$

the level of precision is very acceptable, producing a temperature error of less than 1K at all altitudes for this simulation. However, this random temperature error indicates nothing about the accuracy of the retrieved profile.

#### The Backus and Gilbert Spread

In fig. 4.6, the Backus and Gilbert measure of spread,  $S_i$ , is given as a function of height for the estimators derived from the three covariance matrices.

Below three sh's, there is little difference in the spread for any of the a priori covariance matrices. However, between three and five sh's altitude, it is clear that the EXPT matrix derived estimator provides the best vertical resolution, with the NGC matrix giving only slightly poorer results.

Therefore, this figure, 4.6 would seem to indicate that the GC covariance matrix should not be used as the a priori covariance for the temperature retrieval, since in general this covariance matrix produces a greater spread at some altitudes than do either the NGC or EXPT matrix derived MAP estimators.

For the EXPT a priori covariance matrix then, the spread as given in equation (3.5.2.16) in the height range 1.5 ~ 5 sh is approx. 1.7 ~ 2 sh. Outside this altitude range the spread is greater by as much

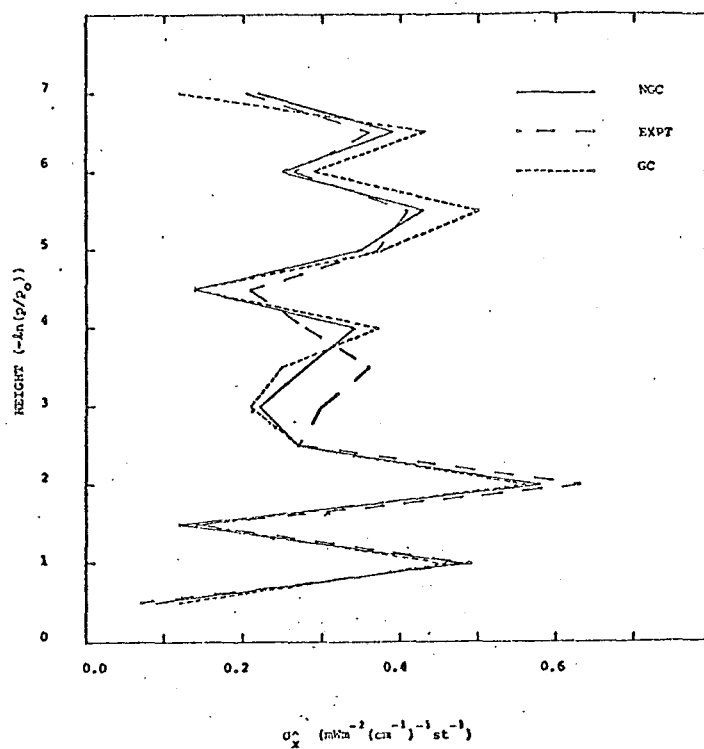


FIGURE 4.5 Random noise radiances,  $\hat{\sigma}_x$ , generated by the MAP estimators derived using  $\hat{\Sigma}$  a priori covariance matrices NGC, GC and EXPT. Satellite noise variance  $0.01\text{mWm}^{-2}(\text{cm}^{-1})^{-1}\text{st}^{-1}$ .

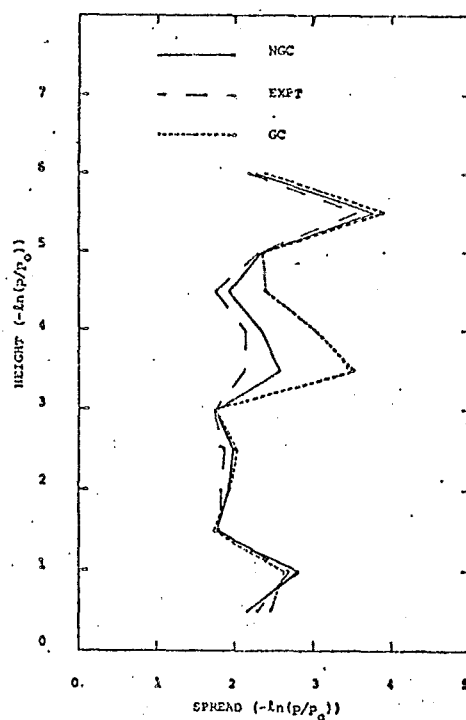


FIGURE 4.6 The Backus and Gilbert spread for the three MAP estimators. Satellite noise variance  $0.01\text{mWm}^{-2}(\text{cm}^{-1})^{-1}\text{st}^{-1}$ .

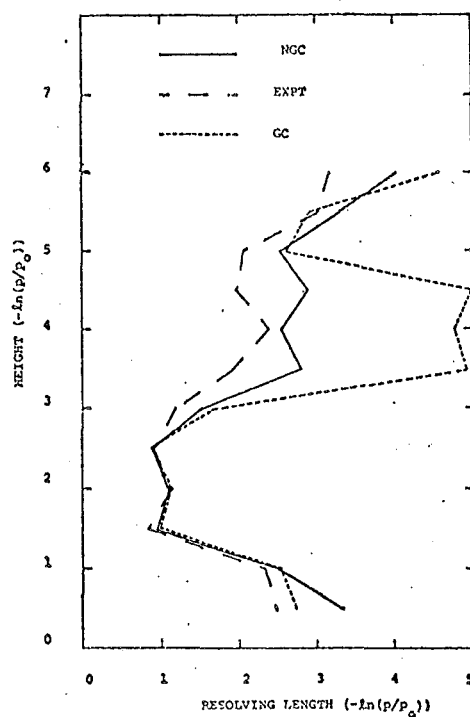


FIGURE 4.7

The Backus and Gilbert measure of resolving length for three given MAP estimators. Satellite noise variance  $0.01 \text{ mWm}^{-2} (\text{cm}^{-1})^{-1} \text{ st}^{-1}$ .

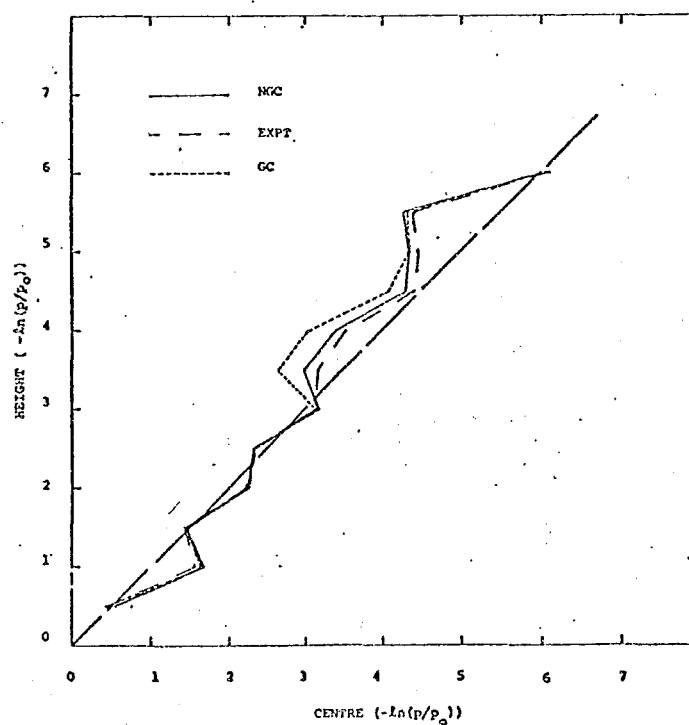


FIGURE 4.8

"Centre" altitudes for the averaging kernels of the three MAP estimators. Satellite noise variance  $0.01 \text{ mWm}^{-2} (\text{cm}^{-1})^{-1} \text{ st}^{-1}$ .

as a factor of two. However, the spread, calculated, using the EXPT covariance matrix, is in general smaller than that arising from the use of either NGC or GC covariance matrices as a priori statistics.

### The Backus and Gilbert Resolving Length

The resolving length, measured in terms of equation (3.5.2.19), is given in figure 4.7 as a function of height and the a priori covariance matrices.

Below 2.5 sh's it matters little which covariance matrix is used as the a priori statistics. However, above this altitude, clearly the EXPT covariance matrix gives superior vertical resolution.

In the region near the tropopause the vertical resolution would seem to be in the range  $0.8 \sim 1$  sh's. Above and below this region the resolution may be decreased by a factor as large as two.

### The Centre of the Averaging Kernels

Figure 4.8 indicates the altitudes of the Backus and Gilbert defined centres of the averaging kernels.

The altitude of the centres,  $C_i$ , at both 1 sh and 3.5 sh's is anomalous. In the case of the averaging kernels for 1 sh, the centre has been shifted upwards by 0.6 sh's, even above the centre for  $A_{15}(Z)$ . Whereas, for the 3.5 sh averaging kernels the reverse has occurred, for with the GC and NGC matrices the centre of the averaging kernels have been depressed in altitude below those of  $A_{30}(Z)$ .

#### 4.4.1.2 Discussion of Results

It is instructive to consider the results presented above, on figs. 4.5, 4.6, 4.7 and 4.8, together with the shape, and evolution with altitude, of the averaging kernels of figs. 4.2, 4.3 and 4.4. This will lead to an understanding of some of the critical factors involved in determining the vertical resolution and the information content of the a priori data. Consequently, the averaging kernels for levels 5, 10, 35, 45, 65 and 70 will be considered in the following work.

#### The Level 5 Averaging Kernel

From an examination of figs. 4.2(i), 4.3(i) and 4.4(i) it can be observed that the Backus and Gilbert formulation for the spread and resolving length of the averaging kernel may not be applicable for the  $A_5(Z)$ 's. This is so, since the formulation as expressed in equation (3.5.2.16) and (3.5.2.19) are given for unimodular functions with tall, narrow peaks centred at or near level  $i$  (of  $A_i(Z)$ ) and with small weight elsewhere. This is clearly not the case for  $A_5(Z)$ . A more correct estimate of the resolving length and spread for  $A_5(Z)$  would possibly be to multiply the calculated Backus and Gilbert spread and resolving length by one half, as only about half the peaked function is given in  $A_5(Z)$ .

This situation arises since the Nimbus IV SCR only has one weighting function peaking below 1 sh and consequently the G matrix of equation (3.5.2.4) weights channel 6 of the SCR heavily on constructing the averaging kernel for this altitude. See table 4.2 and equation (3.5.2.15).

---

TABLE 4.2      G COEFFICIENTS FOR  $A_5(Z)$

---

G Matrix element	Covariance Matrices		
	GC	NGC	EXPT
$G_{66\ 1}$	0.1480	0.1866	0.1336
$G_{66\ 2}$	-0.1954	-0.4142	-0.2809
$G_{66\ 3}$	-0.9561	0.4945	0.2533
$G_{66\ 4}$	1.2319	-0.2721	-0.1112
$G_{66\ 5}$	-0.4531	0.0677	-0.0327
$G_{66\ 6}$	1.1320	0.5715	0.5947

---

From table 4.2 the NGC G matrix elements for channels two, three and perhaps four are similar in magnitude to the coefficients for channel six. However, below 1 sh these channels make no contribution to the value of  $A_5(Z)$  since the magnitudes of the satellite weighting functions for these channels are effectively zero (see fig. 4.1) at these altitudes.

Therefore the resolving lengths of  $A_5(Z)$  given in fig. 4.7 and the spread of  $A_5(Z)$  given in fig. 4.6 should most probably be corrected to values in the range  $1.2 \sim 1.8$  sh's, as already stated above.

Further, by examination of the evolution of the averaging kernels from figs. 4.2(i) to 4.4(i) it is observed that the "sideband" structure is reduced. However, this factor alone does not result in improved vertical resolution, as can be observed by reference to fig. 4.7 for 0.5 sh's altitude. Careful examination of figs. 4.2(i) and 4.3(i) indicates the main peak "width" (as measured at the abscissa origin) in fig. 4.3(i) is greater than that in fig. 4.2(i). The reason for this effect may be understood by referring to table 4.2. The large negative G matrix element  $G_{66 \ 5}$  for the GC covariance matrix has resulted in a narrower peaked function  $A_5(Z)$ , compared with that given using the NGC covariance matrix.

Some observations may be made on examining the covariance matrices in appendix 3. For the GC matrix, the element referring to the variance at 0.5 sh's altitude is  $S'_{x_{66 \ 66}}$ . The value of  $S'_{x_{66 \ 66}}$  is, except for one, greater than all other entries in the 66<sup>th</sup> column of the GC matrix, however for the NGC matrix  $S_{x_{66 \ 66}}$  is less than  $S_{x_{66 \ 67}}$ ,  $S_{x_{66 \ 68}}$  and  $S_{x_{66 \ 69}}$ . Thus indicating that there is a larger covariance between the temperatures at 0.2, 0.3 and 0.4 sh's and those at 0.5 sh's than the variance

at 0.5 sh's. In the case of the EXPT matrix the value for  $S_{x_{66} 66}$  is much larger than any other entry in the 66<sup>th</sup> column of the EXPT matrix. The result for this situation is a decrease in the value of the  $G_{66j}$  ( $j = 1, 2, \dots, 5$ ) elements over those derived from GC and NGC matrices. This has an overall effect, it would seem, of reducing the sidebands magnitude for the EXPT  $A_5(Z)$  more than for the NGC or GC  $A_5(Z)$ . However the peak "width" as defined above remains approximately the same for the NGC and EXPT derived  $A_5(Z)$ .

#### The level 10 Averaging Kernel

Consider the averaging kernels for altitude 1 sh, i.e.  $A_{10}(Z)$ , as given in figs. 4.2(h), 4.3(h) and 4.4(h). There is large sideband structure present in these curves, especially in the region of 2.2 sh's altitude. Clearly then, the centres of these averaging kernels (as defined by equation (3.5.2.18)) will be at an altitude greater than 1 sh, as is clearly demonstrated in fig. 4.8.

The G matrix elements relevant to this altitude are given in table 4.3.



TABLE 4.3 G COEFFICIENTS FOR  $A_{10}(Z)$ 

G MATRIX ELEMENT	GC	COVARIANCE NGC	MATRICES EXPT
$G_{61, 1}$	0.0464	0.0573	0.1217
$G_{61, 2}$	- 0.6494	- 0.6731	- 0.8376
$G_{61, 3}$	3.1427	3.2731	3.3755
$G_{61, 4}$	- 3.1345	- 3.2828	- 3.2193
$G_{61, 5}$	1.2018	1.2748	1.2550
$G_{61, 6}$	0.0465	- 0.0329	0.0085

The large negative sideband at  $\sim 2.2$  sh altitude can be attributed to the large coefficients  $G_{61, 3}$  and  $G_{61, 4}$  since subtracting the satellite weighting function curve four from three (see fig. 4.1) will produce a negative sideband at this altitude. By a similar argument the positive sideband at approximately 4 sh's altitude is related to the value of coefficients  $G_{61, 2}$  and  $G_{61, 3}$ .

Figure 4.7 indicates that the resolving length at 1 sh is better for the EXPT derived  $A_{10}(Z)$  than for either the GC or NGC derived  $A_{10}(Z)$ 's. Further, figs. 4.2(h), 4.3(h) and 4.4(h) indicate that the strong sideband at altitude 2.2 sh's is smaller in magnitude (measured on the abscissa scale) for the EXPT  $A_{10}(Z)$  than for the GC or NGC  $A_{10}(Z)$ 's, both of which have a

sideband of approximately the same magnitude.

Examination of the EXPT, NGC and GC covariance matrices indicates a large covariance between altitude  $\sim 2$  sh's and altitude 1 sh (i.e. elements  $S_{x_{61}, 51}$ ) compared with the variance at altitude 1 sh (i.e. element  $S_{x_{61}, 61}$ ) for NGC and GC covariance matrices. However due to the enhanced variances of the EXPT matrix, this effect is not so pronounced for the EXPT covariance matrix.

#### The level 35 Averaging Kernel

The averaging kernel,  $A_{3.5}(Z)$  for altitude 3.5 sh's is interesting, for from fig. 4.7, it is clear that the vertical resolution is superior for the EXPT covariance derived estimator. The NGC matrix produces slightly poorer resolution but the GC matrix input to G indicates very poor vertical resolution for this altitude. The  $A_{3.5}(Z)$  are given in figs. 4.2(f), 4.3(f) and 4.4(f). Clearly, from inspection of these curves, the main difference is the magnitude of the sideband that peaks at ground level. Since this sideband is much larger for the GC derived  $A_{3.5}(Z)$  than for the EXPT derived  $A_{3.5}(Z)$ , the centre of the GC  $A_{3.5}(Z)$  will be depressed more in altitude than the centre for the EXPT  $A_{3.5}(Z)$ . This is shown to be true in fig. 4.8. Further, it is evident from fig. 4.8 that the negative gradient for the graph in the altitude range  $3 \sim 3.5$  sh's, indicates that there is a lack of intrinsic information in the a priori covariance matrix for these altitudes. A large amount of the

retrieved temperature information at 3.5 sh's altitude is coming from ground level temperatures.

The G matrix coefficients for these averaging kernels ( $A_{35}(Z)$ ) are given in table 4.4.

TABLE 4.4      G      COEFFICIENTS FOR $A_{35}(Z)$			
G MATRIX ELEMENTS	GC	COVARIANCE NGC	MATRICES EXPT
$G_{36-1}$	0.0859	0.1053	0.1197
$G_{36-2}$	- 0.7992	- 0.8413	- 0.9684
$G_{36-3}$	2.2579	2.4886	3.0181
$G_{36-4}$	- 0.9391	- 1.2017	- 1.6689
$G_{36-5}$	- 0.0431	0.0862	0.1629
$G_{36-6}$	0.2968	0.1564	0.0935

Clearly, from this table, the ground weighting function has been suppressed by the EXPT derived  $A_{35}(Z)$ , consequently, the magnitude of this sideband has been reduced.

On referring to the GC covariance matrix, the obvious feature of this matrix for the altitude range 3.5 ~ 5.0 sh's is the high covariances (relative to the variances) between those altitudes and nearly all other altitudes (especially those in the stratosphere). The NGC matrix has a greater difference between the variances and covariances but only for the EXPT matrix are the variances much larger than the covariances with other altitudes.

### The Level 45 Averaging Kernel

Clearly, from the foregoing discussion of the level 35 averaging kernel, similar results and effects could be expected for the  $A_{45}(Z)$ 's. This is evident from inspection of figs. 4.2(d), 4.3(d) and 4.4(d), and indicates the importance of large covariances between levels in reducing the amount of information in the retrieved temperature profiles.

### The Level 65 Averaging Kernel

These averaging kernels demonstrate a short-coming in the simulation results, a problem that occurs for all averaging kernels for altitudes higher than approximately 5.5 sh's. The problem arises due to insufficient statistical temperature data for altitudes above 7.1 sh's, this therefore puts an artificial restriction on the covariance matrices. Consequently, the simulation results have only been able to be calculated for the altitude range 0 - 7.1 sh's.

The 6.5 sh averaging kernels ( $A_{65}(Z)$ ) are given in figs. 4.2(b), 4.3(b) and 4.4(b). From inspection of these curves it is evident that there is large scale sideband structure. Further, the main peak is not "complete" in the Backus and Gilbert sense, consequently the Backus and Gilbert relations for centre, resolving length and spread of the averaging kernel will yield incorrect values, for reasons already explained. Consequently, the values for these quantities have not

been shown for this altitude and above on figs.4.6, 4.7 and 4.8.

The G coefficients for these averaging kernels ( $A_{65}(Z)$ ) are presented in table 4.5 below.

TABLE 4.5 G COEFFICIENTS FOR  $A_{65}(Z)$

G MATRIX ELEMENT	GC	COVARIANCE NGC	MATRICES EXPT
$G_{61}$	1.9106	1.8790	1.7949
$G_{62}$	- 2.3703	- 2.3014	- 2.0424
$G_{63}$	2.7541	2.3764	2.1005
$G_{64}$	- 1.3653	- 0.9353	- 0.9295
$G_{65}$	- 0.1736	- 0.3852	- 0.2285
$G_{66}$	0.0186	0.2486	0.1761

In reference to fig. 4.1, the emphasis placed on satellite weighting functions two and three centred at heights of approximately 3 and 4 sh's, by the G coefficients would seem to indicate a lack of intrinsic information in the weighting functions and a priori covariance matrix at 6 sh's altitude.

Clearly, from table 4.5, the GC derived  $A_{65}(Z)$  will have the smallest sideband at ground level, as is verified in figs.4.2(b), 4.3(b) and 4.4(b).

The calculated Backus and Gilbert characteristics

for these averaging kernels are given in table 4.6. These values are not correct in the Backus and Gilbert sense, but they may be used as a relative indication of the quality of the a priori covariance matrices at this altitude.

---

TABLE 4.6      CHARACTERISTIC VALUES FOR  $A_{65}(Z)$

---

BACKUS AND GILBERT MEASURE	COVARIANCE MATRIX		
	GC	NGC	EXPT
Spread (sh)	3.13	3.76	3.08
Resolving Length (sh)	6.77	9.78	7.74
Centre (sh)	5.51	5.05	5.48

---

Contrary to the trend already established, at this altitude the GC covariance input to the G matrix of equation (3.5.2.15) produces the best vertical resolution.

On inspection of the covariance matrices GC, NGC and EXPT, some comparative differences may be noted. For the GC covariance matrix the off diagonal elements have been reduced, (opposite to the situation for the lower averaging kernels), by the ground correction procedure of equation (4.3.2). Consequently, the covariance of other heights with level 65 have been reduced. The overall result for the  $A_{65}(Z)$  has been a reduction in the

sideband magnitudes, when compared with the NGC  $A_{65}(Z)$ . This is clearly demonstrated in figs. 4.2(b) and 4.3(b). Further, a similar improvement in vertical resolution has resulted for the EXPT covariance matrix over the NGC case, by simply increasing the variance at level 65 in the covariance matrix.

#### The Level 70 Averaging Kernel

The averaging kernels are displayed in figs. 4.2(a), 4.3(a) and 4.4(a).

A limiting factor for a temperature retrieval at this altitude will be the strong bias in the averaging kernels to large values near ground level for the estimators derived from the NGC and EXPT a priori covariance matrices. Consequently, the vertical resolution will be best for the GC covariance derived estimator, followed by the EXPT and NGC  $A_{70}(Z)$ 's. This effect is further demonstrated in the G coefficients for these averaging kernels, (see table 4.7) below.

---

TABLE 4.7      G COEFFICIENTS FOR  $A_{70}(Z)$

---

G MATRIX ELEMENT	GC	COVARIANCE MATRICES	
		NGC	EXPT
$G_{11}$	0.8134	0.8704	0.8970
$G_{12}$	- 0.4382	- 0.5622	- 0.6748
$G_{13}$	0.5605	1.2405	1.1911
$G_{14}$	- 0.5722	1.3461	- 1.0956
$G_{15}$	0.3058	0.6868	0.4909
$G_{16}$	0.0158	- 0.3982	- 0.2898

---

where, clearly the GC covariance G elements put greatest weight on the highest satellite weighting function, (see equation 3.5.2.15), and the lower weighting functions are suppressed. Whereas, for the NGC and EXPT  $A_{70}(Z)$ 's the largest weights are placed on satellite weighting functions 3 and 4, centred below 3 sh altitude.

#### 4.4.1.3 Summary

From the foregoing discussion of sections 4.4.1.1 and 4.4.1.2, some deductions may be made :

- (i) The vertical resolution in the region of the tropopause is approximately  $0.8 \sim 1$  sh. Above and below this region the vertical resolution decreases to approximately 2 sh's.
- (ii) The random error in the retrieved temperature profile will be less than 1K.
- (iii) A lack of intrinsic "information" in the a priori covariance matrices is evidenced by large (compared with the main peak of  $A_i(Z)$ ) sideband structure. In particular, this will result in two effects:-
  - (a) The centre of the averaging kernel  $A_i(Z)$  may be raised, or depressed about the level  $i$ , depending on whether the sidebands are above or below the level  $i$ .
  - (b) The vertical resolution is decreased by this sideband structure.



- (iv) The large sideband structure in  $A_i(Z)$  for the given covariance matrices arises due to large off diagonal covariances, compared with the variances at the levels,  $i$ .
- (v) The magnitude (and or width) of the sideband structure may be reduced by :-
  - (a) Reducing the correlation in temperature between levels in the atmosphere, here attempted with the EXPT covariance matrix derived MAP estimator.
  - (b) By ground correction above level 60.
- (vi) The covariance matrices EXPT, GC and NGC have large off diagonal covariances (compared with the diagonal variance) near 1 sh altitude and in the stratosphere.

#### 4.4.2 Satellite Noise Variance Aspects

In this section the effect of changing the satellite noise variance will be discussed.

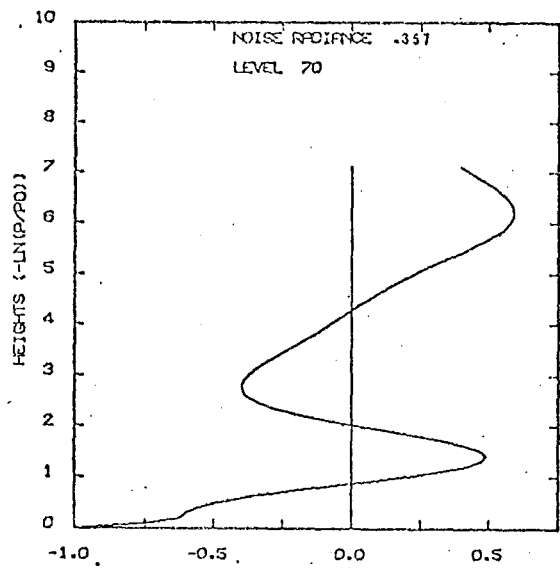
The averaging kernels using the NGC covariance matrix and satellite noise variance  $0.1 \text{ mWm}^{-2} (\text{cm}^{-1})^{-1} \text{ st}^{-1}$  are given for selected levels in fig. 4.9. On comparison of these curves with those given in fig. 4.2, it can be seen that an effect of the increased noise variance is a "smoothing" of the averaging kernels, and therefore suppression of some fine structure shown in fig. 4.2.

#### The Noise Radiance

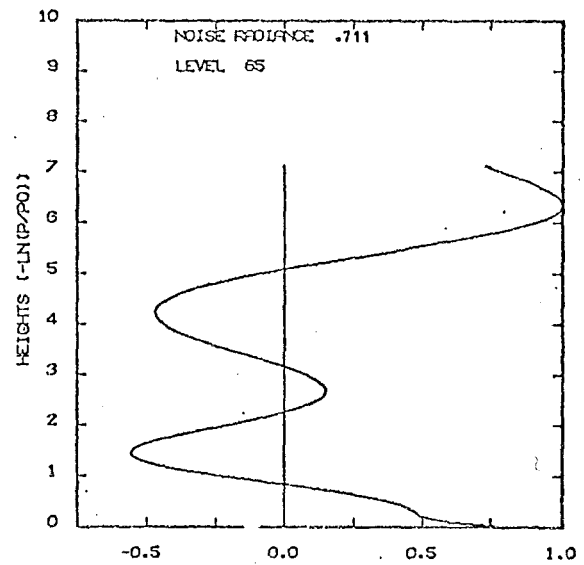
The random noise radiance is that calculated from equation (3.5.2.23), and is given as a function of height in fig. 4.10 for the estimators of both NGC and GC a priori covariance matrices. From these curves, it can be observed that the random noise radiance in the retrieved profiles will be approximately  $(0.45 \pm 0.2) \text{ mWm}^{-2} (\text{cm}^{-1})^{-1} \text{ st}^{-1}$ . The noise amplification over the SCR noise is therefore:

$$\frac{\hat{\sigma}_x}{\sigma_e} \approx 1.4 \pm 0.6$$

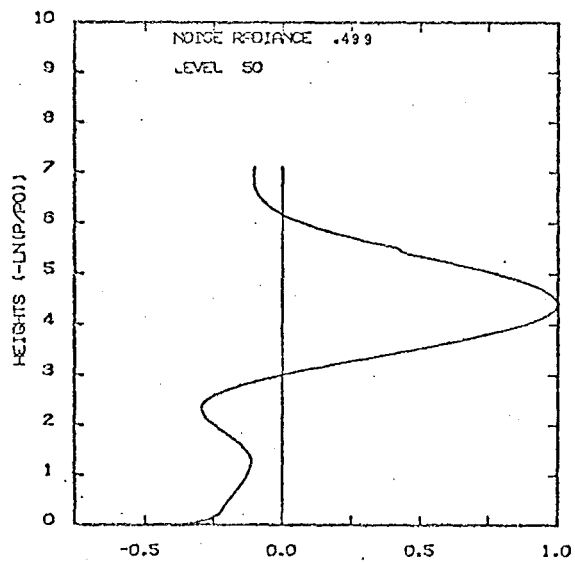
Thus, the noise amplification for a satellite noise variance of  $(0.1) \text{ mWm}^{-2} (\text{cm}^{-1})^{-1} \text{ st}^{-1}$  is decreased by a factor of two over that for a satellite noise variance of  $(0.01) \text{ mWm}^{-2} (\text{cm}^{-1})^{-1} \text{ st}^{-1}$ . However, the absolute error in the retrieved profile will still be smaller for a satellite noise variance of  $(0.01) \text{ mWm}^{-2} (\text{cm}^{-1})^{-1} \text{ st}^{-1}$ .



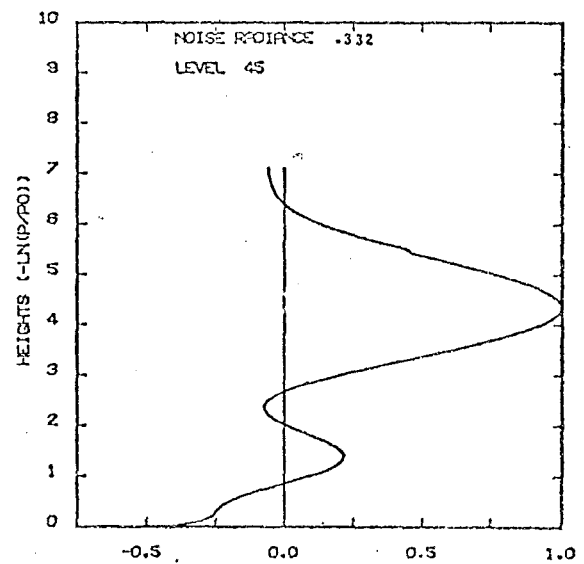
a



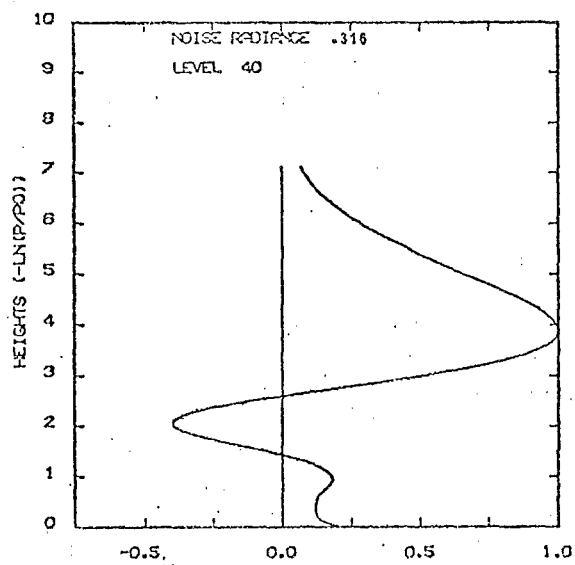
b



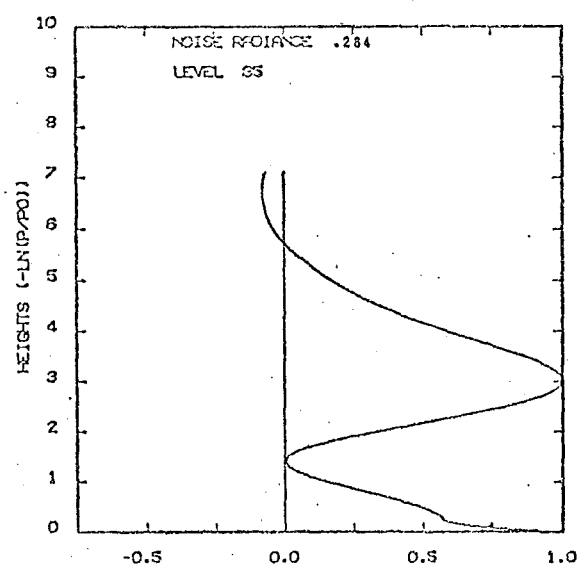
c



d



e



f

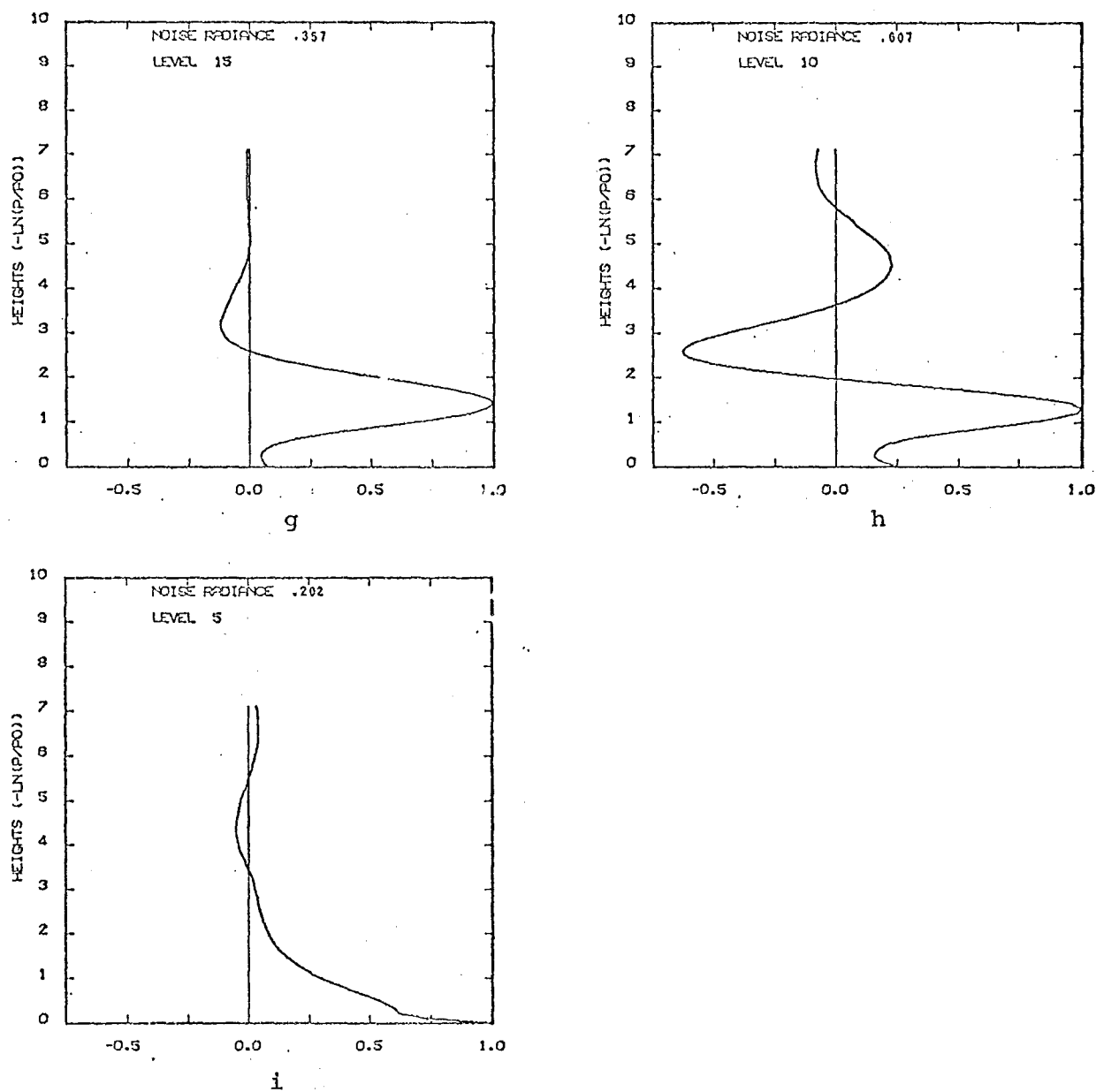


FIGURE 4.9 Averaging kernels for a MAP estimator derived using the NGC a priori covariance matrix and satellite noise variance  $0.1 \text{ mWm}^{-2} (\text{cm}^{-1})^{-1} \text{ st}^{-1}$ .

This noise radiance for the  $(0.1) \text{ mWm}^{-2} (\text{cm}^{-1})^{-1} \text{st}^{-1}$  satellite variance corresponds to a temperature profile error variance of less than 1K at all heights.

#### 4.4.2.1 Comparison of Results

As found in section 4.4.1.1, the GC covariance matrix tends to give the poorer vertical resolution for the same satellite noise variance, in this case  $(0.1) \text{ mWm}^{-2} (\text{cm}^{-1})^{-1} \text{st}^{-1}$ . This is displayed in fig. 4.11, and as found before, an improved resolving length for the GC matrix  $A_i(Z)$ 's over that for the NGC matrix  $A_i(Z)$ 's occurs above approximately 5 sh's altitude.

Consequently, in the following work it will only be necessary to compare the NGC estimator results with those of the EXPT covariance matrix derived estimator.

#### The Backus and Gilbert Resolving Length.

The resolving lengths, as functions of height, are given in fig. 4.12. Clearly, from this figure, the vertical resolution resulting from a satellite noise of  $(0.01) \text{ mWm}^{-2} (\text{cm}^{-1})^{-1} \text{st}^{-1}$  is superior to that of the vertical resolution for the  $(0.1) \text{ mWm}^{-2} (\text{cm}^{-1})^{-1} \text{st}^{-1}$  satellite noise, as might be expected.

The situation at 4 sh's altitude may be understood after considering fig. 4.9(e) and fig. 4.2(e). In fig. 4.2(e) the "width" (as measured at the abscissa origin) of the large negative sideband is large in comparison with the

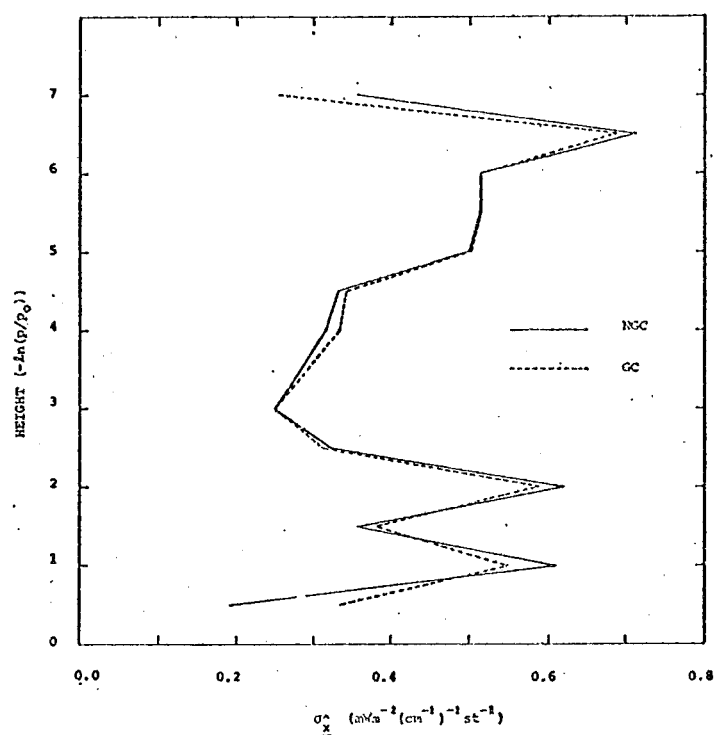


FIGURE 4.10

Random noise radiances,  $\hat{\sigma}_x$ , generated by MAP estimators derived using a priori covariance matrices NGC and GC. Satellite noise variance  $0.1 \text{ mWm}^{-2} (\text{cm}^{-1})^{-1} \text{ st}^{-1}$ .

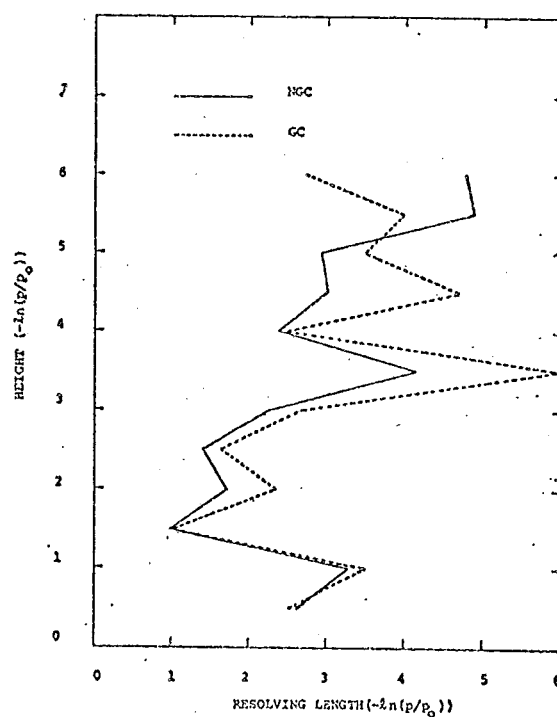


FIGURE 4.11

Backus and Gilbert resolving lengths for MAP estimators derived from NGC and GC a priori covariance matrices. Satellite noise variance  $0.1 \text{ mWm}^{-2} (\text{cm}^{-1})^{-1} \text{ st}^{-1}$ .

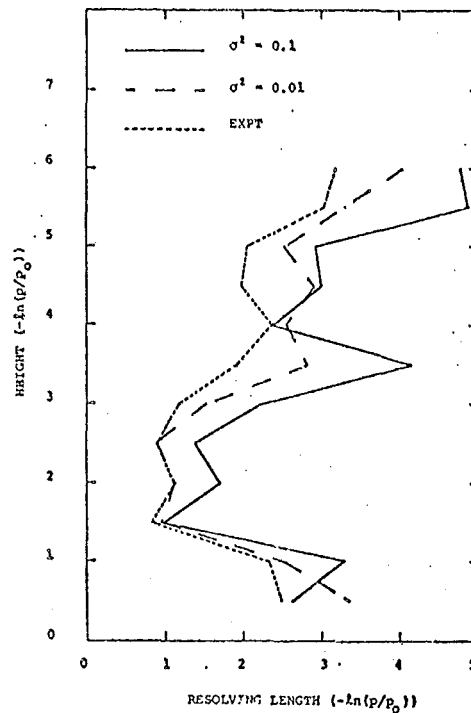


FIGURE 4.12

A comparison of Backus and Gilbert resolving lengths for satellite noise variances of 0.01 and 0.1  $\text{mWm}^{-2}(\text{cm}^{-1})^{-1}\text{st}^{-1}$  for the NGC derived MAP estimator. The EXPT results ( $\sigma^2 = 0.01 \text{ mWm}^{-2}(\text{cm}^{-1})^{-1}\text{st}^{-1}$ ) are given for reference.

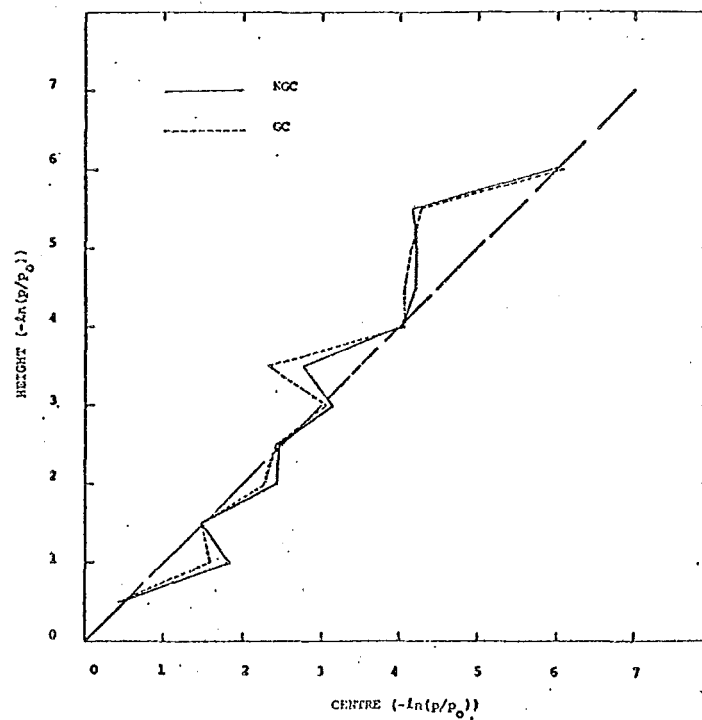


FIGURE 4.13

"Centre" altitudes for averaging kernels of MAP estimators derived using NGC and GC a priori covariance matrices. Satellite noise variance  $0.1 \text{ mWm}^{-2}(\text{cm}^{-1})^{-1}\text{st}^{-1}$ .

width of the peak in  $A_{40}(Z)$ . However, in fig. 4.9(e), although the main peak of  $A_{40}(Z)$  is much wider than for fig. 4.2(e), the negative sideband "width" in fig. 4.9(e) is much smaller relative to the "width" of the main peak in fig. 4.9(e). Consequently, the resolving length as determined by equation (3.5.2.19) is smaller for the case of satellite noise variance equal to  $(0.1) \text{mWm}^{-2} (\text{cm}^{-1})^{-1} \text{st}^{-1}$  rather than for a satellite noise of  $(0.01) \text{mWm}^{-2} (\text{cm}^{-1})^{-1} \text{st}^{-1}$ .

Results for the EXPT covariance  $A_i(Z)$ 's are also given in fig.4.12 for a comparison.

#### The Backus and Gilbert Centre

Analysis of the altitude of the centres of the  $A_i(Z)$  for an SCR noise variance of  $(0.1) \text{mWm}^{-2} (\text{cm}^{-1})^{-1} \text{st}^{-1}$  indicates that similar comments to those in sections 4.4.1.1, 4.4.1.2 and 4.4.1.3 apply here. However, the lack of intrinsic information in the a priori covariance matrices and SCR weighting functions at altitudes near 3.5 sh's and in the region  $4.5 \sim 5.5$  sh's appears to be accentuated by the higher satellite noise, as can be observed from inspection of fig.4.13. The cause of the altitude depression of the centre of  $A_{35}(Z)$  is clearly demonstrated in fig. 4.14. (For comparison see fig. 4.3(f)).



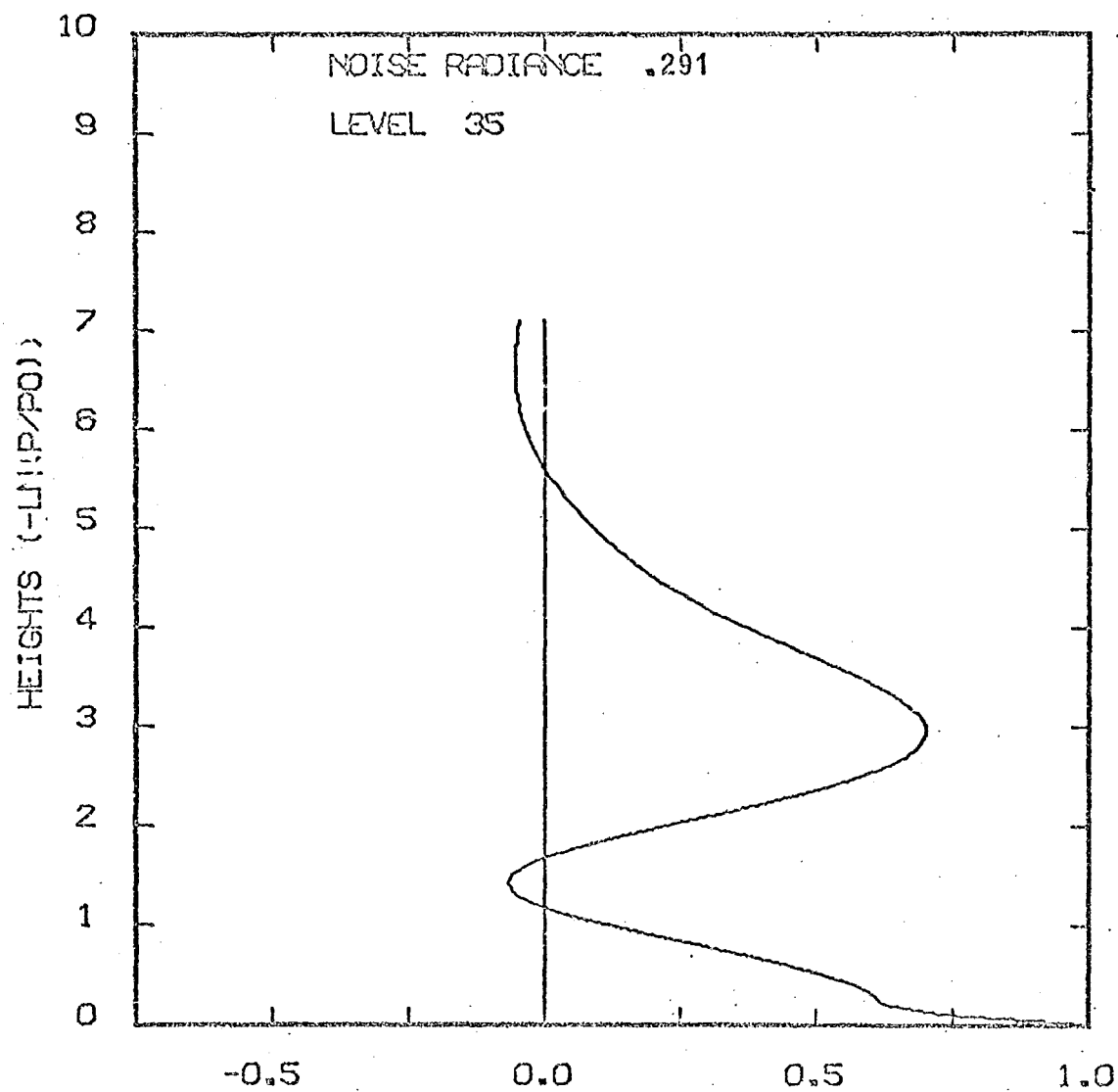


FIGURE 4.14

Averaging kernel at level 35 for the MAP estimator derived using the GC a priori covariance matrix. Satellite noise variance  $0.1 \text{ mWm}^{-2} (\text{cm}^{-1})^{-1} \text{ s}^{-1}$ .

#### 4.4.3 Summary of Results from Backus and Gilbert Diagnostics

The questions proposed in the introduction to section 4.4 and discussed obliquely in the intervening sections, are considered here:-

- (i) The vertical resolution of the MAP estimated temperature profiles is very dependent upon the a priori covariance matrix used.
- (ii) If the covariance matrix, for particular levels, has large off diagonal covariances compared with the diagonal covariance (i.e. variance) then the vertical resolution for these levels will be poor.
- (iii) Ground correction of the covariance matrix (NGC) in general reduces the amount of information available for the retrieval and consequently will result in poorer (with regard to vertical resolution) retrievals. However, at high altitudes (above 5.5 sh's) this situation is reversed, and the GC matrix derived estimator produces the best vertical resolution.
- (iv) The "intrinsic information" content of the EXPT, NGC and GC covariance matrices varies with altitude. In particular, the matrices lack intrinsic information near 3.5 sh's altitude and in the high stratosphere. It seems that retrievals may be reliably made for altitudes up to 7.1 sh's (given the present limitations of height), however, where there is a lack of intrinsic information

in the covariance matrices, the vertical resolution will be poor.

- (v) The random temperature error in the MAP estimated temperature profile, for the satellite noise variances examined here, will be less than  $\pm 1\text{K}$ , i.e. the precision of the retrieval is better than  $\pm 1\text{K}$ .
- (vi) Increasing the SCR noise variance from  $(0.01) \text{ mWm}^{-2} (\text{cm}^{-1})^{-1} \text{ st}^{-1}$  to  $(0.1) \text{ mWm}^{-2} (\text{cm}^{-1})^{-1} \text{ st}^{-1}$  has the effect of "smoothing" the averaging kernels and in general decreases the vertical resolution of the MAP estimator.
- (vii) Sidebands in the averaging kernels arise mainly from large off diagonal covariances in the a priori covariance matrix.
- (viii) The vertical resolution of the MAP estimator is better than that of the weighting functions for sufficiently high quality a priori covariance matrices (i.e. those that do not have a lack of intrinsic information).
- (ix) The question of whether deviations in the retrieved profiles from the actual profiles may be predicted by examination of the given Backus and Gilbert diagnostics, a priori, will be considered in section 4.7.

## 4.5 RETRIEVAL CALCULATIONS

In this section, MAP estimated retrieval profiles are presented for satellite radiances calculated for the 10th June, 1970 Wallops Island temperature profile. Three differing a priori covariance matrices will be discussed, as well as two satellite noise variances, thus coinciding with the previous analysis of section 4.4.

### 4.5.1 The First Guess Profile

In keeping with previous conventions in this work, the height above ground level will be expressed in terms of scale heights (sh's), and the temperatures as black body radiances at the linearization wavenumber.

The a priori first guess temperature profile used for all retrievals is the sample mean of the 49 temperature profiles used to construct the covariance matrix NGC. This temperature profile, together with the Wallops Island temperature profile to be retrieved, are illustrated in fig. 4.15.

### 4.5.2 The Satellite Radiances

The Wallops Island temperature profile for retrieval (see fig. 4.15) has been determined by the same method as used to calculate input profiles for deduction of the a priori covariance matrices.

Satellite radiances have been calculated by applying equation (3.2.3):-

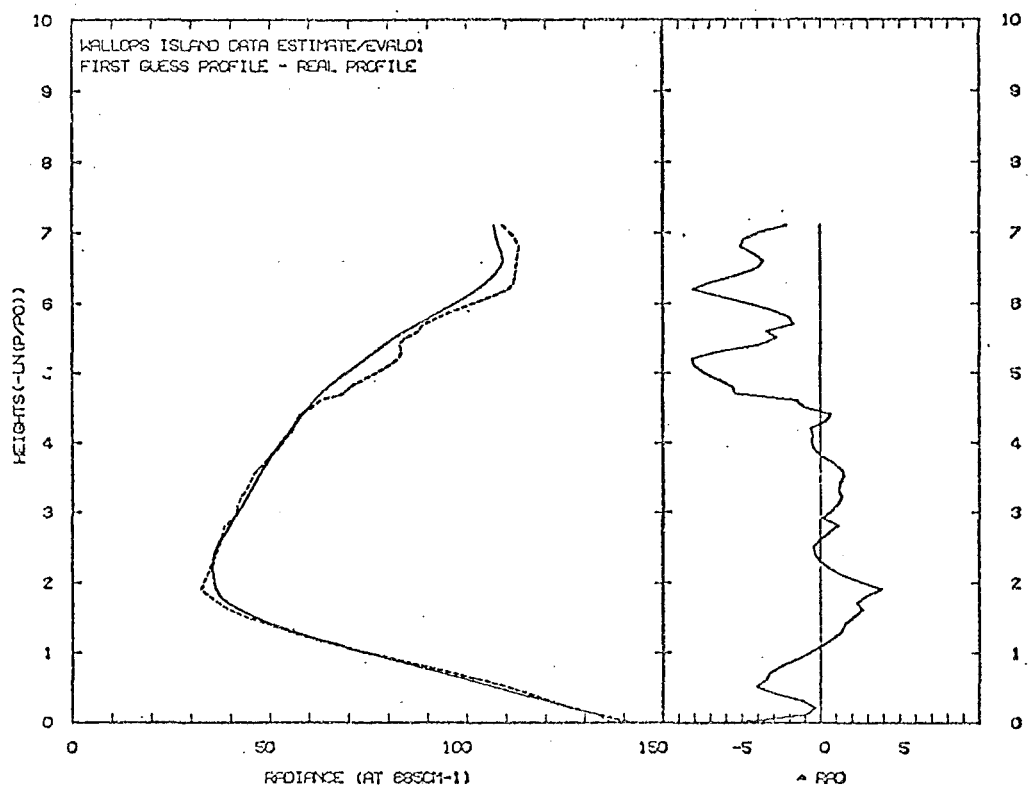


FIGURE 4.15 First guess profile and the temperature profile to be retrieved:-

— first guess profile

..... profile to be retrieved.

$\Delta$ RAD refers to the difference between the first guess profile and the profile for retrieval.

$$I(\bar{v}_i, 0) = - \int_{\infty}^{-\ln p_0} B[T(y)] K_i(y) dy \quad \dots (3.2.3)$$

where

$i = 1, 2, \dots, 6$  is the satellite channel number,

$T(y)$  is the Wallops Island temperature profile calculated from rocket and balloon data (expressed in K), and,

$K_i(y)$  is the  $i^{\text{th}}$  satellite weighting function.

All other variables are as previously defined.

#### 4.5.3 The Retrieval Results

The following calculations are for clear column radiance retrievals, no cloud effects have been included in the following analyses. The problem of clouds will be dealt with at the stage of operational retrievals.

The retrieval method is that of the MAP estimator developed in chapter three, sections 3.2 and 3.3. The a priori data has been determined from a sample of Wallops Island temperature profiles as indicated in sections 4.3 and 4.5.2, and the sequential MAP estimator equations have been used for all retrieval calculations. The major advantage of the sequential estimator that will be used here, is the property that it is possible to observe the effect on the retrieval profile of adding further satellite observations to the estimator. Consequently for the retrieval presented here, this property will be utilized whenever the results will be informative.

#### 4.5.3.1 Presentation of Retrieval Results

Figure 4.16(a, b, c, d, e, f) displays the results of a retrieval using the a priori NGC covariance matrix and satellite noise variance of  $0.01 \text{ mWm}^{-2} (\text{cm}^{-1})^{-1} \text{st}^{-1}$ .

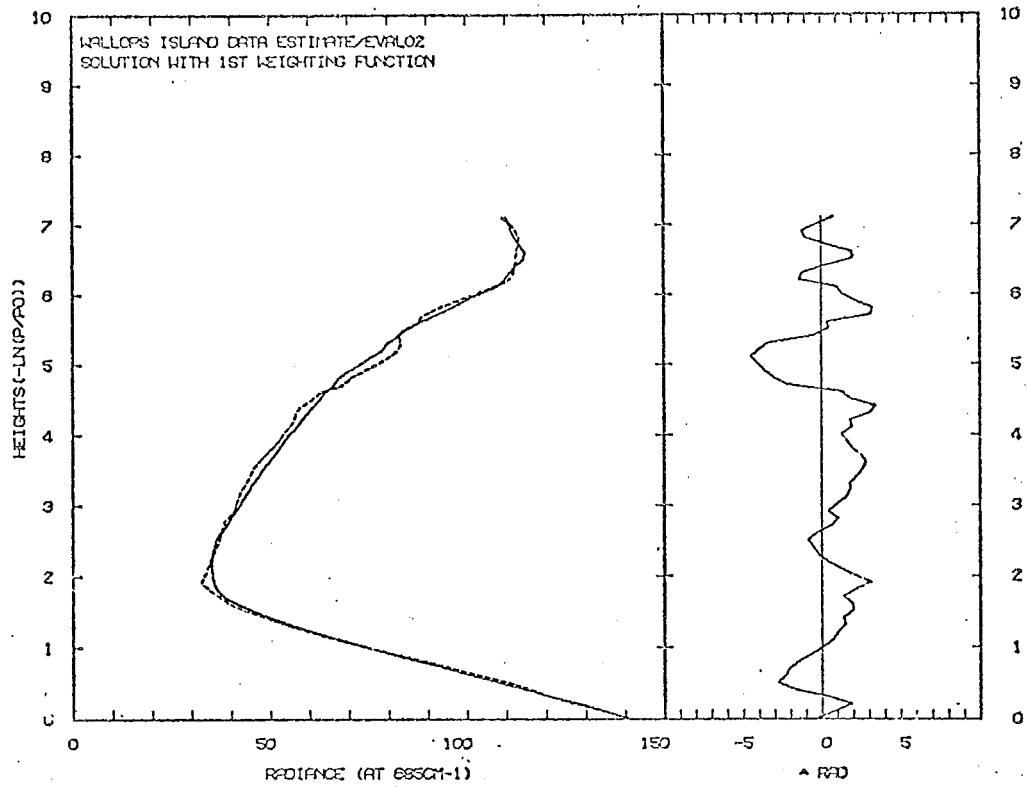
The final solution for a retrieval using the GC covariance matrix and a satellite noise variance of  $0.01 \text{ mWm}^{-2} (\text{cm}^{-1})^{-1} \text{st}^{-1}$  is given in fig. 4.17, where as in fig. 4.18 the satellite noise variance is the same as in the above cases, but the a priori covariance used is the EXPT matrix.

The stepwise sequential results for the GC and EXPT a priori matrix calculations have not been given as the essential features are displayed in fig.4.16 (a, b, c, d, e), and little useful information would be gained by presenting the calculations. It is the final result, it would seem, that is important in indicating the differences induced in the retrieval solution by changing the a priori covariance matrix.

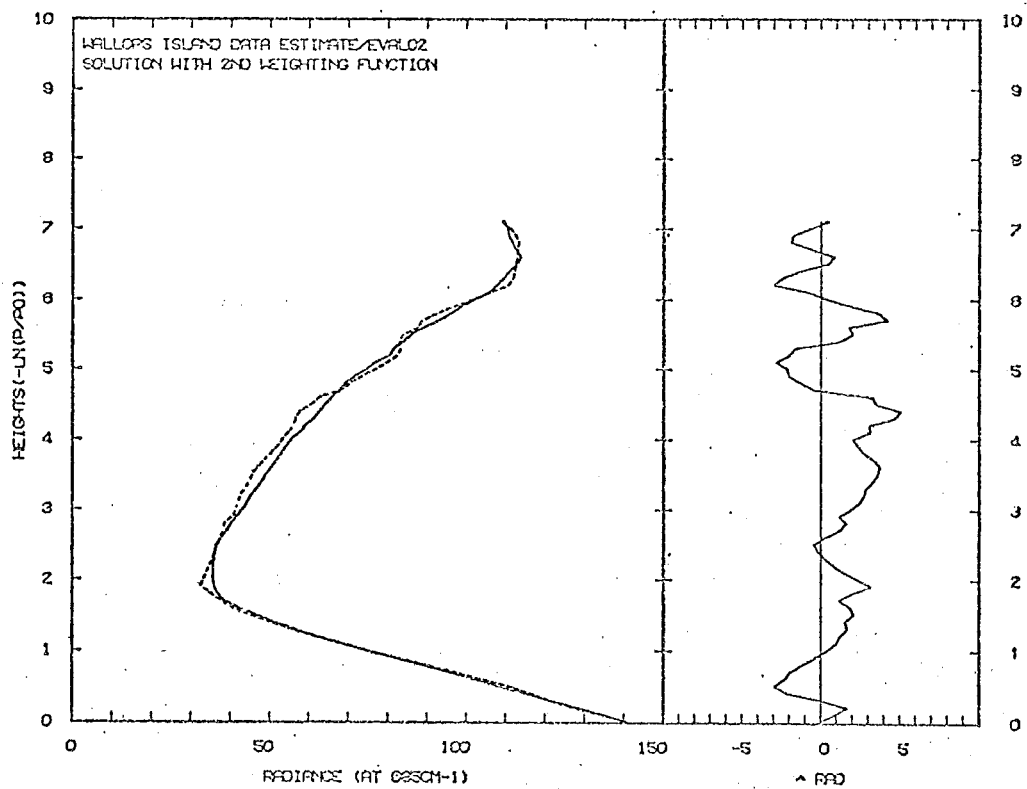
For the case where the satellite noise variance is  $0.1 \text{ mWm}^{-2} (\text{cm}^{-1})^{-1} \text{st}^{-1}$ , the results of the sequential estimation are given in fig. 4.19 (a,b,c,d,e,f). The NGC matrix has been used as the a priori covariance in this calculation.

#### 4.5.3.2 Discussion of Results

This discussion is presented in three parts where each part refers to an important aspect of the temperature profiles retrieved with the MAP estimators.

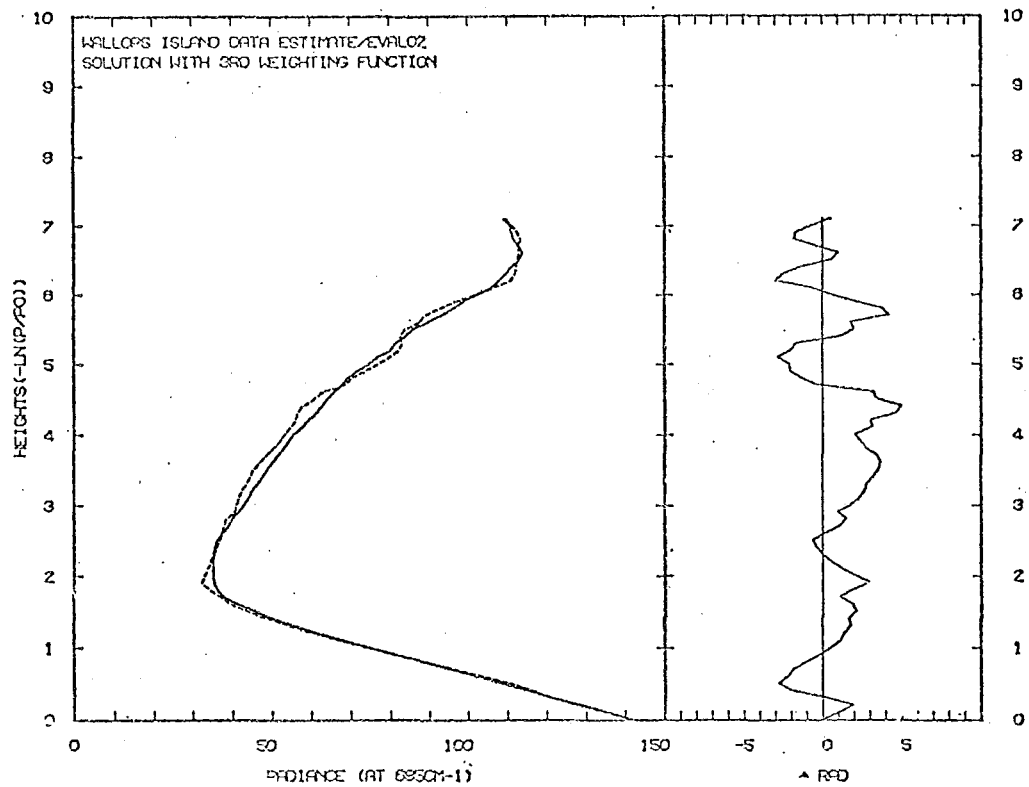


a

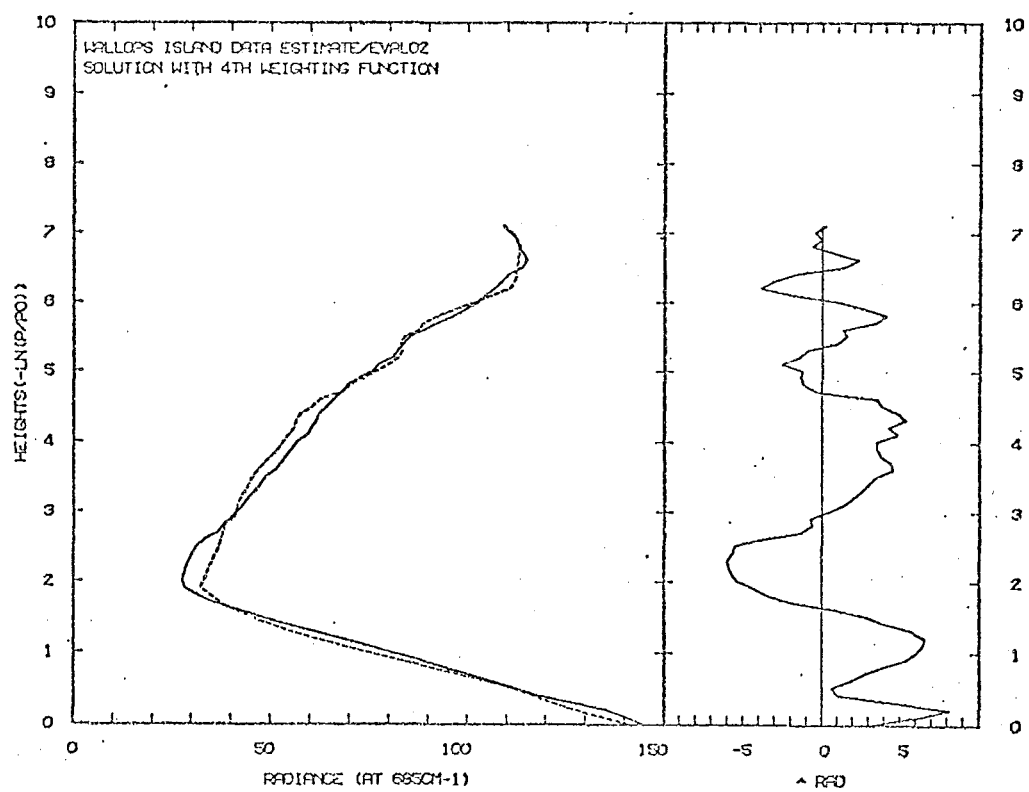


b

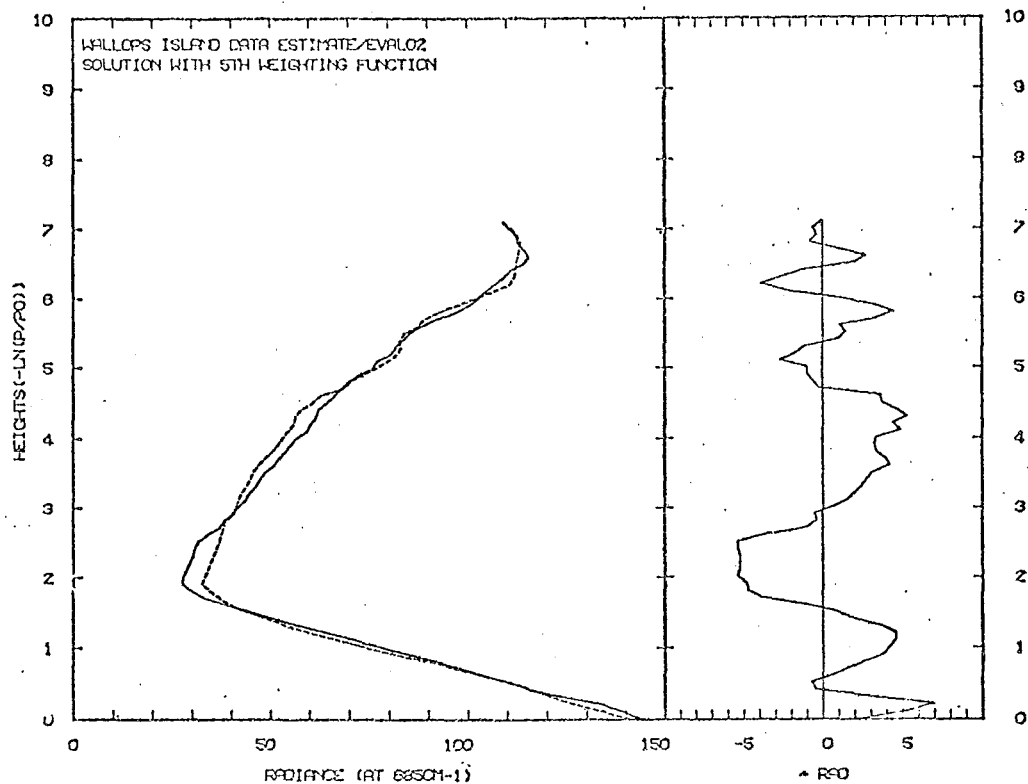




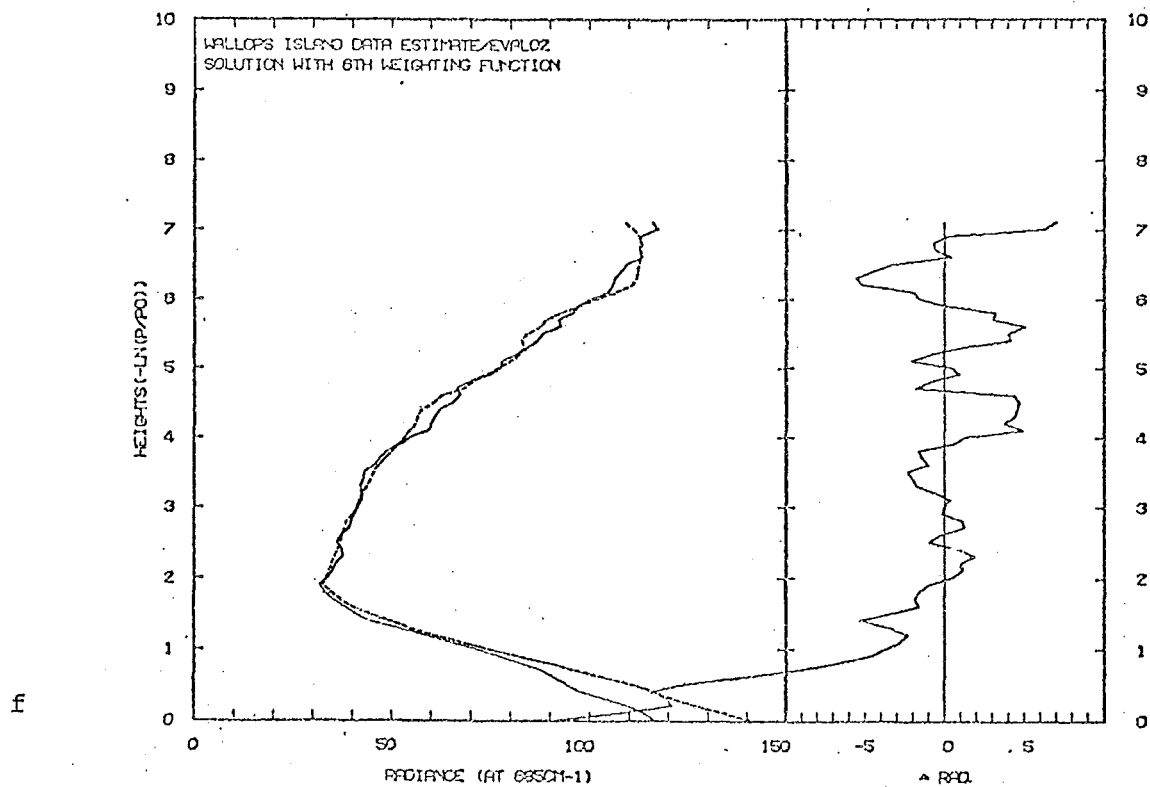
c



d



e



f

FIGURE 4.16 Sequential retrieval results using the MAP estimator derived using the NGC a priori covariance matrix. Satellite noise variance  $0.01 \text{ mWm}^{-2} (\text{cm}^{-1})^{-1} \text{ s}^{-1}$ .

— Sequential solution profile  
 .... profile to be retrieved.

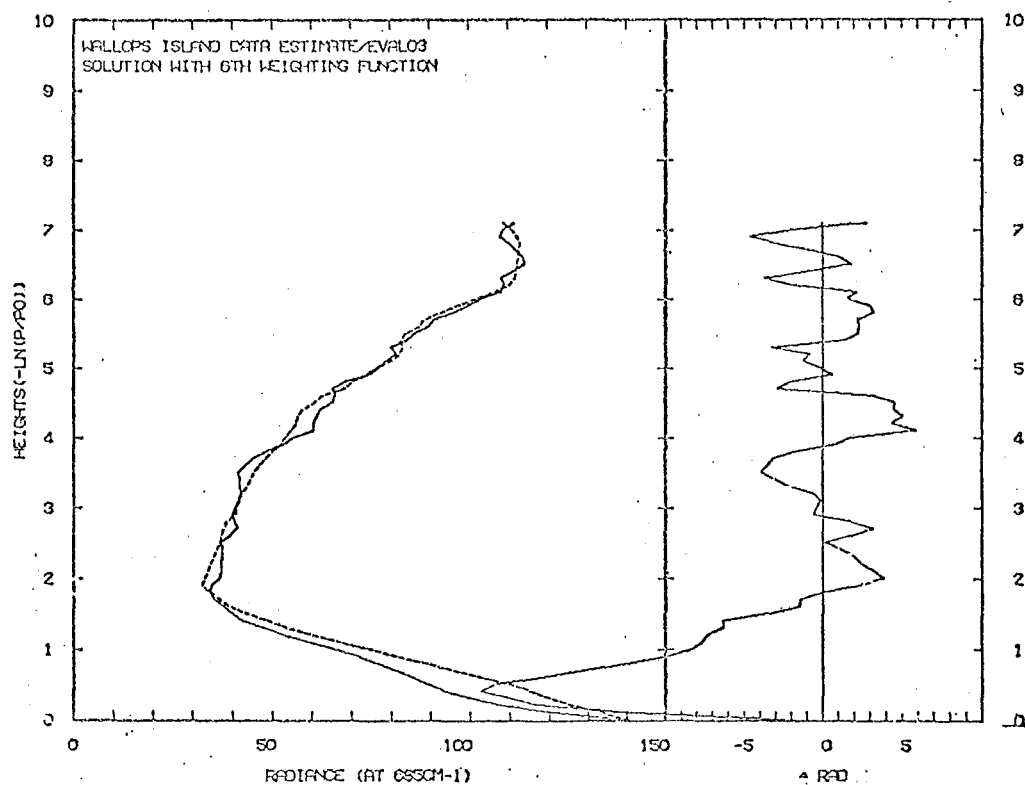


FIGURE 4.17 Final retrieval results for MAP estimator using the GC a priori matrix and satellite noise variance  $0.01 \text{ mWm}^{-2} (\text{cm}^{-1})^{-1} \text{ st}^{-1}$ .

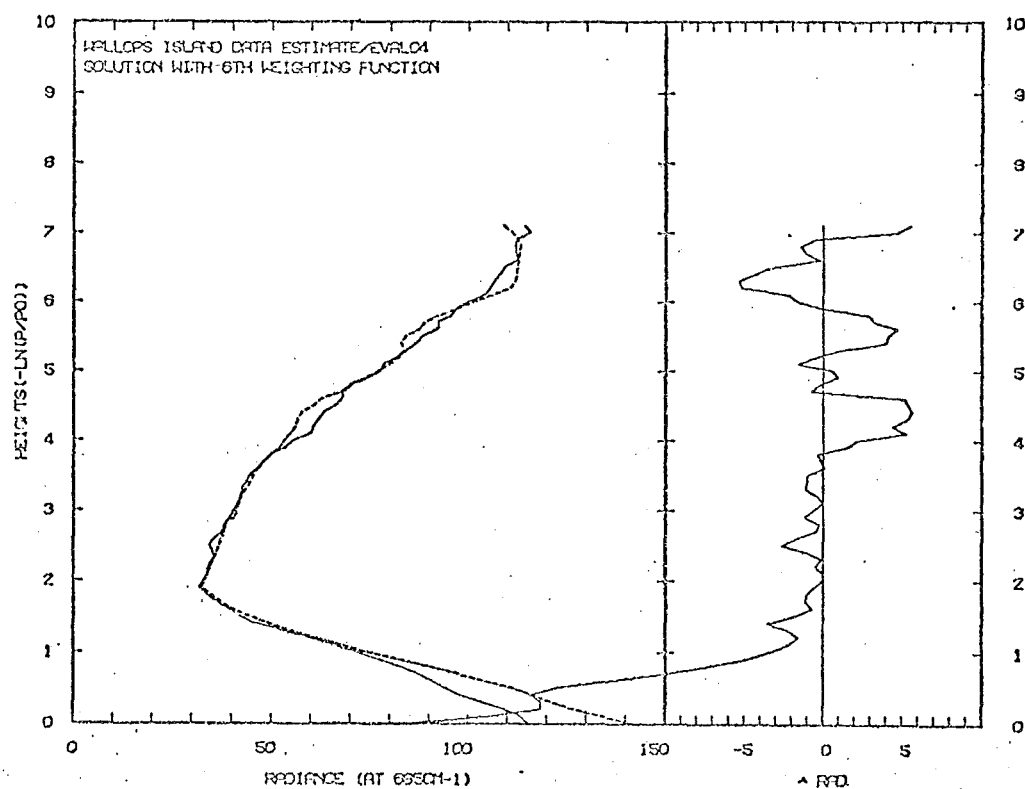


FIGURE 4.18 Final retrieval results for MAP estimator using the EXPT a priori matrix and satellite noise variance  $0.01 \text{ mWm}^{-2} (\text{cm}^{-1})^{-1} \text{ st}^{-1}$ .

### Covariance Matrix Aspects

The sequential MAP estimator is given by equation (3.3.5), reproduced below:

$$\hat{\underline{x}}_{i+1} = \hat{\underline{x}}_i + \hat{\underline{S}}_i \underline{k}_{i+1}^T (y_{i+1} - \underline{k}_{i+1} \hat{\underline{x}}_i) / (\underline{k}_{i+1} \hat{\underline{S}}_i \underline{k}_{i+1}^T + \sigma_{i+1}^2) \quad \dots (4.5.3.2.1)$$

Clearly, the covariance matrix  $\hat{\underline{S}}_i$  is important in determining the final estimated profile. The effect of the different a priori covariance matrices NGC, GC and EXPT on the MAP estimator may be observed by reference to figs.4.16(f), 4.17 and 4.18. In each of these case  $\sigma_{i+1}^2$ , the satellite noise variance is constant, and the same, so that all differences observed are due to the a priori covariance matrix differences.

In each case the MAP estimator introduces unphysical noise into the solutions. This is particularly noticeable in fig.4.17, for the GC matrix results. However, with the assistance of the Backus and Gilbert diagnostics of section 4.4 it is possible to put limits on the true physical noise in the retrieval. These limits may be set by referring to calculations of resolving lengths for the MAP estimators (see fig. 4.7). The Backus and Gilbert resolving lengths can therefore be regarded as filters of the solution profile noise, in order that only physically significant features of the estimated profile(s) will be detected in any ensuing analysis.

In the case of the EXPT matrix derived MAP estimator (fig. 4.18) the accuracy of the retrieved profile in the altitude range  $\sim 1$  sh to  $\sim 4$  sh's is of the order of  $\pm 1 \text{mWm}^{-2} (\text{cm}^{-1})^{-1} \text{st}^{-1}$  corresponding to a temperature error of approximately  $\pm 1.2\text{K}$ . For the altitude range  $\sim 4$  to  $7.1$  sh's the accuracy of the retrieval is somewhat poorer, and is in the range  $\pm 4 \text{mWm}^{-2} (\text{cm}^{-1})^{-1} \text{st}^{-1}$  corresponding to a temperature error of approximately  $\pm 3\text{K}$ . However, below  $1$  sh altitude the temperature retrieval is most inaccurate and therefore this estimator cannot be relied upon to produce reliable estimates of the temperature at these heights.

The accuracy of the GC matrix derived MAP estimator (results in fig. 4.17) in the altitude range  $\sim 1.5$  sh's to  $7.1$  sh's corresponds to a maximum temperature error of approximately  $\pm 4.2\text{K}$  in the region of the tropopause and lower stratosphere. The temperature error in the upper stratosphere will however be only about  $\pm 2.5\text{K}$ . Below  $1.5$  sh's the retrieval is completely inaccurate.

For the NGC derived MAP estimator the solution profile (see fig. 4.16) accuracy in the altitude range  $\sim 1$  sh to  $\sim 4$  sh's is approximately  $\pm 2 \text{mWm}^{-2} (\text{cm}^{-1})^{-1} \text{st}^{-1}$  corresponding to a temperature error of approximately  $\pm 2.5\text{K}$ .

Whereas in the altitude range  $\sim 4$  sh's to 7.1 sh's the radiance error is larger, at approximately  $\pm 4 \text{ mWm}^{-2} (\text{cm}^{-1})^{-1} \text{ st}^{-1}$ , corresponding to a temperature error of approximately  $\pm 3\text{K}$  (owing to the non linearity of the Planck black body function) for the upper atmosphere. Below 1 sh the retrieval profile is in large error, as in both other cases given above.

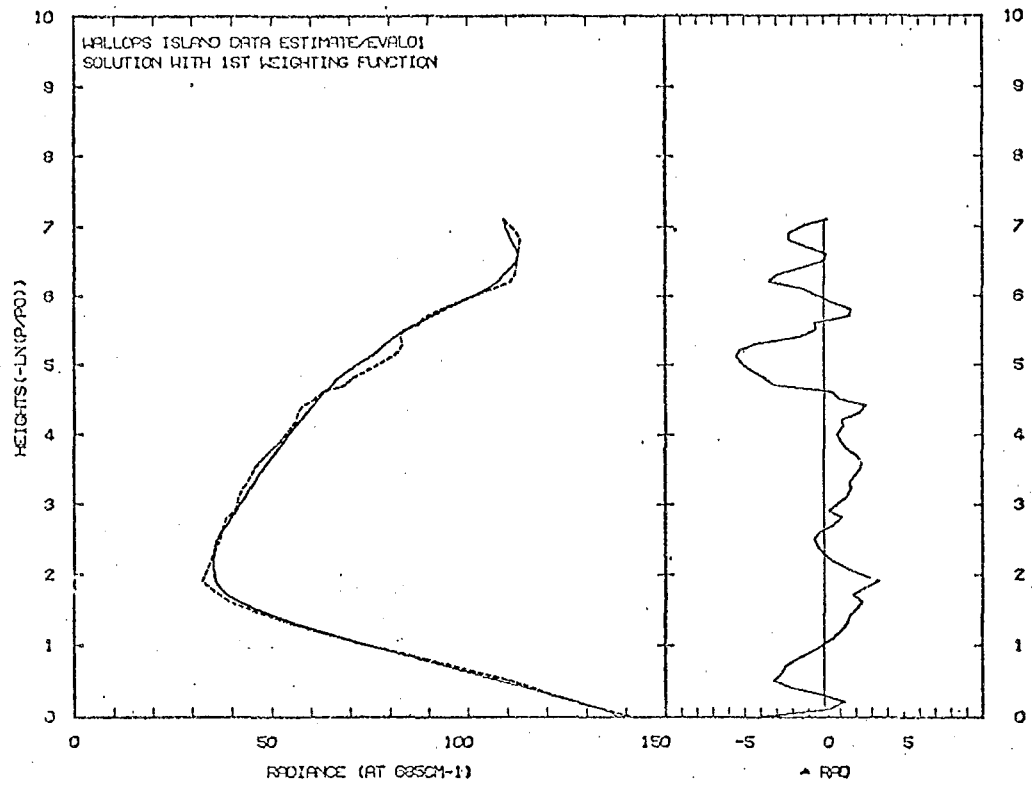
Therefore, from the above it would seem that for the present simulation study, the EXPT covariance matrix derived estimator will retrieve a temperature profile with approximately  $\pm 1\text{K}$  accuracy in the altitude range of the mid troposphere to the mid stratosphere. Above this height however, the GC covariance matrix derived estimator produces more accurate retrievals, the error being approximately  $\pm 2.5\text{K}$ . Further, not only is the temperature error smaller in the upper stratosphere for the GC covariance derived estimator, but it also appears more "randomised" since it does not grow with altitude, as in the case of the EXPT and NGC derived estimators.

The large error in the retrieved profiles near ground level arises because, for each estimator a priori covariance NGC, EXPT and GC, there is a large covariance, and variance in the temperatures near the ground level. Consequently, when the product  $\hat{S}_5 \underline{k}_6$  of the MAP estimator is evaluated,

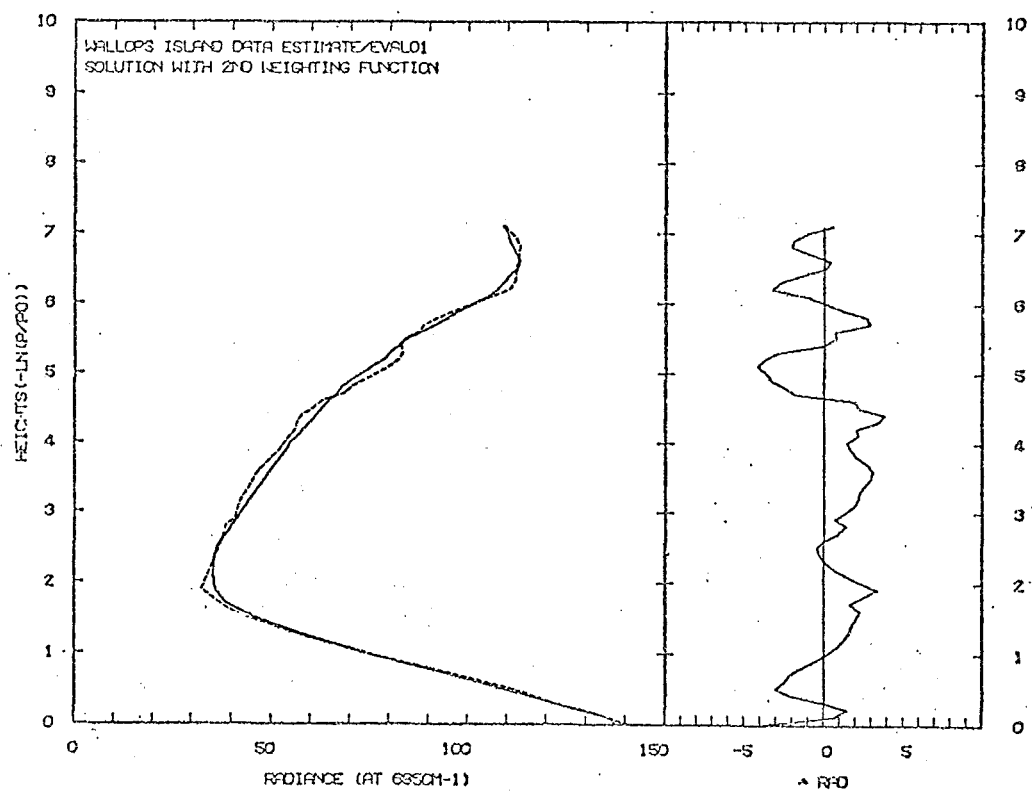
large corrections to ground level temperatures are applied to the  $\hat{\underline{x}}_5$  profile. Further, the errors in the solution profile at high altitudes above approximately 6 sh's generated at the  $\hat{\underline{x}}_6$  step are also induced by the product  $\hat{S}_5 \underline{k}_6$ . This occurs also because for each a priori matrix there are large covariances between high altitudes and heights near ground level, so causing large corrections to the  $\hat{\underline{x}}_6$  profile above 6 sh's when generating the solution profile  $\hat{\underline{x}}_6$ .

This effect is clearly displayed in the averaging kernels for altitude 7.0 sh's (see figs. 4.2(a) and 4.4(a)). In the case of the GC covariance derived estimator the ground correction procedure forces the profile to have the same value at ground level as the first guess, but this procedure does not sufficiently reduce the covariance values near ground level to reduce the large errors below 1.5 sh's. However, as already noted, the GC covariance derived estimator produces a more accurate retrieval profile above approximately 6 sh's, due to the suppression of the ground information in the covariance matrix. This effect is demonstrated in the averaging kernels of figs. 4.3(a) and 4.3(b) when compared with figs. 4.4(a) and 4.4(b).

Figure 4.16 (a, b, c, d, e) is included to indicate the effect on the solution profile of adding satellite observations to the virtual data. From these diagrams the importance of using all the satellite radiance

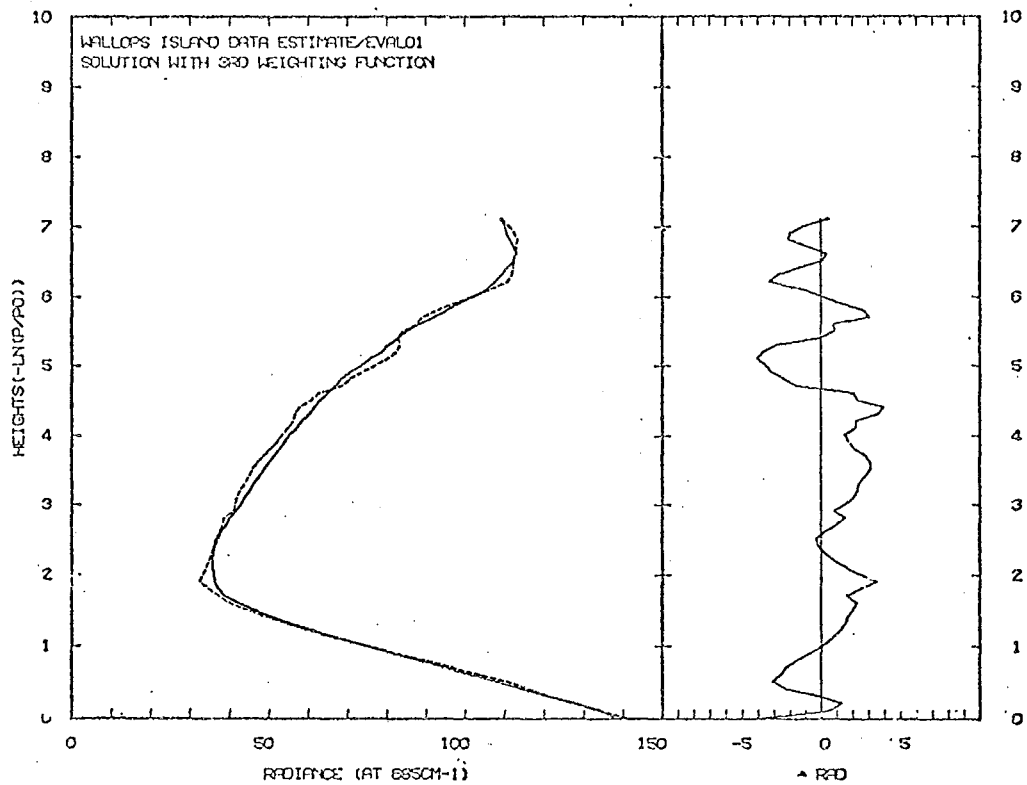


a

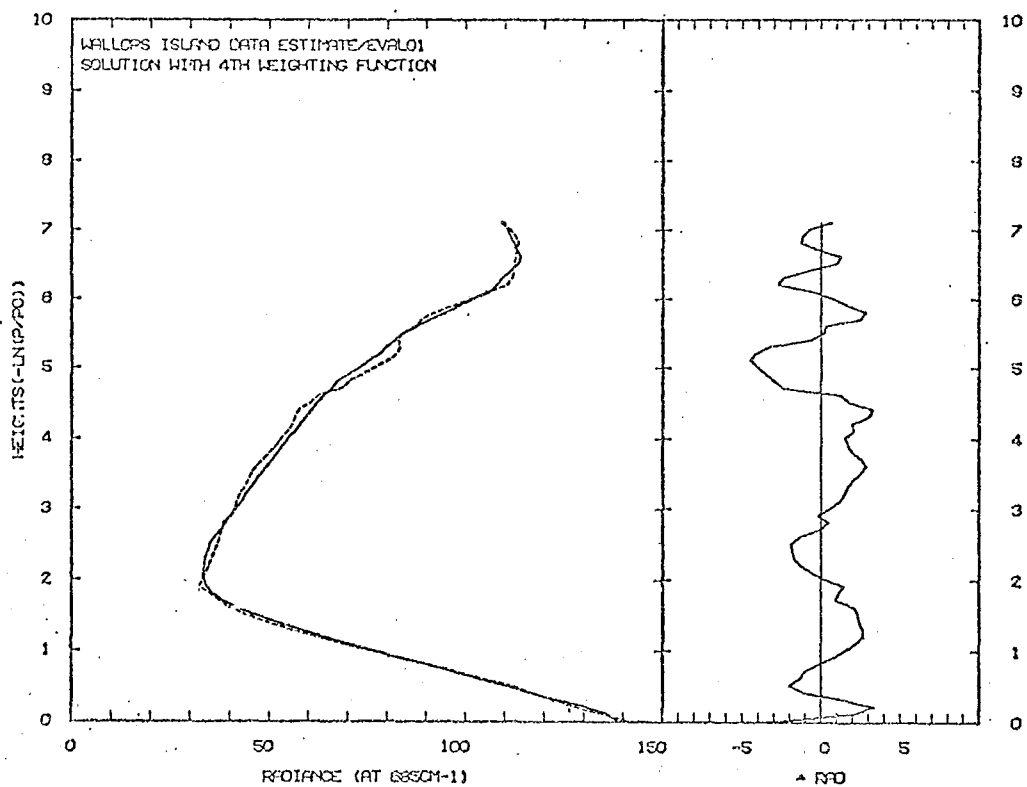


b





c



d

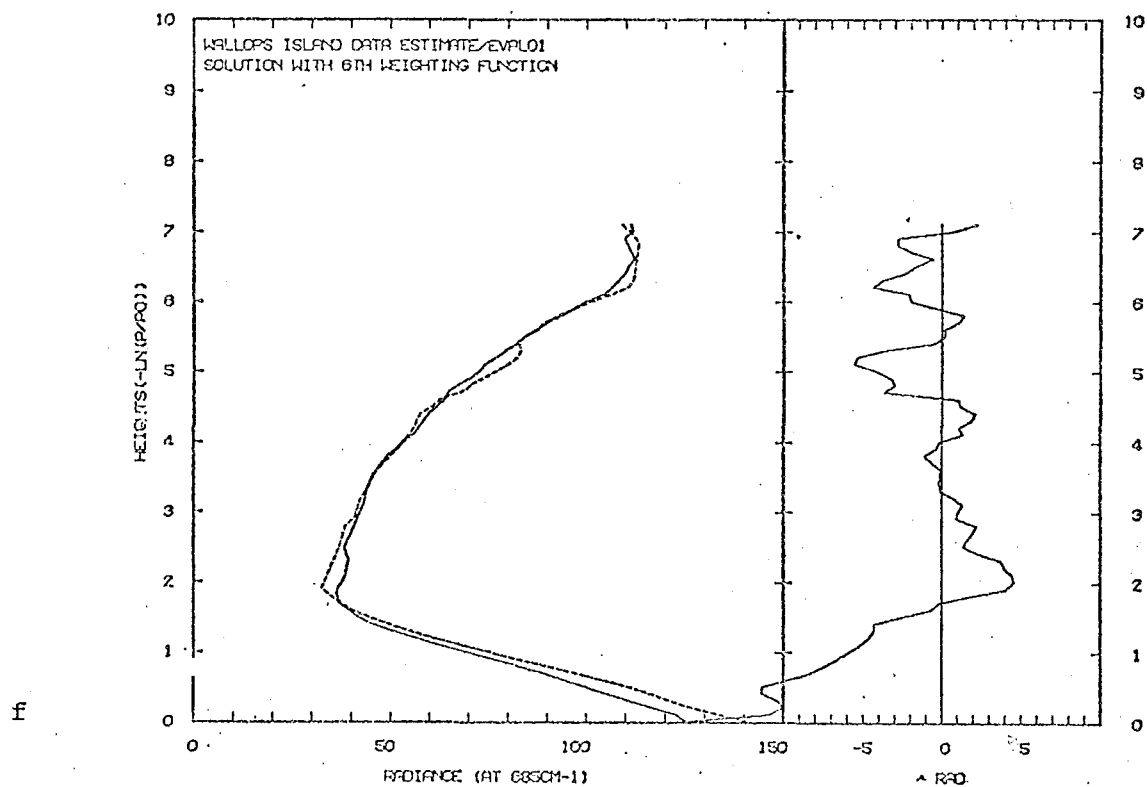
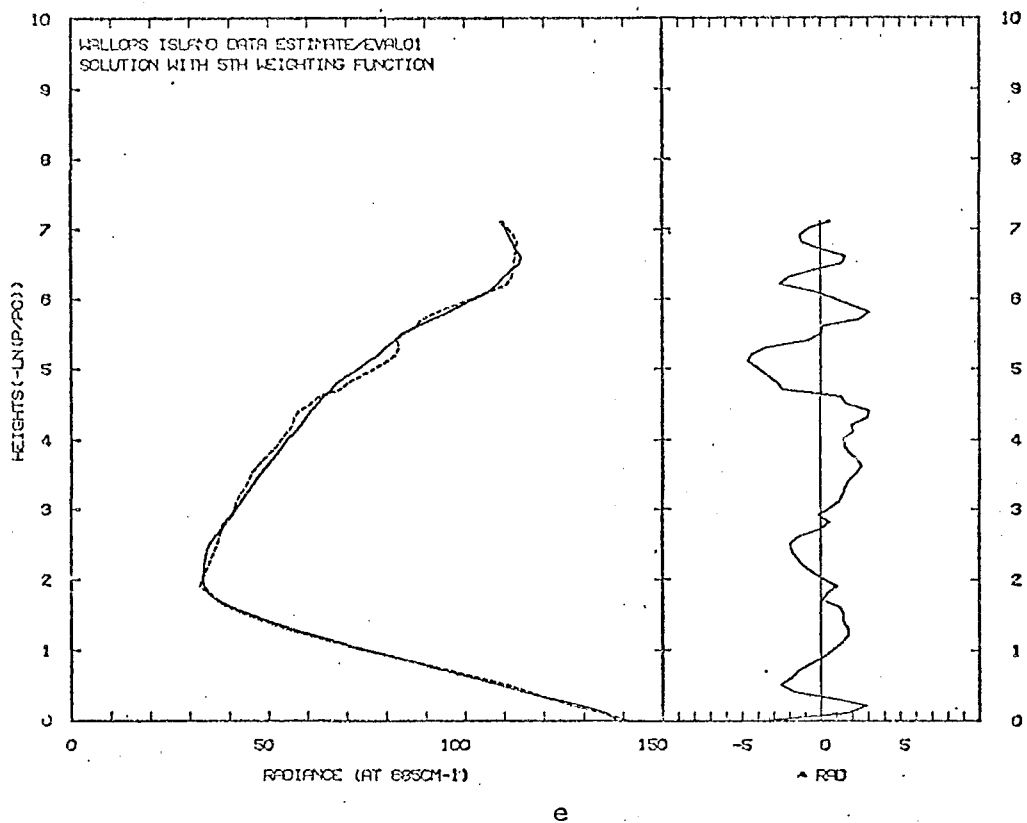


FIGURE 4.19 Sequential retrieval results from MAP estimator derived using the NGC a priori matrix and satellite noise variance  $0.1 \text{ mWm}^{-2} (\text{cm}^{-1})^{-1} \text{ st}^{-1}$ .

— sequential solution  
..... profile to be retrieved.

observations is clearly demonstrated.

Examination of all results presented thus far indicates a noticeable change in the accuracy of the retrieved profiles above approximately 4 sh's. Apart from true atmospheric temperature variations at these heights, probably part of this increasing inaccuracy can be attributed to the change over from balloon derived temperature profiles to lower quality rocket derived profiles at these altitudes. This situation may cause increased off diagonal covariances to be introduced into the covariance matrices since they are constructed from a set of single profiles as detailed in section 4.3.

#### Satellite Noise Aspects

On comparing fig. 4.19 (a,b,c,d,e,f) with fig.4.16 (a,b,c,d,e,f), the main differences in the retrieval arising from increasing the satellite noise variance, are demonstrated.

Increasing the satellite noise,  $\sigma_{i+1}^2$ , in equation 4.5.3.2.1) increases the denominator of this equation without disturbing other terms. Consequently, the satellite noise behaves like a filter on the solution retrieval profile resulting in a smoothing of the estimated temperature profile. The increased noise therefore effectively constrains the solution to be closer to the first guess profile since increasing

the noise reduces the effective information content of the satellite measured radiances (see table 4.8). Thus, in the solution, more weight is placed on the correctness of the first guess profile of the virtual data as compared to the satellite measured radiances.

Therefore, it is to be expected, that for a given first guess profile (see fig. 4.15) and the above observations for different satellite noises, that the retrieval may be less accurate in the high noise case than in the case for low satellite noise. This loss in accuracy is therefore most apparent at heights where the first guess profile deviates greatly from the actual profile. For example, in the case of the simulation profile this occurs in the high stratosphere, as is clearly demonstrated by examining figs. 4.16(f) and 4.19(f). The same effect also occurs at the tropopause, see fig. 4.19(f).

For the case where the satellite noise variance is  $0.1 \text{ mWm}^{-2} (\text{cm}^{-1})^{-1} \text{ st}^{-1}$  (fig. 4.19), in the height range  $\sim 2$  sh's to  $\sim 5$  sh's the accuracy of the retrieval is approximately  $\pm 4.5 \text{ mWm}^{-2} (\text{cm}^{-1})^{-1} \text{ st}^{-1}$  corresponding to a temperature error of the order of  $\pm 5\text{K}$ . Above this region the temperature error is approximately  $\pm 3\text{K}$ , however, below  $\sim 2$  sh's the temperature error is too large for the estimator to yield realistic temperature structure at these heights.

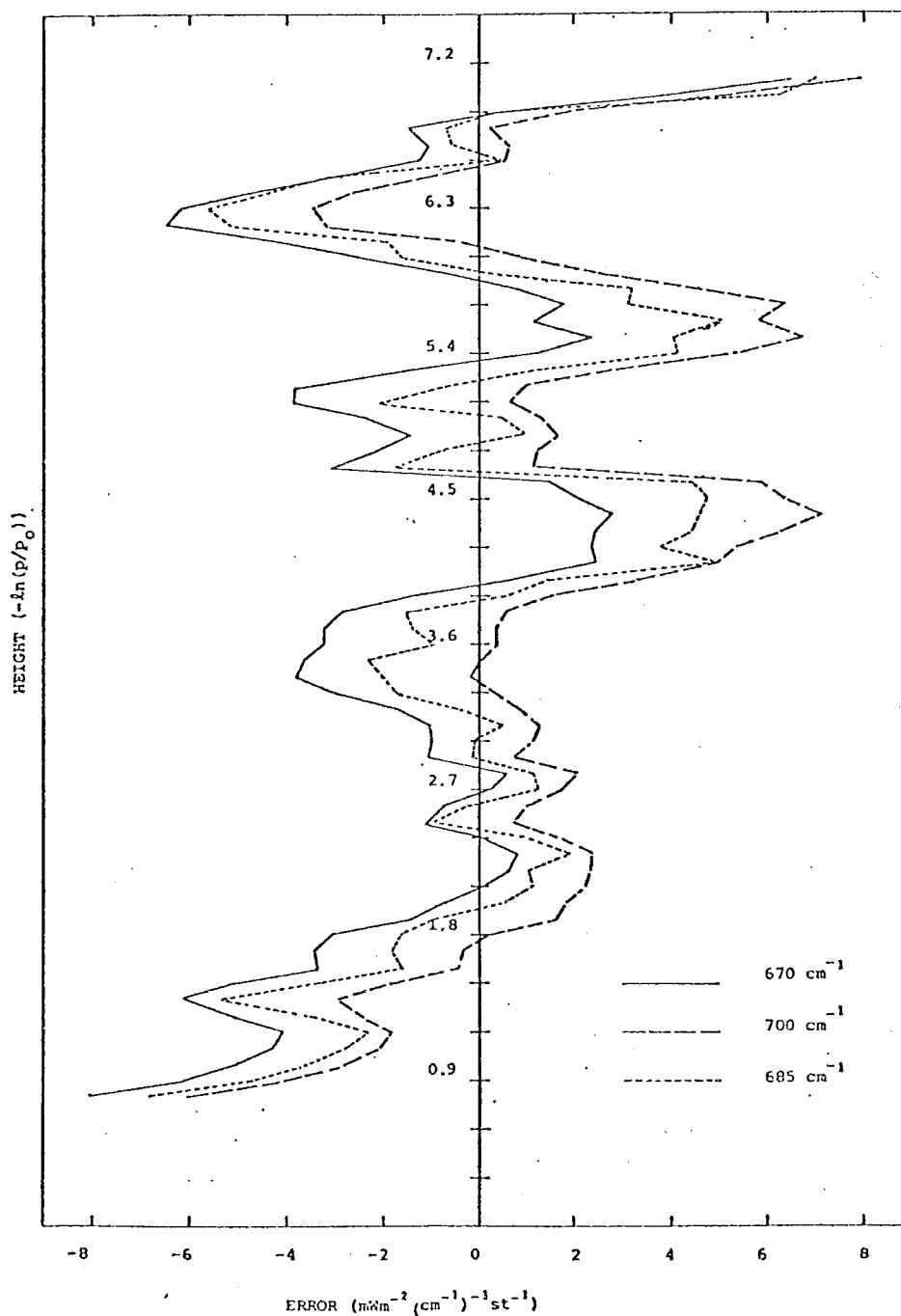


FIGURE 4.20 A comparison of the errors between the true profile and the MAP estimated retrieval profiles (using NGC statistics and satellite noise variance  $0.01\text{mWm}^{-2}(\text{cm}^{-1})^{-1}\text{st}^{-1}$ ) for different linearization wavenumbers.

### Linearization Aspects

The equation of radiative transfer has been linearized so that the problem can be solved by linear methods. This linearization is expressed by equation (3.2.1)

$$B[T(y)] \equiv B[\bar{\nu}, T(y)] \quad \dots (3.2.1)$$

where  $\bar{\nu}$  is the linearization wavenumber.

The value of  $\bar{\nu}$  used in this simulation study has been selected from the following values:-  $670\text{cm}^{-1}$ ,  $680\text{cm}^{-1}$ ,  $685\text{cm}^{-1}$  and  $700\text{cm}^{-1}$ , by examining the final error between the retrieved profile  $\hat{x}$ , and the real profile  $x$  in each case.

The net effect of changing the linearization wavenumber is for the retrieval profile to be laterally shifted about the actual profile and thereby introducing a systematic error that changes with altitude. The effect is demonstrated in fig. 4.20.

From these results, a linearization wavenumber of  $685\text{cm}^{-1}$  was selected for the Nimbus IV weighting functions.

#### 4.5.3.3 Summary of Discussion

- (i) An incorrect choice of the linearization wavenumber will introduce an altitude dependent systematic error into the retrieval temperature profile.
- (ii) As the satellite noise variance is increased, the retrieval profile is constrained to be closer to the a priori first guess profile.

- (iii) Given the Nimbus IV set of weighting functions used in this study, the large covariances between high altitudes and ground level, and the large variances near ground level in the a priori data, have produced significant errors in the MAP estimated profile. These errors occur at altitudes in the high stratosphere and near ground level.
- (iv) For the simulation carried out here, the EXPT covariance derived MAP estimator provides the best retrieval accuracy of approximately  $\pm 1.2\text{K}$  for mid-troposphere to mid-stratosphere heights. Above these heights the GC covariance derived MAP estimator provides the best accuracy, being approximately  $\pm 2.5\text{K}$  up to the stratopause.

#### 4.6 COVARIANCE ANALYSIS

An understanding of some important factors, of the MAP estimated retrieval profile, may be gained by determining an estimate of the 95% confidence regions at each level of discretization.

The theoretical background for determining confidence regions of a correlated covariance matrix has been presented in section 3.4, and is now applied to the results calculated in section 4.5.

This section is divided into three subsections. The first will contain the formal results of the analysis, whilst the second will be a discussion of the analysis results. The third subsection is a summary of the conclusions drawn, for the covariance analysis.

##### 4.6.1 Presentation of Analysis Results

An eigen analysis of the initial virtual covariance observations, and final MAP estimated solution covariance matrices has been carried out in accordance with the theoretical discussion of section 3.4.

##### Confidence Regions

For an  $\alpha$  value of 0.05 in equation (3.4.21), indicating the 95% confidence region, and using equation (3.4.26) the confidence regions for the a priori NGC matrix have been calculated for the sample mean profile (the first guess profile). The results of this analysis are presented in fig. 4.21, where, as in all previous work the temperatures are expressed in black body radiances.



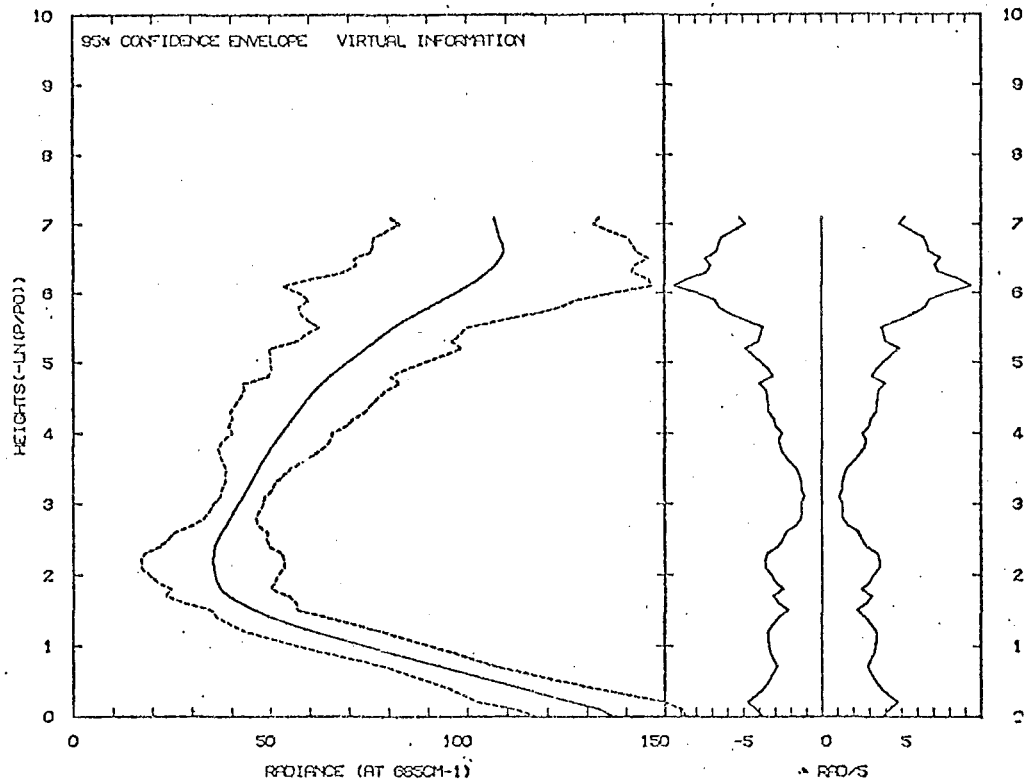


FIGURE 4.21 The 95% confidence regions about the first guess profile for the NGC a priori covariance matrix.

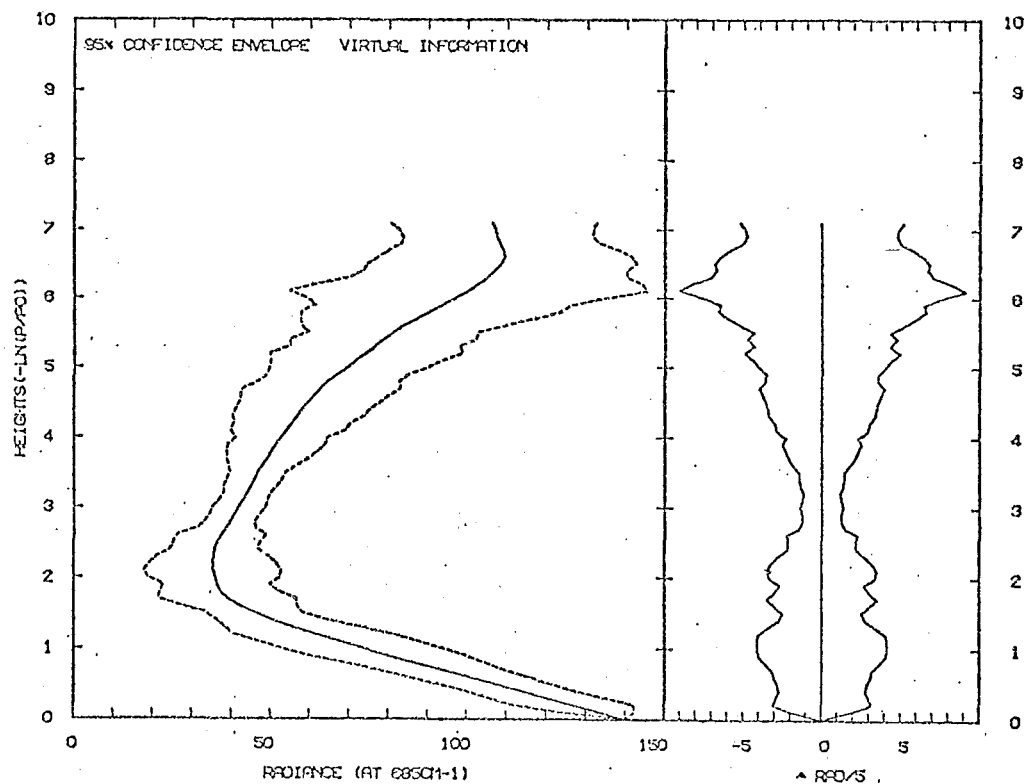


FIGURE 4.22 The 95% confidence regions about the first guess profile for the GC a priori covariance matrix.

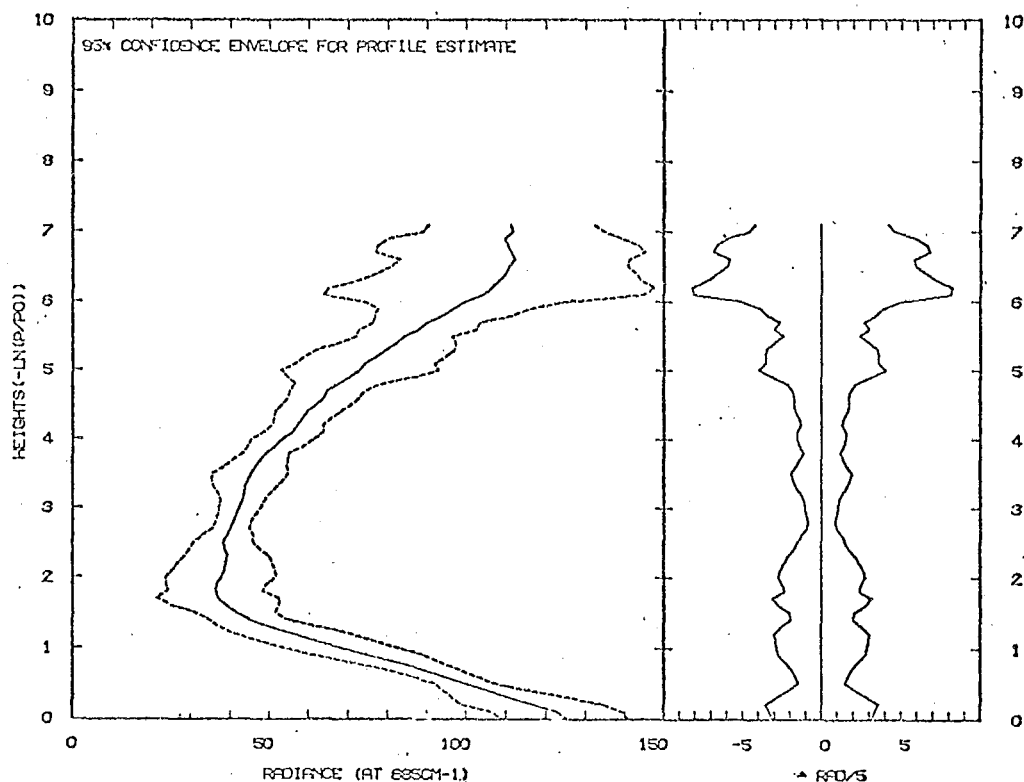


FIGURE 4.23 The retrieval profile confidence regions for the MAP estimator derived using the NGC a priori matrix and satellite noise variance  $0.1 \text{ mWm}^{-2} (\text{cm}^{-1})^{-1} \text{ st}^{-1}$ .

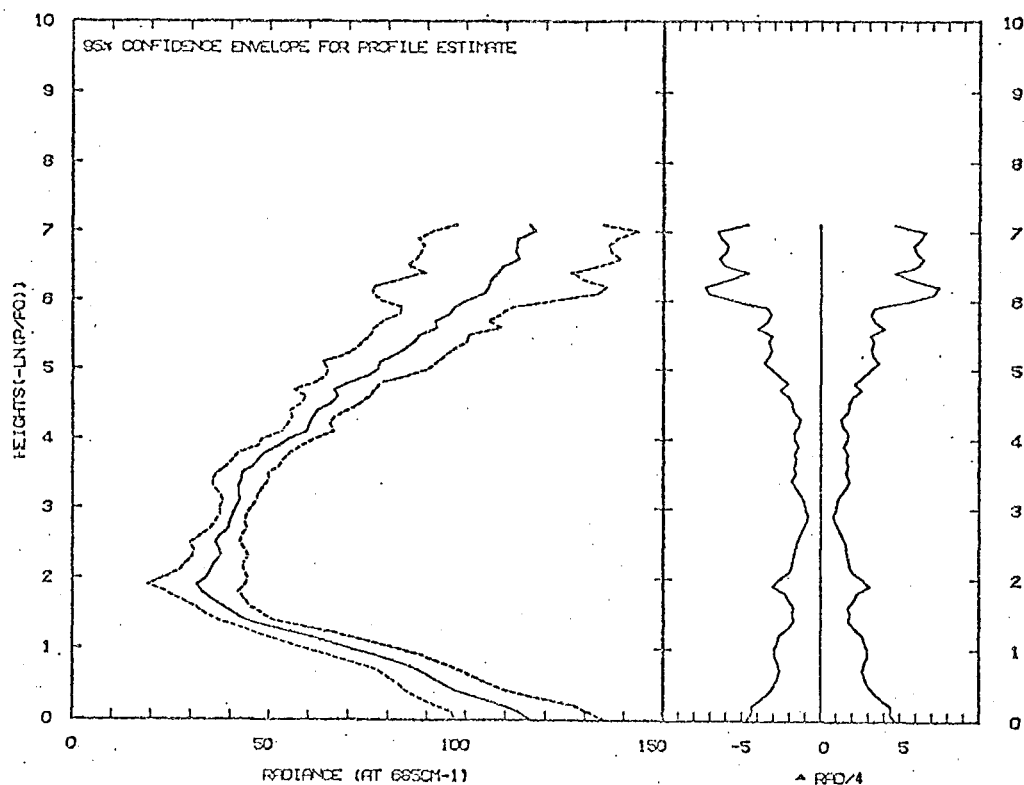


FIGURE 4.24 As above, except satellite noise variance is  $0.01 \text{ mWm}^{-2} (\text{cm}^{-1})^{-1} \text{ st}^{-1}$ .

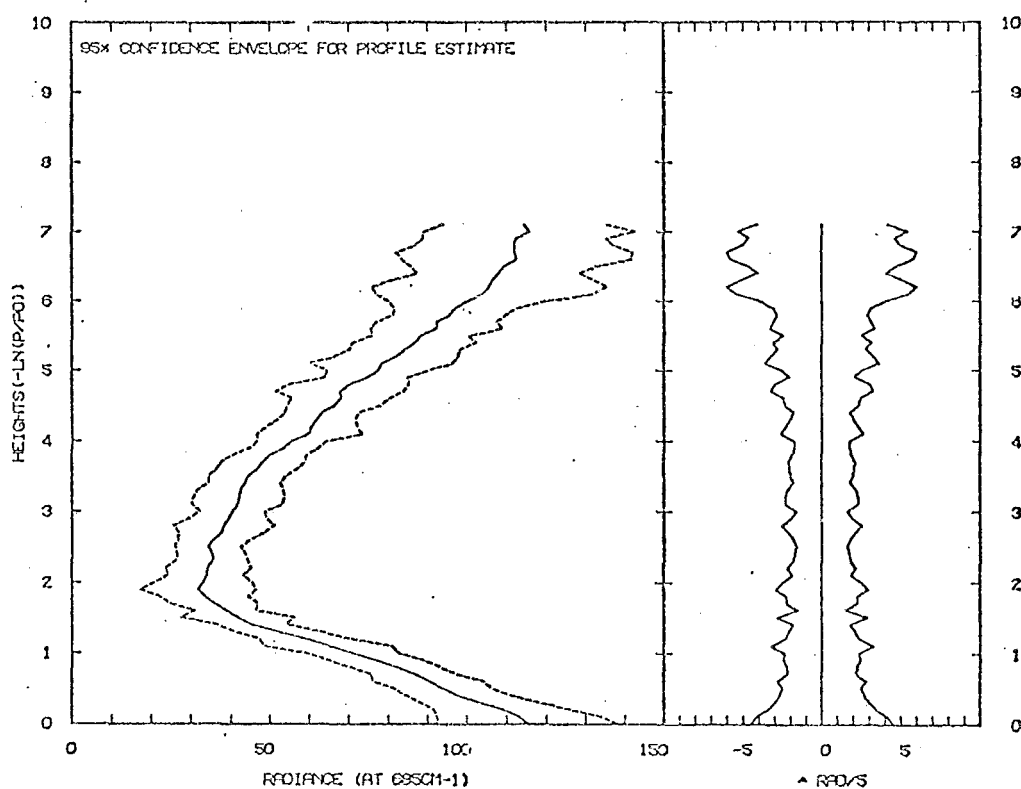


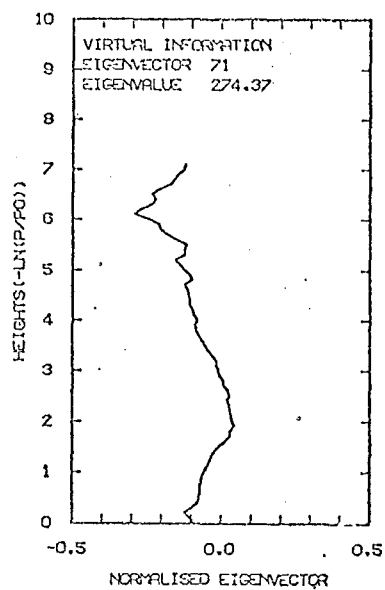
FIGURE 4.25 Retrieval profile confidence regions for the MAP estimator derived using the EXPT a priori covariance matrix and satellite noise variance  $0.01 \text{ mWm}^{-2} (\text{cm}^{-1})^{-1} \text{ s}^{-1}$ .

at the linearization wavenumber. From this diagram, the 95% confidence regions of the a priori covariance matrix about the first guess profile have a magnitude of approximately  $\pm 28\text{K}$  in the high stratosphere. However, below these heights the confidence regions are smaller, being approximately  $\pm 12\text{K}$ .

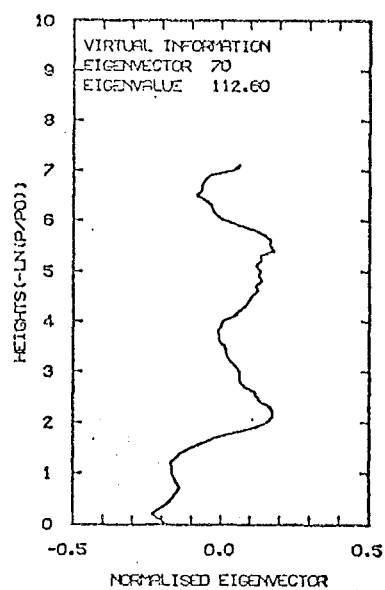
Similar calculations have been performed for the GC covariance matrix, about the first guess profile. These results are presented in fig. 4.22 where the confidence regions imply similar temperature deviations as in fig. 4.21. However, due to the ground correction procedure the GC matrix implies zero probability for any ground level temperature other than that of the first guess profile.

The 95% confidence regions have also been calculated for the MAP estimated retrieval profiles and covariance matrices. The results of the calculations are presented in fig. 4.23 where the a priori virtual data are the first guess profile and the NGC covariance matrix. A satellite noise variance of  $0.1 \text{ mWm}^{-2} (\text{cm}^{-1})^{-1} \text{ st}^{-1}$  has been used. Whereas in fig. 4.24, a satellite noise variance of  $0.01 \text{ mWm}^{-2} (\text{cm}^{-1})^{-1} \text{ st}^{-1}$  is assumed for a calculation using the same virtual observations as for fig. 4.23.

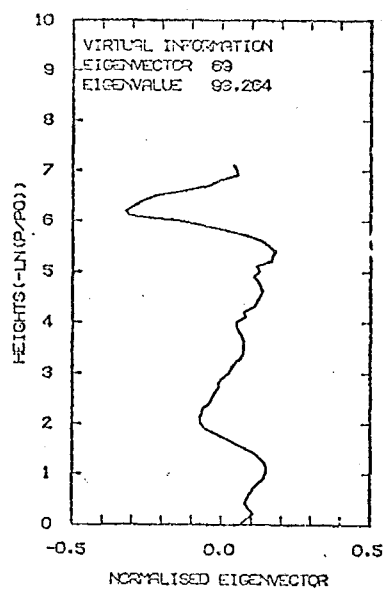
The confidence regions for the retrieval profile estimated using the EXPT covariance matrix and first guess profile are given in fig. 4.25. The satellite noise variance is  $0.01 \text{ mWm}^{-2} (\text{cm}^{-1})^{-1} \text{ st}^{-1}$ .



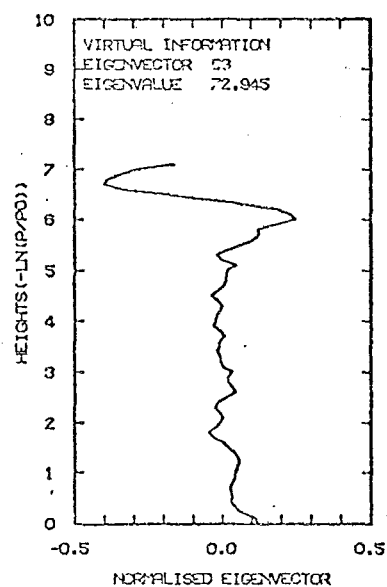
a



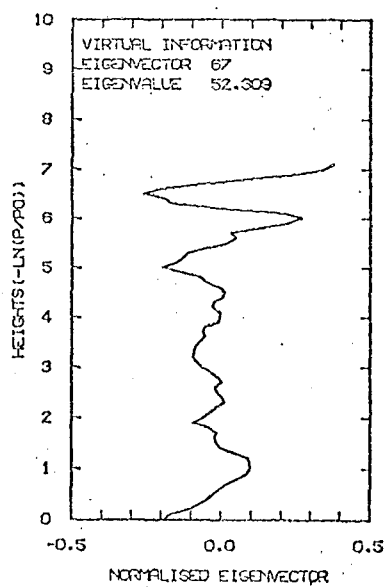
b



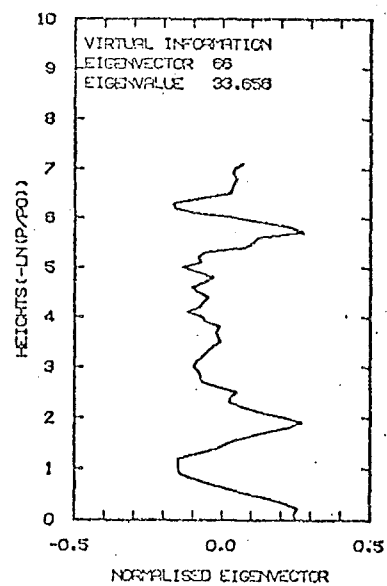
c



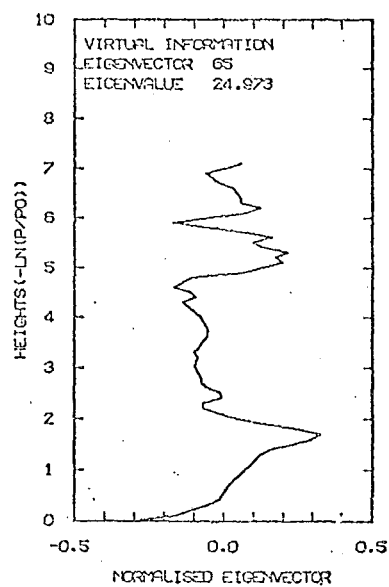
d



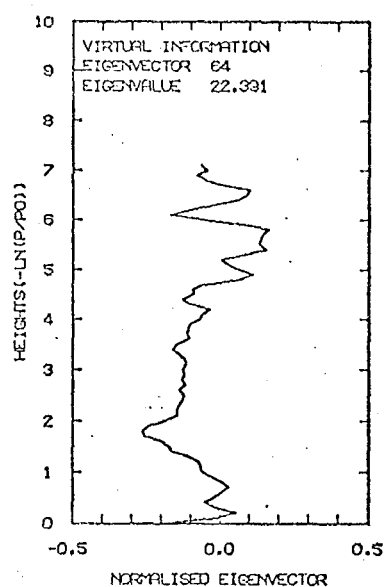
e



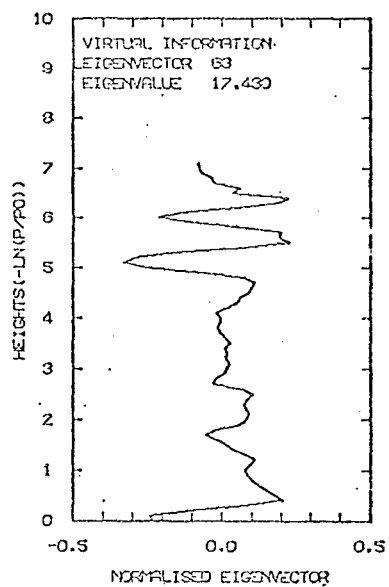
f



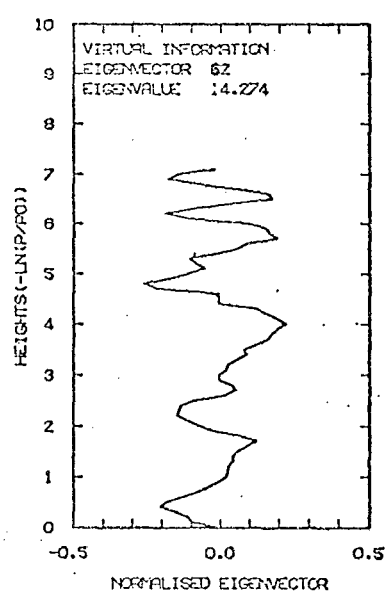
g



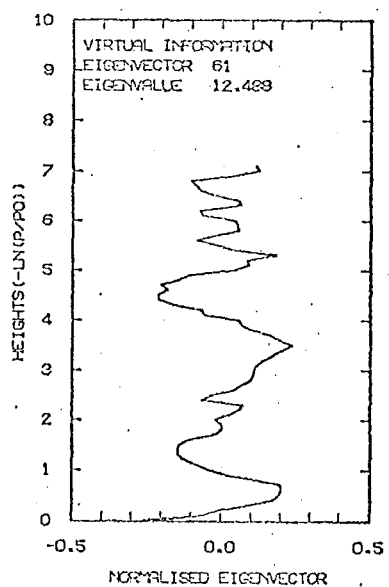
h



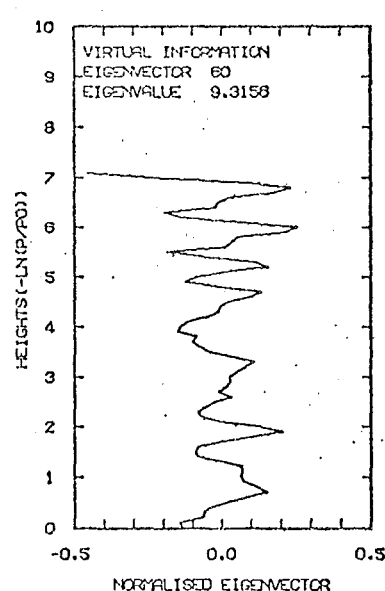
i



j



k



l

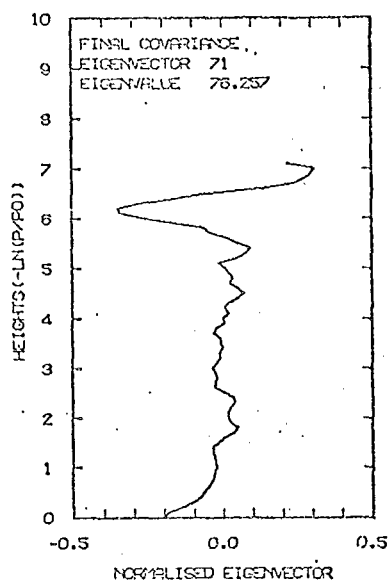
FIGURE 4.26 Eigenvectors for twelve largest eigenvalues of the NGC a priori matrix.

For fig. 4.23 the magnitude of the temperature deviation for the 95% confidence regions of the retrieval profile are of the order of  $\pm 24\text{K}$  at high stratosphere, stratopause heights, and approximately  $\pm 8\text{K}$  in the lower stratosphere and about  $\pm 12\text{K}$  in the troposphere. The results of fig. 4.24 are similar to those in fig.4.23, however the magnitude of the temperature deviation has been reduced by approximately  $2\text{K}$  over those for fig. 4.23, at most levels of discretization. For the case of fig. 4.25 the size of the confidence regions are similar to the two other cases, except in the stratosphere, where the magnitude of the temperature deviation is larger than in these cases, it being approximately  $\pm 12\text{K}$ .

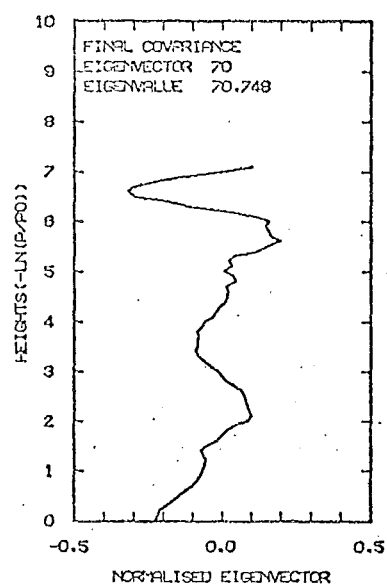
The results for the GC calculation show few deviations from those expressed in fig. 4.24 and are therefore not presented.

#### Eigenvectors and Eigenvalues of the Covariance Matrices

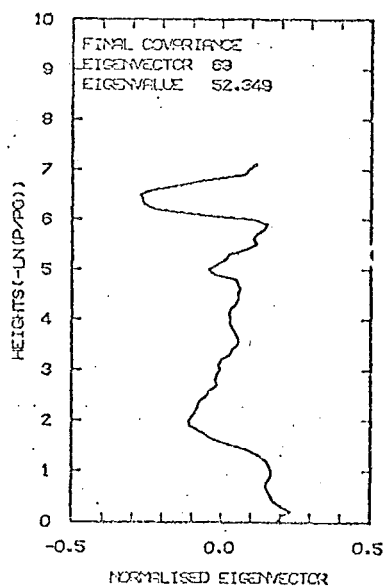
For each covariance matrix in the present study there are  $p(=72)$  eigenvectors and eigenvalues. The twelve eigenvectors corresponding to the twelve largest eigenvalues of the NGC a priori covariance matrix are presented in fig. 4.26. The corresponding set of eigenvectors and eigenvalues is given in fig.4.27 for the MAP estimated solution covariance matrix for satellite noise variance of  $0.01 \text{ mWm}^{-2} (\text{cm}^{-1})^{-1} \text{ st}^{-1}$ . The other sixty eigenvectors are not shown for reasons that will be given in the following section.



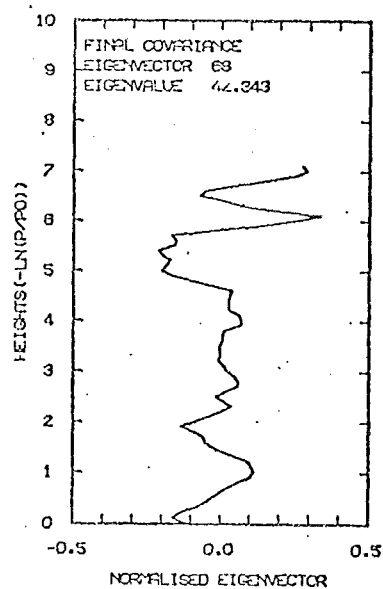
a



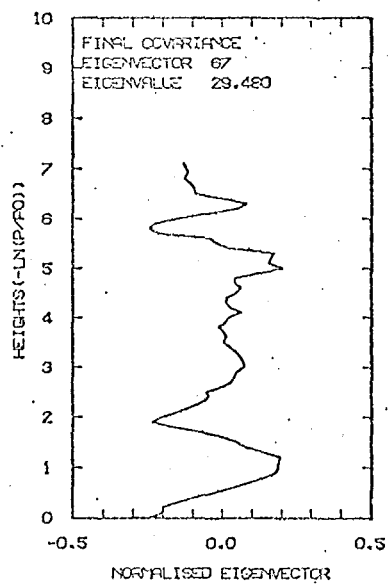
b



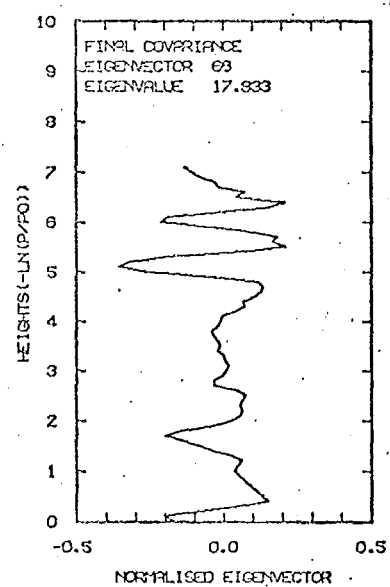
c



d

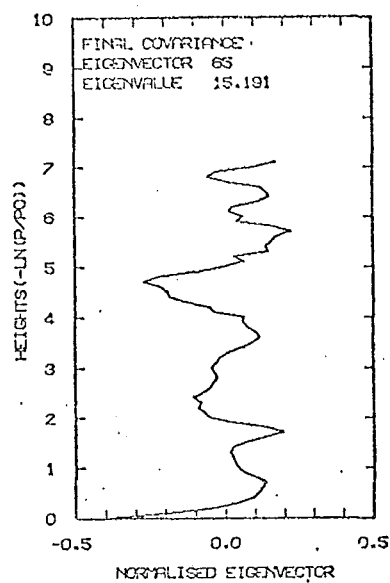


e

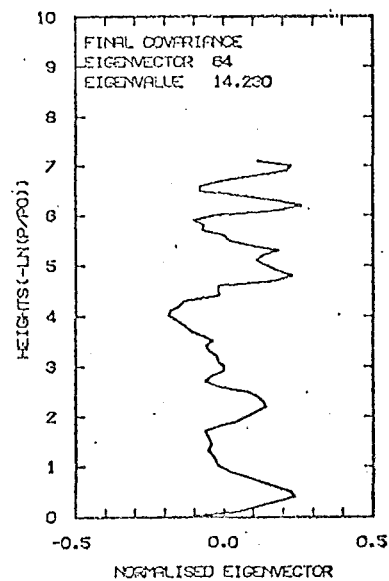


f

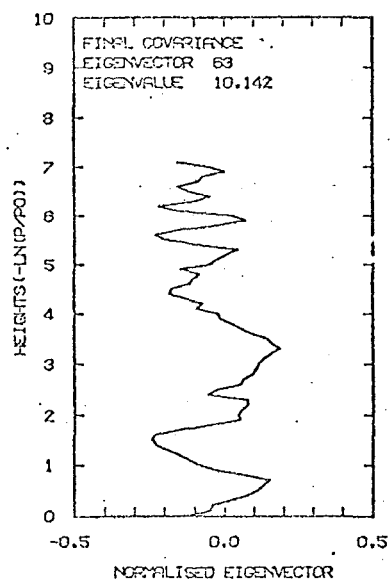




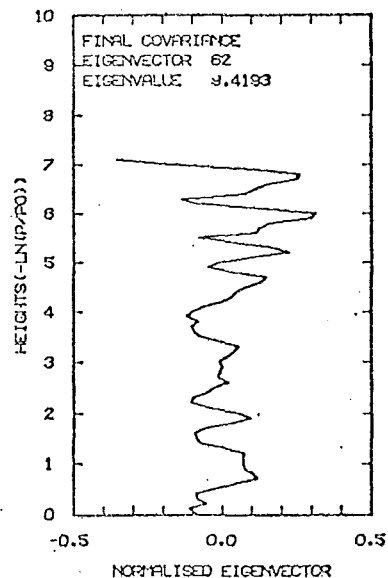
g



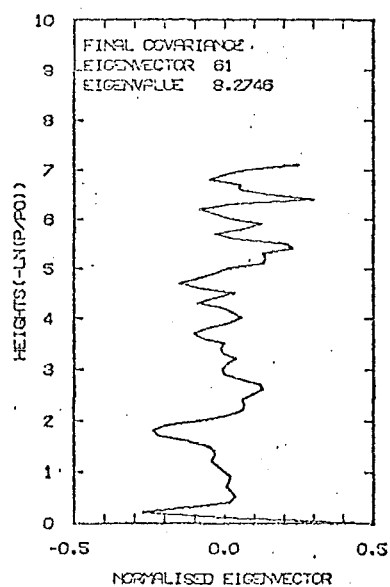
h



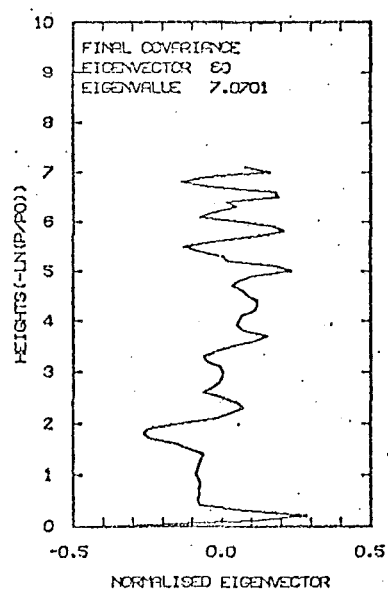
i



j



k



l

FIGURE 4.27 Eigenvectors for twelve largest eigenvalues of the retrieval covariance matrix for NGC MAP estimator.

#### 4.6.2. Discussion of Covariance Analysis Results

The confidence regions of the a priori covariance matrix as illustrated in fig. 4.21 indicate the variation of the atmospheric temperature with altitude for the given sample of temperature profiles making up the covariance matrix. The first guess profile and its covariance (the a priori data) is treated as a set of virtual observations by the MAP estimator. Clearly, the virtual observations constitutes a large set of rather "noisy" measurements.

As stated in section 3.3, these a priori observations act as a constraint on the solution profile by specifying (or setting limits on) unmeasured parameters of the retrieved temperature profile. Therefore with probability 0.95 all realistic temperature profiles will lie within the confidence regions of the first guess profile, that is, the error hyperellipsoid of the first guess profile. Consequently, the solution profile will lie within the a priori covariance hyperellipsoid with probability 0.95.

The MAP estimator is a random variable, and therefore, given the 95% confidence regions of the MAP estimated profile, there is probability 0.95 that the true profile lies within these regions.

Clearly the magnitude of the solution profile's confidence regions depend on the virtual observations

used in the MAP estimator.

Comparing the virtual observations constraints analysis of fig.4.21 with fig. 4.23, the MAP estimated solution covariance analysis. It is clear that on adding the satellite measurements to the virtual observations via the MAP estimator results in smaller confidence regions for the solution profile than for the a priori first guess profile, as is expected. The solution error hyperellipsoid is therefore smaller than the a priori covariance hyperellipsoid, and is contained within the latter. Further, on comparison of the NGC covariance analysis of fig. 4.21 with the solution covariance analysis for satellite noise variance of  $0.1 \text{ mWm}^{-2} (\text{cm}^{-1})^{-1} \text{ st}^{-1}$  in fig. 4.23 and the solution covariance analysis for satellite noise variance  $0.01 \text{ mWm}^{-2} (\text{cm}^{-1})^{-1} \text{ st}^{-1}$  in fig. 4.24. It may be observed that reducing the satellite noise in the MAP estimator also reduces magnitude of the confidence regions for the estimated solution profile.

If the confidence regions are regarded as a measure of the accuracy for the retrieved profile, then clearly all retrievals will be very poor and the first guess profile would be as good an estimate of the temperature structure as the MAP estimated profile. However, this is not the case, since the large confidence regions

arise because there are few satellite measurements compared with the number of parameters to be estimated. Therefore, the solution covariance (error hyperellipsoid) is large since it still contains much of the a priori atmospheric covariance.

The accuracy of the retrieval is better understood by examining the components of the vector  $\hat{\underline{x}} - \underline{x}_0$ . No component of this vector (except below 1 sh altitude) is larger than approximately  $\pm 8 \text{ mWm}^{-2} (\text{cm}^{-1})^{-1} \text{ st}^{-1}$ , corresponding to a temperature deviation of not more than  $\pm 5\text{K}$ . All components of this vector are much smaller than the solution confidence regions. Therefore, the accuracy of the retrieved profile is principally determined by the quality (accuracy) of the first guess profile. Since the MAP estimator in all cases studied does not cause large deviations in the estimated profile from the first guess profile.

However, the true temperature profile  $\underline{x}$  will with probability 0.95, lie within the confidence regions of the solution profile, as previously stated.

The confidence regions are more useful for another purpose. A single number measure of the amount by which the error ellipsoid has been decreased in volume by use of the MAP estimator and satellite observations may be derived by considering the volumes of the  $p$  dimensional hyperrectangles of the a priori and solution confidence regions.

The volumes of the hyperrectangles of figs. 4.21, 4.23 and 4.24 have been calculated and are presented in table 4.8 below:

TABLE 4.8 HYPER-RECTANGLE VOLUMES

COVARIANCE MATRIX FOR ANALYSIS	VOLUME ( $\text{mWm}^{-2}(\text{cm}^{-1})^{-1}\text{st}^{-1})^{7/2}$	RATIO OF VOLUMES
A priori	$5.12 \times 10^{89}$	1.0
$0.1 \text{ mWm}^{-2}(\text{cm}^{-1})^{-1}\text{st}^{-1}$ case	$9.35 \times 10^{79}$	$5.5 \times 10^9$
$0.01 \text{ mWm}^{-2}(\text{cm}^{-1})^{-1}\text{st}^{-1}$ case	$5.04 \times 10^{73}$	$1.0 \times 10^{16}$

The entries in the column labelled "ratio of volumes" are the ratios of the a priori volumes to the solution volumes. Therefore if "information content" of the satellite observations is regarded as a measure of the factor by which the uncertainty in the temperature profile is decreased by the act of measuring it, then the "ratio of volumes" may be used as a measure of the information content of the satellite observations. Clearly then, from the results of table 4.8, as the satellite noise is reduced the information content of the observations increases as is expected.

Alternatively, a better measure of the "information content" of the satellite measurements would be the ratio of the volumes of the actual error hyperellipsoids calculated by considering the determinants of the a priori covariance matrix and the solution estimate covariance matrix. However, in the case of nearly ill-conditioned covariance matrices, the determinants cannot be calculated accurately. Therefore, although there are errors in using the ratios of the volumes of the confidence regions, they do give an indication of the overall information content in the satellite measurements.

For all covariance matrices under study here, the relation

$$\frac{\lambda_P}{\lambda} \gg 1 \quad \dots (3.4.1.1)$$

is satisfied, therefore all are ill-conditioned (or nearly so) and therefore the values of the confidence regions have been used as a measure of information content of the satellite observation.

From equation (3.4.26) it is also to be expected that the essential shape of the confidence regions may be constructed from a small number of the eigenvectors of the covariance matrices. A representative set of eigenvectors have been given in figs. 4.26 and 4.27. Thus, on examination of these eigenvectors and equation (3.4.26) it is clear

that the confidence regions will be largest in the high-stratosphere and troposphere.

If the "total variance" of the population of profiles is defined as the sum of the variances of its individual components, that is, the trace of the matrix, then under a similarity transformation, the trace of a matrix is not changed and the "total variance" is just the sum of the eigenvalues. Therefore, the eigenvectors with the largest eigenvalues explain most of the total variance. See table 4.9.

TABLE 4.9 EIGENVALUES OF THE NGC COVARIANCE MATRIX

Eigenvector Number	Eigenvalue	Percent Variance	Cumulative Variance
72	274.34	34.2	34.2
71	112.60	14.1	48.3
70	98.26	12.3	60.6
69	72.95	9.1	69.7
68	52.31	6.5	76.4
67	33.65	4.2	80.4
66	24.97	3.1	83.5
65	22.39	2.8	86.3
64	17.43	2.2	88.5
63	14.27	1.8	90.3
62	12.49	1.6	91.9
61	9.32	1.2	93.1
60	8.13	1.0	94.1

For this case, ten eigenvalues account for more than 90% of the total variance. Consequently, the hyperellipse has been "stretched" along these principal axes (eigenvectors).

This same effect is also evident in the solution covariance matrix as it also, is ill-conditioned, as can be seen from table 4.10 below.

TABLE 4.10 EIGENVALUES OF THE SOLUTION COVARIANCE MATRIX FOR SATELLITE NOISE  $0.01 \text{ mWm}^{-2} (\text{cm}^{-1})^{-1} \text{st}^{-1}$  AND NGC A PRIORI DATA

Eigenvector Number	Eigenvalue	Percent Variance	Cumulative Variance
72	76.26	18.9	18.9
71	70.75	17.5	36.4
70	52.35	13.0	49.4
69	42.34	10.5	59.9
68	29.48	7.3	67.2
67	17.83	4.4	71.6
66	15.19	3.8	75.4
65	14.23	3.5	78.9
64	10.14	2.5	81.4
63	9.42	2.3	83.7
62	8.27	2.0	85.7
61	7.07	1.8	87.5
60	6.59	1.6	89.1

With only 12 eigenvalues, approximately 90% of the total variance is accounted for, again indicating the non hypersphericity of the hyperellipsoid.

A similar analysis can be carried out for the



solution covariance arising from using the EXPT data and satellite noise  $0.01 \text{ mWm}^{-2} (\text{cm}^{-1})^{-1} \text{st}^{-1}$ . When this is done it is found that the twelve largest eigenvalues account for only 44% of the total variance, and no one eigenvalue accounts for more than 8% of the total variance. Clearly the effects of ill conditioning are much less for this matrix than for the others used in this study.

The confidence regions for the MAP estimated profile using the EXPT a priori virtual measurements are given in fig. 4.25. Comparing fig. 4.25 with figs. 4.23 or 4.24 illustrates two major differences:-

- (i) The magnitude of the high stratosphere/stratopause confidence regions are smaller in fig. 4.25, and
- (ii) The magnitude of the lower stratosphere/troposphere confidence regions are approximately the same for fig. 4.25 but rather different in the other figures.

Thus the hyperellipsoid is more hyperspherical for the EXPT case since the covariance matrix is less well correlated (ill conditioned) than in the other cases discussed in this study.

The set of eigenvectors for either the a priori covariance matrix or the MAP estimated solution covariance matrix may also be used as a basis set for a representation of the solution profile having the form:

$$\hat{\underline{x}} = \sum_{i=1}^n a_i \underline{\ell}_i$$

where

$\underline{x}$  is the solution profile vector, the  
 $\underline{l}_i$  are the basis vectors and the  
 $a_i$  are projection coefficients.

If  $n \ll p$ , then this is an efficient representation of the temperature profile vector. However, for the solution profiles calculated in this simulation study and for the given sets of basis vectors (i.e. the sets of eigenvectors for the NGC, GC, EXPT and all solution covariance matrices) it has been found that this representation is not efficient. The integer  $n$  is always of the order  $p$  for a correct specification of the vector  $\hat{\underline{x}}$ , where for a correct specification, the difference between the solution profile  $\hat{\underline{x}}$  and the profile generated by this representation must be less than one tenth of the magnitude of the confidence regions at all levels of discretization.

#### 4.6.3 Summary of Discussion of Covariance Analysis

Where there are highly correlated and therefore nearly ill-conditioned covariance matrices the magnitudes of the confidence regions at some levels of discretization are large compared to other levels. Further, only a small number of the largest eigen values and corresponding eigenvectors are important in determining the confidence regions of the estimated solution profile. Similarly, only a small number of eigenvalues are necessary to account for a large percentage of the "total variance".

For covariance matrices that are less well correlated the confidence regions for the solution profile do not show such large variations in magnitude with altitude. Correspondingly a larger number of eigenvectors and eigenvalues are needed in order to calculate the confidence regions of the solution profile, and to account for a large percentage of the total variance.

The ratio of the volumes of the confidence regions of the virtual data and the solution profile is useful as an overall measure of the information content of the satellite measurements.

The use of the eigenvectors of the a priori or solution covariance matrices as a basis set for the representation of the solution profile, is not efficient in all cases of this simulation study.

The quality (accuracy) of the first guess profile is the main factor in determining the accuracy of the MAP estimated retrieval profile.

#### 4.7 CONCLUSIONS FOR SIMULATION STUDY

From the results and discussions of previous sections in this chapter, the following conclusions have been drawn.

The Backus and Gilbert diagnostics, as derived in section 3.5, are valuable in determining the quality of the a priori data. In particular, the following conclusions have been deduced:-

- (i) The a priori covariance matrix is important in determining the vertical resolution of the MAP estimated retrieval profile.
- (ii) An a priori matrix that has highly correlated entries will have poor vertical resolution at the corresponding heights.
- (iii) At heights where there is a lack of "intrinsic information" (defined in section 3.5) in the a priori data, poor vertical resolution in the retrieval will result.
- (iv) Increasing satellite noise decreases the vertical resolution of the retrieved profile.
- (v) Vertical resolution of the retrieved profiles may be better, or worse, than the resolution of the satellite weighting functions, depending on the quality of the a priori data, as stated in (i) above.
- (vi) The precision and error magnification for the retrieved profile are easily determined.

- (vii) Strong sidebands in the averaging kernels are a result of strong off diagonal covariances in the covariance matrix.

The covariance analysis developed in section 3.4 has also proved to be useful in understanding some characteristics of the MAP estimated retrieval profile. The following deductions have resulted:-

- (viii) For near ill-conditioned matrices, the confidence regions may in general be determined from a small number of the eigenvectors and eigenvalues.
- (ix) A measure of the information content of the satellite observations may be derived by examining the volumes of the confidence regions for the a priori and solution covariance matrices.
- (x) The accuracy of the first guess profile is the main factor in determining the absolute accuracy of the estimated retrieval profile.

Finally, the retrieval results of section 4.5 indicate:-

- (xi) Choosing the wrong linearization wavenumber introduces an altitude dependent systematic error in the solution.
- (xii) Increasing the satellite noise constrains the retrieval solution to be closer to the a priori first guess profile.

(xiii) From the simulation results, retrieval accuracy has been found to be best in the mid troposphere to mid stratosphere altitude range. However, it may be poorer by a factor of two above these heights, depending on point (x) above.

(xiv) Large weighting in the averaging kernels at levels not near the analysis level will introduce errors into the solution profile at some levels. These errors may be predicted a priori in some cases.

## APPENDIX I

NIMBUS IV . . . . . SCR . . . . . WEIGHTING FUNCTIONS

In this work the weighting functions are represented by the analytic functions given below.

The height variable,  $Z$ , is expressed as :-

$$Z = - \ln(p/p_0)$$

where  $p$  and  $p_0$  are as already defined.

Channel A

$$y(Z) = \exp-[a_1 + a_2 (Z-a_6) + a_3 (Z-a_6)^2 + a_4 (Z-a_6)^3 + a_5 (Z-a_6)^4] + a_7 \exp-[a_8 (Z-a_9)^2]$$

Channel B

Two separate functions are required for a suitably accurate fit to the discretized data points:-

(i) for  $Z \leq 5.4$

$$y(Z) = \exp-[a_1 + a_2 (Z-a_6) + a_3 (Z-a_6)^2] \times (a_4 Z + a_5 Z^2)$$

(ii) For  $Z \geq 5.4$

$$y(Z) = a_7 \exp-[a_8 (Z-a_9)^2]$$

Channel C

$$y(Z) = \exp-[a_1 + a_2 (Z-a_6) + a_3 (Z-a_6)^2 + a_4 (Z-a_6)^3 + a_5 (Z-a_6)^4] \times (a_7 + a_8 Z + a_9 Z^2)$$

Channel D

$$y(Z) = \exp-[a_1 + a_2(Z-a_6) + a_3(Z-a_6)^2 + a_4(Z-a_6)^3 + a_5(Z-a_6)^4] \times (a_7 + a_8Z + a_9Z^2).$$

Channel E

$$y(Z) = \exp-[a_1 + a_2(Z-a_6) + a_3(Z-a_6)^2 + a_4(Z-a_6)^3 + a_5(Z-a_6)^4] \times (a_7 + a_8Z + a_9Z^2)$$

Channel F

Two separate functions are required for a suitably accurate fit to the discretized data points:-

(i) For  $Z \geq 0.17$

$$y(Z) = \exp-[a_1 + a_2(Z-a_6) + a_3(Z-a_6)^2 + a_4(Z-a_6)^3 + a_5(Z-a_6)^4] + a_7 \exp-[a_8(Z-a_9)^2]$$

(ii) For  $Z \leq 0.17$

$$y(Z) = -0.6429 Z + 0.2363.$$

The coefficients  $a_i$ ,  $i = 1, 2, \dots, 6$  are given in table 1.1 below:



TABLE 1.1

	Channel	Channel	Channel	Channel	Channel	Channel
	A	B	C	D	E	F
$a_1$	2.977567	4.130931	1.825558	3.014476	2.540197	1.919749
$a_2$	0.030070	0.081956	0.135437	-0.253694	0.504519	0.139179
$a_3$	0.612385	0.425562	0.665981	1.066743	1.340218	1.551304
$a_4$	-0.203292	1.193764	-0.215337	-0.266736	-0.755421	-0.590243
$a_5$	0.027237	-0.023867	0.028406	0.022430	0.159017	0.061235
$a_6$	6.396557	4.159521	2.569883	2.055876	1.376097	0.200756
$a_7$	0.029149	48.052378	-0.588145	-1.165643	-0.335004	0.003193
$a_8$	0.427481	0.035406	0.316914	1.429447	1.342166	4.100470
$a_9$	5.133507	-8.592527	-0.502054	-0.026566	-0.021751	3.350990

## APPENDIX 2

MATRIX INVERSION LEMMA

Let  $A$  be  $p \times m$  and  $B$  be  $m \times p$  matrices and let  $I_m$  be the  $m \times m$  identity matrix.

Then

$$-A(I_m + BA) = -(I_p + AB)A \quad \dots (2.1)$$

$$\therefore -A(I_m + BA)(I_m + BA)^{-1} = -(I_p + AB)A(I_m + BA)^{-1} \quad \dots (2.2)$$

$$-AB = -(I_p + AB)A(I_m + BA)^{-1}B \quad \dots (2.3)$$

$$\text{and } I_p = I_p + AB - AB \quad \dots (2.4)$$

$$\therefore I_p = (I_p + AB) - (I_p + AB)A(I_m + BA)^{-1}B \quad \dots (2.5)$$

Premultiplying equation (2.5) by  $(I_p + AB)^{-1}$  gives

$$(I_p + AB)^{-1} = I_p - A(I_m + BA)^{-1}B \quad \dots (2.6)$$

If  $\hat{S}_{MAP}$  is defined to be

$$\begin{aligned} \hat{S}_{MAP} &\equiv (K^T S_\epsilon K + S_x^{-1})^{-1} \\ &= (S_x K^T S_\epsilon K + I_p)^{-1} S_x \end{aligned} \quad \dots (2.7)$$

and if  $\hat{S}_{MAP}$  is chosen to be  $(I_p + AB)^{-1}S_x$  then from equation (2.6) and (2.7)

$$A = S_x K^T S_\epsilon \quad \dots (2.8)$$

$$\text{and } B = K \quad \dots (2.9)$$

the following equation arises

$$\hat{S}_{MAP} = [I - S_x K^T S_\epsilon (I + K S_x K^T S_\epsilon)^{-1} K] S_x \quad \dots (2.10)$$

therefore

$$\hat{S}_{\text{MAP}} = S_x - S_x K^T (K S_x K^T + S_\epsilon)^{-1} K S_x \quad \dots (2.11)$$

This equation is the matrix inversion lemma.

By a suitable matrix multiplication equation (2.1) may be rewritten thus:-

$$(I_p + AB)^{-1} A = A(I_m + BA)^{-1}$$

If the substitutions of equations (2.7), (2.8) and (2.9) are applied, the following result occurs:-

$$\hat{S}_{\text{MAP}} K^T S_\epsilon = S_x K^T (K S_x K^T + S_\epsilon)^{-1} \quad \dots (2.12)$$

## APPENDIX 3

## A PRIORI COVARIANCE MATRICES

## (i) The NGC Covariance Matrix.

	71	70	69	68	67	66	65	64	63
71	17.27478	16.22573	13.24240	9.83206	7.61915	5.69110	3.39596	2.62703	2.25396
70	16.22573	19.18861	17.12511	14.23911	11.77558	9.09043	5.70215	3.55225	1.63191
69	13.24240	17.12511	19.75092	18.17239	15.69563	12.65910	9.23334	6.21314	3.46165
68	9.83206	14.23911	18.17239	20.23278	19.63146	17.75197	14.30006	10.15879	6.80953
67	7.61915	11.77558	15.69563	19.63146	22.03503	21.84450	18.79743	13.75406	9.67961
66	5.69110	9.09043	12.65910	17.75197	21.84450	26.10963	24.85555	19.54975	16.20876
65	3.39596	5.70215	9.23334	14.30006	18.79943	24.85555	28.66065	24.66072	21.63527
64	2.62703	3.55225	6.21314	10.15879	13.75406	19.54975	24.66072	25.37306	24.02450
63	2.25396	1.63191	3.46165	6.80953	9.67961	16.20876	21.63527	24.02450	27.92662
62	5.39059	3.53745	4.53726	6.71054	8.32288	14.53539	20.08235	22.91042	29.35033
61	9.4.334	7.70306	7.56610	8.10863	7.96714	12.03364	18.58450	22.01883	26.61619
60	9.11484	7.18230	6.68405	5.58622	4.83187	6.92515	12.10332	14.26178	17.37618
59	8.58911	6.63793	6.12144	5.11677	4.57030	6.27936	9.41471	10.66607	11.95282
58	8.74046	7.44045	6.23442	5.30116	5.16011	7.63182	9.04736	9.29753	10.08690
57	6.41770	5.01610	3.68370	3.30851	3.63787	6.20791	7.62820	7.53439	7.85469
56	6.17475	4.63410	3.44326	2.68642	2.35052	3.78121	3.89997	4.22643	5.05276
55	5.62737	4.40759	2.82807	2.13563	1.94419	2.32276	1.83384	2.60210	2.79281
54	5.46442	4.72630	3.46795	3.28090	3.63504	3.04716	2.59569	2.44829	2.55317
53	4.10607	4.07534	4.11720	4.13274	5.15721	5.76792	4.17922	3.54634	3.73423
52	4.36281	4.59492	5.05725	5.03447	6.05167	6.89869	6.37684	4.58551	5.16160
51	3.01386	2.96569	2.74093	2.64461	3.81577	5.42050	6.91017	5.22258	5.93251
50	1.61331	2.18174	2.19127	2.44799	3.84926	5.49066	6.20610	4.71713	5.50937
49	1.84189	2.65198	2.33091	2.74997	3.36616	4.62515	4.42695	3.96479	5.16205
48	2.42650	3.23395	3.07322	2.82701	2.73389	2.88092	2.33251	2.18256	3.05993
47	3.11173	4.31367	4.90417	4.70878	4.42782	4.52400	4.07606	3.72351	4.42583
46	4.09608	4.53073	5.19427	4.64575	4.09023	4.09172	2.79091	2.50115	3.25792
45	5.20360	5.21261	5.67919	4.93907	4.51150	4.63782	3.28095	2.99259	3.02495
44	4.83763	4.96572	4.98207	4.44143	4.21276	4.31685	3.44076	2.84392	3.14573
43	3.58718	3.62998	3.77634	3.80018	4.08651	4.50401	3.93865	3.02681	3.67732
42	3.16276	3.29223	3.28516	3.49779	4.06179	4.86132	4.55162	3.68068	3.84559
41	3.77531	3.89848	3.93054	3.93362	4.24698	4.63120	4.12492	3.37007	3.85490
40	3.36471	3.21171	3.41604	3.51332	4.04735	4.67687	4.57291	3.56525	3.57820
39	3.65104	3.62435	4.04860	4.09174	4.51096	5.09455	4.87814	3.91859	4.09507
38	2.26225	2.31972	3.04303	3.34744	4.14230	4.91942	4.84281	3.66445	4.29359
37	1.70495	1.85413	2.37426	2.28164	3.07014	4.04090	3.89841	2.96953	3.74913
36	1.81805	2.00809	2.73871	2.50125	2.99925	3.46946	3.25007	2.40711	2.86754
35	1.47333	1.34952	2.05250	1.73258	2.30618	2.38377	2.34165	1.89692	2.03952
34	0.47600	0.72842	1.65309	1.72675	2.25081	2.70340	2.03758	1.41934	1.45041
33	-0.76591	-0.11129	0.83344	1.11481	1.46519	1.09041	1.27199	0.83108	0.76255
32	-0.95149	-0.49301	-0.15658	0.24186	0.79227	0.61974	0.77468	0.71384	0.53767
31	-1.00424	-0.46205	-0.47495	-0.14543	0.21986	0.32611	0.54234	0.72019	0.92961
30	-1.07401	-0.92470	-1.07963	-1.10473	-0.99844	-0.67833	-0.55563	0.01462	0.75519
29	-0.50834	-0.40265	-0.60590	-0.66622	-0.75444	-0.73580	-0.64152	-0.09436	0.77410
28	-0.30714	-0.52545	-1.05567	-1.20631	-1.34467	-1.38360	-1.38964	-0.71763	0.90240
27	-0.01299	-0.56460	-1.37228	-1.67332	-1.85073	-1.94612	-1.91998	-0.86090	-0.12036
26	-0.84984	-1.81512	-2.75080	-2.92152	-2.83741	-2.93678	-2.67815	-1.17117	-0.66563
25	-0.12344	-0.83853	-2.01763	-2.18749	-2.22182	-2.40610	-2.40381	-1.18326	-1.06556
24	0.59666	0.49217	-0.91823	-1.16671	-1.38198	-1.80032	-2.02168	-0.96244	-0.80275
23	1.03440	1.04752	-0.83098	-1.48600	-1.78565	-2.01254	-2.31184	-1.07934	-0.51962
22	0.40433	0.26561	-1.67988	-2.12333	-2.29067	-2.36649	-2.40826	-1.10167	-0.69761
21	-0.42913	-0.72988	-2.47063	-2.43468	-2.40178	-2.24853	-2.28939	-1.13715	-0.76179
20	-1.31337	-1.53817	-2.54849	-1.95200	-1.94968	-2.00071	-1.97813	-1.37999	-1.42947
19	-1.98930	-2.14867	-2.15413	-1.17261	-1.19045	-1.38352	-1.42531	-1.49313	-1.66146
18	-0.15493	-0.31371	-0.39528	0.30609	0.03311	-0.27532	-0.71702	-1.77665	-2.13716
17	0.16086	-0.27524	-0.68138	-0.30918	-0.47165	-0.75299	-1.19166	-2.67483	-2.99442
16	-0.10193	-0.66209	-0.86070	-0.52096	-0.40145	-0.58836	-0.58672	-1.44996	-1.74042
15	-0.03791	-0.45279	0.05315	0.29343	0.19779	-0.06473	0.02542	-0.57148	-0.65024
14	0.13168	-0.15872	0.79921	0.53234	0.50815	-0.01218	-0.04760	-0.56044	-0.67900
13	0.35475	0.21461	1.36784	0.71922	0.37735	-0.32970	-0.68285	-0.77541	-0.63737
12	0.98231	1.06315	2.39655	1.31899	0.44411	-0.45450	-1.00447	-0.57272	-0.36729
11	1.52482	1.66046	3.03824	1.69211	0.99473	0.03598	-0.53803	-0.16396	0.12301
10	2.06744	2.25686	3.67915	2.46500	1.54615	0.52754	-0.07078	0.24535	0.60961
9	2.13450	2.41459	3.85404	2.48538	1.91377	1.10724	0.66534	0.99344	1.32014
8	1.67594	2.08172	3.60639	2.74909	2.35196	1.95521	1.75165	1.83062	1.80449
7	1.29193	1.80127	3.40759	2.65958	2.77935	2.75403	2.77943	2.59712	2.25804
6	1.19589	1.68810	3.37775	3.01972	2.99672	3.20371	3.46974	3.27539	2.89463
5	1.09822	1.58558	3.37687	3.18297	3.20284	3.64080	4.15085	3.94857	3.51549
4	1.02405	1.51739	3.36769	3.34951	3.41396	4.01551	4.68091	4.33917	3.73945
3	0.77138	1.34455	3.64788	3.94396	4.35210	5.27691	6.16209	4.68398	4.44709
2	0.29930	0.89392	3.97114	4.73272	5.65236	6.96844	8.00044	5.10553	5.62165
1	-1.23538	-1.28794	1.41846	2.62746	3.86063	5.35078	7.13440	4.66761	5.26772
0	-1.76023	-3.03850	0.77800	1.91129	3.19685	4.08562	6.63425	5.63958	4.38698

\* The indices 71, 70, ..., 0 refer to the levels of discretization. The matrix elements referred to in the text are numbered conventionally from 0, 1, ..., 71. Therefore in order to obtain a matrix element,  $S_{ij}$ , in terms of the indices given, use the following relations :-

$$S_{ij} = \text{NGC/GC}(71-i, 71-j).$$

	62	61	60	59	58	57	56	55	54
71	5.39059	9.46364	9.11484	8.58911	8.74046	6.41770	6.17475	5.62737	5.46442
70	3.53745	7.70306	7.18230	6.83793	7.44045	5.01610	4.63410	4.40759	4.72230
69	4.53726	7.56610	6.68405	6.12144	6.23442	3.68370	3.44326	2.82807	3.46795
68	6.71854	8.10863	5.53622	5.11677	5.30116	3.30851	2.68642	2.13563	3.28090
67	8.32288	7.96014	4.85187	4.57030	5.16011	3.63787	2.35052	1.94419	3.63504
66	14.53539	12.03364	6.92515	6.27966	7.63182	6.20791	3.78121	2.32276	3.84716
65	20.88835	18.58450	12.10332	9.41431	9.04736	7.62820	3.89997	1.85324	2.57969
64	23.91042	22.01803	14.26178	10.64607	9.29753	7.58430	4.22641	2.60210	2.64829
63	29.12033	26.61619	17.37018	11.95232	10.06690	7.86469	5.05276	2.79281	2.52317
62	35.61792	35.94365	24.79352	17.22335	13.43791	10.15254	7.30874	3.57725	2.66327
61	35.94365	41.62133	31.94649	22.95112	17.12437	12.51343	9.10178	4.67351	3.43437
60	24.79352	31.94649	29.90824	23.05482	17.85747	13.61812	10.26603	6.11309	4.94591
59	17.22035	22.95412	23.05482	21.31175	17.80253	14.18389	11.09945	7.52151	6.52917
58	13.43791	17.12437	17.65007	17.80253	18.93398	17.17272	13.58734	10.79038	10.27759
57	10.15254	12.51343	13.61812	14.10389	17.17272	18.99446	15.51837	12.60504	11.21923
56	7.30874	9.10178	10.26603	11.09945	13.58734	15.51837	15.92926	13.12924	12.03824
55	3.57725	4.67351	6.11309	7.52151	10.79038	12.60504	13.12924	13.57154	12.25726
54	2.66327	3.43437	4.94591	6.52917	10.27759	11.33923	12.03824	12.25726	14.26962
53	3.82387	3.95458	4.50755	4.95035	7.30034	8.55319	9.41588	8.79571	11.69725
52	6.17543	6.90234	7.34610	6.90704	8.62508	9.27950	9.91906	8.42601	11.24768
51	7.28775	7.66970	7.24354	6.61945	7.99624	8.94430	8.79204	7.00005	8.17656
50	5.89147	4.77224	4.28334	4.11241	6.20992	7.54643	8.18741	6.84950	8.33842
49	5.42141	4.28408	3.58574	4.07990	6.23219	7.40765	8.16436	7.47625	8.17656
48	3.62179	3.32539	3.70550	4.78431	6.53929	7.36362	8.00274	7.74034	7.68776
47	5.56768	5.85613	5.87993	6.29446	7.65904	8.45096	8.35505	7.43543	7.57945
46	3.32667	4.61647	5.35021	6.00845	7.06194	7.69087	8.06302	6.87421	7.51499
45	3.66556	4.29767	4.66354	5.56387	6.91731	7.21636	7.47912	6.22242	7.07167
44	4.07941	4.92324	5.12590	5.74894	6.84728	7.16430	7.04306	5.96898	6.63939
43	4.39278	5.12742	5.43268	5.88654	6.86978	7.18318	6.49398	5.71644	6.15551
42	4.35618	5.02105	4.96515	5.25740	5.88650	5.84712	5.30425	4.73775	5.09637
41	4.27263	4.94493	4.81702	4.68662	5.40793	4.79016	4.77623	4.55979	4.63051
40	3.75747	4.33354	4.34042	4.16080	4.25753	3.52552	3.16143	3.09378	3.01879
39	4.43520	4.81907	4.74369	4.26027	4.34248	3.71734	3.33763	3.24148	3.12667
38	4.25094	4.37234	4.54764	4.05714	4.36642	4.20158	3.33053	3.09869	3.25340
37	3.49106	3.43764	3.72357	3.44476	3.99781	4.08305	3.20981	2.70734	2.63060
36	2.20229	2.09588	2.59668	2.35429	3.21947	3.50768	2.81614	2.63129	2.70492
35	1.21917	0.99175	1.50806	1.79601	2.42831	3.02354	2.34366	2.55949	2.75447
34	0.54112	0.29774	0.71679	1.19824	1.53303	2.09205	1.81270	2.02232	2.43546
33	-0.22292	-0.35782	0.23621	0.51956	0.69433	1.26048	1.24630	1.65171	2.10724
32	-0.37849	-0.68419	-0.52773	-0.19036	0.00567	0.34616	0.42217	1.21197	1.77362
31	0.20849	-0.01474	-0.14224	0.06623	0.09519	0.45662	0.66242	1.18525	1.55768
30	0.61516	0.50134	0.18038	0.32736	0.09481	0.55057	1.07314	1.26343	1.31732
29	0.70319	0.20886	0.49827	0.58305	0.12569	0.16042	0.73167	0.75985	0.72466
28	0.06870	0.36545	0.19636	0.23501	-0.29117	-0.47724	-0.08307	0.13378	0.07589
27	0.05214	0.57595	0.58759	0.70708	0.12673	-0.03340	0.35518	0.74183	0.39338
26	-0.72725	-0.71001	-0.51453	-0.11815	-0.23078	0.45827	0.72167	0.96366	0.66320
25	-1.20672	-1.37871	-1.36043	-0.68976	-0.24756	0.70949	0.93631	1.18700	0.82906
24	-0.87430	-0.65559	-1.30064	-0.77234	-0.30331	0.43161	0.91910	1.15482	0.92952
23	-0.62976	-0.84893	-1.20190	-0.52536	0.07356	0.25154	0.58570	0.95869	1.01124
22	-0.60381	-1.04416	-1.50164	-0.81077	0.27732	0.73420	0.67737	1.14425	1.31288
21	-0.63166	-1.16193	-1.59059	-0.46766	0.56827	1.27498	1.00079	1.16413	1.37029
20	-1.51153	-1.80796	-2.14912	-1.01983	0.25009	1.33775	0.74676	0.67310	1.14633
19	-2.39831	-3.03570	-3.22504	-2.20704	-0.54408	1.05309	0.04531	-0.04568	0.60350
18	-2.33667	-2.47912	-2.36253	-2.53961	-1.12969	0.57122	0.01350	-0.34106	-0.24733
17	-2.49725	-2.49115	-2.30420	-3.36338	-2.41846	-0.76231	-0.52322	-0.77391	-1.29334
16	-1.27445	-1.27698	-1.58444	-2.63514	-2.08471	-0.57116	-0.10101	-0.43833	-0.44727
15	-0.39026	-0.30447	-0.54424	-1.64920	-1.5791	-0.36806	0.27729	0.07725	-0.11175
14	0.08061	0.41155	0.53201	-0.69202	-1.02210	-0.14231	0.58929	0.38981	0.04755
13	0.25819	0.81793	1.17215	0.04712	-0.45063	-0.10516	0.71641	0.55227	0.02546
12	0.85363	1.72601	2.02171	0.74931	0.09467	-0.02008	0.84445	0.57099	0.10693
11	1.27630	2.25711	2.64962	1.33716	0.72069	0.34465	1.05895	0.79988	0.42432
10	1.69973	2.78713	3.27638	1.92675	1.34723	0.70860	1.27493	1.02929	0.74725
9	2.24039	3.15530	3.69047	2.39774	1.91544	1.16230	1.63573	1.24787	1.06136
8	2.49839	3.04805	3.71103	2.59301	2.25550	1.65540	1.95167	1.25404	1.24698
7	2.76579	2.98382	3.70775	2.72646	2.51684	2.08124	2.14825	1.22077	1.33333
6	3.24163	3.24248	3.55653	2.78089	2.69684	2.37517	1.96054	1.28715	1.20983
5	3.70693	3.48983	3.39019	2.81434	2.87115	2.67979	1.79542	1.34738	1.08430
4	3.71480	3.36363	3.06468	2.83026	3.04984	2.93934	1.49737	1.36861	0.87287
3	4.71462	4.64562	4.79264	4.29969	4.39308	4.01329	1.82153	1.46251	1.24346
2	6.37100	6.56974	7.25893	6.34502	6.14739	5.35835	2.76851	1.52467	1.87311
1	6.05625	6.13692	6.50335	5.50017	4.60582	4.00812	1.46365	0.80468	1.30112
0	5.14240	5.44493	5.75375	5.12188	3.61033	2.82797	0.55238	0.65859	0.27229

	53	52	51	50	49	48	47	46	45
71	4.10607	4.36281	3.01386	1.81331	1.84199	2.42650	3.11173	4.09608	5.20360
70	4.07534	4.59492	2.96549	2.18174	2.65198	3.23395	4.31367	4.53073	5.21261
69	4.11720	5.05725	2.74093	2.19127	2.33091	3.07322	4.90417	5.19427	5.67919
68	4.13274	5.03447	2.64481	2.44799	2.74997	2.82701	4.70978	4.64575	4.93987
67	5.19721	6.05167	3.81577	3.84926	3.30616	2.73389	4.42782	4.09023	4.51150
66	5.76792	6.98969	5.42050	5.49066	4.62515	2.85092	4.52400	4.07172	4.63762
65	4.17922	6.37684	6.91017	6.20610	4.42895	2.33251	4.07606	2.79091	3.28095
64	3.54034	4.98551	5.62258	4.71713	3.96479	2.18856	3.72235	2.50115	2.89258
63	3.73423	5.16180	5.93251	5.50937	5.16205	3.05993	4.42583	3.20792	3.02495
62	3.82387	6.17543	7.28775	5.89147	5.42141	3.62178	5.56768	3.60667	3.66556
61	3.95419	6.80234	7.66970	4.77224	4.28408	2.32539	5.85613	4.61647	4.29767
60	4.50755	7.34610	7.24354	4.28334	3.58114	3.70550	3.87993	5.35021	4.66354
59	4.95035	6.87704	6.61945	4.11241	4.07990	4.78431	6.29446	6.00845	5.56367
58	7.30034	8.62508	7.99624	6.20992	6.23219	6.53929	7.60904	7.06194	6.91731
57	8.55319	9.27950	8.94420	7.54643	7.40765	7.36362	8.45096	7.69087	7.21426
56	9.41563	9.91006	8.79204	6.16741	8.16436	8.06724	8.35505	8.06382	7.47912
55	8.70291	8.42601	7.00005	6.84950	7.49625	7.74034	7.43548	6.87421	6.22542
54	11.68725	11.24768	8.92836	6.85842	8.17856	7.96976	7.57945	7.51498	7.07167
53	13.93268	13.59551	10.70369	10.53964	8.33037	6.90266	6.99993	7.09083	6.41650
52	13.59551	15.57393	13.19646	12.50751	9.40589	7.95642	8.64923	8.04749	7.74906
51	10.70369	13.19646	14.00799	12.51196	8.79802	6.46263	7.11497	5.85135	5.89150
50	10.53986	12.50751	12.51196	13.09568	9.67970	7.72134	7.75834	6.50942	6.08136
49	8.33037	9.40589	8.79802	9.87970	9.70466	8.11447	7.78188	6.13538	5.39224
48	6.90266	7.95642	6.46263	7.72134	8.11449	9.58942	9.44253	7.24921	6.14541
47	6.99993	8.64923	7.11497	7.75834	7.78188	9.44253	10.68947	9.02549	7.80574
46	7.09083	8.04749	5.85135	6.50942	6.13538	7.24921	9.02549	10.68947	8.76966
45	6.41650	7.74906	5.89150	6.08136	5.39224	6.14541	7.80574	8.76966	8.77034
44	5.94751	7.25907	5.87630	5.89809	5.25606	5.97516	7.59075	8.01576	7.90193
43	5.27759	6.57661	5.44300	5.79112	5.15005	5.76682	7.24434	7.46891	6.83922
42	4.41251	5.62446	4.76820	5.08279	4.34133	4.64395	5.51634	5.69925	5.23572
41	4.09933	5.55298	4.77154	4.90749	4.24941	4.12840	4.96920	5.37234	5.06314
40	2.63719	3.67621	3.18232	3.26468	2.63396	2.43730	3.09218	3.35032	3.14474
39	2.64667	3.98066	3.29695	3.45303	2.88224	2.67494	3.28193	3.53517	3.33427
38	3.40036	4.29253	3.58062	3.69085	2.92198	2.49008	3.10280	3.34383	2.99436
37	3.41467	4.14477	3.63438	3.74003	2.78013	2.24534	2.96876	3.24756	2.84764
36	3.34706	3.74408	3.17642	3.29500	2.32572	1.97145	2.72618	3.10667	2.69629
35	3.46096	3.65562	3.00337	3.00507	1.70523	1.86675	2.67460	3.06811	2.69193
34	3.27998	3.65854	2.64262	2.94375	1.67566	1.78673	2.58803	3.06252	2.60915
33	2.57531	2.98799	2.34579	2.60654	1.62726	1.76595	2.46890	2.69164	2.16464
32	2.24344	2.50952	1.96704	2.14498	1.45013	1.60299	2.06729	2.19265	1.71754
31	1.95657	2.16370	1.84246	2.15827	1.69430	1.73963	2.15670	2.39290	1.70621
30	1.74356	1.69087	1.81252	2.18532	1.70148	1.78929	2.14017	2.45360	1.65559
29	1.08449	1.26260	1.22470	1.42636	1.17611	1.34745	1.59779	1.93641	1.17957
28	0.25214	0.82472	0.62954	0.60709	0.31192	0.47071	0.65438	1.03721	0.55017
27	0.30461	0.73532	0.58040	0.63940	0.43451	0.74647	0.85833	1.12961	0.71337
26	0.08369	0.26393	0.37321	0.21841	0.10241	0.61289	0.89352	1.12640	0.63268
25	-0.08161	-0.07414	0.03969	-0.06227	0.18911	1.04625	1.00772	0.84553	0.67350
24	0.01669	0.04040	0.10680	0.31987	0.58522	1.38522	1.23271	1.15161	0.90665
23	0.13963	0.04653	-0.15635	0.40824	0.73404	1.40847	1.10402	1.32306	1.03441
22	0.10669	-0.03396	-0.17033	0.43126	0.77951	1.57602	1.12557	1.01621	0.89676
21	-0.03002	-0.21109	-0.21351	0.15202	0.61443	1.31992	0.77363	0.37175	0.28524
20	-0.33642	-0.43159	-0.46379	-0.36638	0.11754	0.72002	0.20470	-0.40001	-0.32220
19	-0.41167	-0.53757	-0.52032	-0.80047	-0.69427	-0.38318	-0.67107	-1.31822	-1.02413
18	-0.24605	-0.07085	-0.13363	-0.84249	-1.08665	-1.43442	-1.23750	-1.66222	-1.41280
17	-0.54740	-0.70903	-0.10279	-0.89964	-1.52108	-2.39013	-1.90391	-2.12524	-1.85569
16	0.02133	0.07570	0.39678	-0.28258	-0.80813	-1.84741	-1.52628	-1.43296	-1.02930
15	0.47811	0.53135	0.67784	0.14219	-0.71454	-1.24608	-0.72942	-0.57197	-0.07591
14	0.62414	0.74557	0.72677	0.75736	-0.26847	-0.83133	-0.01218	0.19092	0.64235
13	0.60467	0.71873	0.45005	-0.04463	-0.29767	-0.60971	0.42076	0.71366	1.12151
12	0.83370	1.02248	0.54622	-0.07310	-0.22423	-0.35733	0.93867	1.25956	1.67670
11	1.24515	1.53739	0.87495	0.25539	0.09385	-0.03819	1.25226	1.46852	1.87673
10	1.65640	2.05145	1.20252	0.60296	0.41081	0.23070	1.57648	1.67665	2.07941
9	1.97433	2.43219	1.55207	1.03120	0.79594	0.69342	1.90930	1.77001	2.13940
8	1.99154	2.47560	1.77702	1.33209	0.86651	0.98928	2.06222	1.59073	1.79639
7	1.91197	2.39710	1.84727	1.46427	0.82099	1.19191	2.16034	1.37994	1.44146
6	1.67106	1.99366	1.51013	1.04122	0.67086	1.06805	1.97319	1.03214	1.16880
5	1.43246	1.59851	1.24865	0.62933	0.53399	0.94499	1.80260	0.69499	0.91264
4	0.98297	0.90283	0.59895	-0.07228	0.19938	0.71174	1.54103	0.35675	0.61355
3	1.48571	1.47655	1.49376	0.78387	0.69621	1.07561	1.97433	0.75713	0.55558
2	2.44260	3.16245	3.11128	2.36810	1.63926	1.82070	2.72359	1.40765	1.50603
1	2.10487	3.21268	3.54055	2.73078	2.01537	1.36823	2.03564	0.84155	0.84159
0	0.04654	2.50863	2.54708	1.39131	1.01721	1.05646	2.24938	1.12712	1.56621

	44	43	42	41	40	39	38	37	36
71	4.88763	3.59718	3.16276	3.77531	3.36431	3.65104	2.26225	1.70495	1.81905
70	4.96572	3.82998	3.29223	3.89948	3.21171	3.67435	2.31972	1.85413	2.00809
69	4.98207	3.77434	3.28516	3.93054	3.41604	4.04860	3.04303	2.37426	2.73871
68	4.44143	3.80018	3.49779	3.93362	3.51332	4.09174	3.34744	2.28164	2.50125
67	4.21276	4.06651	4.06179	4.24698	4.04735	4.51096	4.14230	3.07014	2.97925
66	4.31885	4.50401	4.86132	4.63120	4.67687	5.09485	4.91942	4.04090	3.46946
65	3.44076	3.93865	4.55182	4.12492	4.57291	4.87814	4.84281	3.89841	3.25007
64	2.84392	3.02681	3.68068	3.39007	3.56525	3.91859	3.68445	2.94953	2.40711
63	3.14573	3.67332	3.84559	3.85490	3.57020	4.09609	4.20359	3.74713	2.86754
62	4.07941	4.39278	4.38618	4.27263	3.97547	4.43520	4.25074	3.49106	2.70229
61	4.91324	5.12742	5.02109	4.94493	4.35354	4.81907	4.32234	3.43764	2.69568
60	5.12590	5.43268	4.96515	4.81702	4.34042	4.74369	4.54764	3.79357	2.19688
59	5.74894	5.82654	5.25740	4.68662	4.16800	4.26027	4.05714	3.44876	2.55327
58	6.84726	6.66978	5.68650	5.40793	4.25953	4.34248	4.36662	3.99781	3.21947
57	7.16430	7.18818	5.84712	4.79016	3.52552	3.71234	4.20158	4.08305	3.57758
56	7.04306	6.49598	5.30425	4.77623	3.16143	3.33763	3.33053	3.20981	2.81614
55	5.96898	5.71644	4.73775	4.55979	3.09378	3.24148	3.00869	2.70934	2.62329
54	6.63039	6.15051	5.09637	4.63051	3.03679	3.12069	2.83080	2.83080	2.70692
53	5.94751	5.27759	4.41251	4.09933	2.63719	2.84687	3.40036	3.41487	3.34706
52	7.25907	6.57661	5.62446	5.55288	3.67621	3.98066	4.29253	4.14477	3.74426
51	5.87830	5.44300	4.76520	4.77154	3.18232	3.29095	3.58562	3.63438	3.17642
50	5.89809	5.79112	5.08279	4.90749	3.26668	3.45303	3.68005	3.74003	3.29590
49	5.25606	5.15005	4.34133	4.24941	2.63396	2.88524	2.92598	2.79513	2.73572
48	5.97916	5.76682	4.64395	4.12040	2.43738	2.67494	2.49008	2.24534	1.97145
47	7.59075	7.24434	5.51634	4.96920	3.09218	3.28193	3.18280	2.96876	2.72618
46	8.01576	7.46391	5.69925	5.37234	3.35032	3.53517	3.34383	3.24756	3.10667
45	7.90193	6.83922	5.23572	5.06314	3.14774	3.32427	2.99836	2.84964	2.69029
44	7.89134	6.60133	5.06163	4.80757	3.01687	3.21178	3.06627	2.96189	2.66520
43	6.80133	7.13104	5.61835	5.28619	3.70214	3.81880	3.71871	3.51626	2.97214
42	5.06163	5.61835	4.99828	4.74009	3.58900	3.69246	3.38471	3.17624	2.64598
41	4.80757	5.20619	4.74009	5.47676	4.04172	4.05159	3.54655	3.30466	2.78250
40	3.01487	3.70214	3.58900	4.04172	3.97468	3.95036	3.44718	3.09315	2.55420
39	3.21178	3.81880	3.69246	4.05159	3.95036	4.32525	3.62523	3.43671	2.85973
38	3.06637	3.71871	3.38471	3.54655	3.46718	3.62523	3.52860	3.71096	3.17134
37	2.96189	3.51626	3.17624	3.30466	3.09315	3.43671	3.71096	3.91023	3.42307
36	2.85520	2.97214	2.64598	2.78250	2.58420	2.85973	3.17124	3.42307	3.39786
35	2.65473	2.76480	2.34324	2.32874	2.10313	2.33864	2.67444	2.94115	3.11142
34	2.45486	2.72393	2.30566	2.31740	2.01097	2.20191	2.50943	2.64446	2.61924
33	2.05023	2.44268	1.97692	1.88897	1.60323	1.70995	2.00699	2.09962	2.25652
32	1.73534	1.95518	1.52713	1.46805	1.05764	1.15983	1.34106	1.31021	1.44527
31	1.74508	1.89930	1.58125	1.47888	1.00949	1.14213	1.22505	1.23605	1.31036
30	1.67257	1.83205	1.44487	1.26799	0.81051	0.88087	0.95140	1.10743	1.22177
29	1.17971	1.26792	1.02286	0.97132	0.68669	0.71664	0.66651	0.80396	0.66249
28	0.56361	0.65623	0.55458	0.61484	0.46267	0.39391	0.24726	0.42482	0.47239
27	0.65622	0.72156	0.67791	0.82448	0.49095	0.33471	0.10949	0.24950	0.33259
26	0.54546	0.42399	0.20412	0.01867	-0.30138	-0.44962	-0.49647	-0.34957	-0.21775
25	0.65881	0.02124	-0.30946	-0.76912	-0.93318	-0.92431	-1.00496	-0.89642	-0.71102
24	0.94969	0.22366	-0.29468	-0.67416	-0.95035	-0.82298	-1.04007	-0.95902	-0.79529
23	0.92454	0.30582	-0.05336	-0.43788	-0.88113	-0.77103	-0.93117	-0.71962	-0.57334
22	0.77767	0.27786	-0.20482	-0.64340	-1.00760	-0.96795	-0.99692	-0.85142	-0.75576
21	0.41605	0.01210	-0.47204	-1.01109	-1.22539	-1.11570	-1.04816	-0.92041	-1.04575
20	-0.00533	-0.34722	-0.87026	-1.49354	-1.52025	-1.37908	-1.10629	-1.14986	-1.27438
19	-0.88526	-0.90114	-1.40523	-1.91722	-1.69247	-1.43716	-0.87248	-0.69431	-0.99613
18	-0.84300	-1.10643	-1.40901	-1.54283	-1.11098	-0.81065	-0.34693	-0.36728	-0.26860
17	-1.31809	-1.44301	-1.55032	-1.32578	-0.61046	-0.39141	-0.10290	-0.17497	-0.09531
16	-0.44290	-0.77185	-0.97363	-0.69708	-0.21339	-0.10118	0.18454	0.22315	0.17155
15	0.39851	0.04729	-0.24998	0.02084	0.1173	0.57625	0.85750	0.88097	0.75319
14	0.95650	0.70169	0.33215	0.56892	0.99980	1.21159	1.47648	1.47815	1.26739
13	1.25205	1.03351	0.63975	1.03952	1.12993	1.31973	1.45305	1.46333	1.29151
12	1.62673	1.40866	0.99529	1.54731	1.38049	1.53711	1.52971	1.52329	1.37661
11	1.85054	1.67136	1.25552	1.87482	1.67199	1.82071	1.79347	1.60844	1.64799
10	2.07295	1.93369	1.51622	2.20248	1.96453	2.10527	2.06704	2.09431	1.91983
9	2.05982	1.95892	1.63897	2.29115	2.10307	2.20810	2.18390	2.22539	2.05124
8	1.85857	1.62299	1.50593	1.84998	2.00191	2.12105	2.16645	2.16674	2.01621
7	1.27686	1.30592	1.34484	1.47446	1.90762	2.06021	2.18587	2.13989	2.01396
6	1.11818	1.11327	1.13278	1.07734	1.66493	1.87287	2.17743	2.16335	2.05079
5	0.97706	0.92525	0.89486	0.72640	1.42545	1.67374	2.16228	2.17919	2.05104
4	0.89247	0.80615	0.65992	0.38346	1.17364	1.47527	2.15285	2.21025	2.12782
3	1.49901	1.47813	1.20377	0.89138	1.54206	1.92970	2.90662	2.97772	2.77580
2	2.26878	2.35817	2.00575	1.63691	2.08050	2.60592	3.94468	4.09217	3.61689
1	1.67504	1.96114	1.67594	1.47239	1.91197	2.38820	3.68516	3.53470	2.95458
0	1.94975	2.34105	2.01672	2.04120	2.32266	2.55587	3.29011	2.67509	2.12699

	35	34	33	32	31	30	29	28	27
71	1.47333	0.47600	-0.76681	-0.95149	-1.00424	-1.07401	-0.56634	-0.30714	-0.01299
70	1.34992	0.72842	-0.11129	-0.49301	-0.46205	-0.92470	-0.40265	-0.52545	-0.54460
69	2.05250	1.69309	0.88344	-0.15458	-0.47695	-1.07963	-0.65590	-1.05567	-1.37228
68	1.73258	1.72675	1.11481	0.24186	-0.14543	-1.10473	-0.66622	-1.20681	-1.67332
67	2.30618	2.25091	1.46519	0.79227	0.21986	-0.99844	-0.75444	-1.34467	-1.85073
66	2.36677	2.20540	1.09041	0.61974	0.32611	-0.87838	-0.73880	-1.38360	-1.74612
65	2.34165	2.03758	1.27199	0.77468	0.54234	-0.55563	-0.64152	-1.38764	-1.91998
64	1.68692	1.41934	0.83108	0.71384	0.72019	0.01462	-0.09436	-0.71783	-0.86090
63	2.03982	1.41541	0.76255	0.53767	0.92961	0.79019	0.73410	0.02140	-0.13056
62	1.21917	0.54112	-0.22292	-0.37849	0.20849	0.61516	0.70319	0.06870	0.05214
61	0.99115	0.29774	-0.35782	-0.68419	-0.01474	3.50134	0.60886	0.38545	0.57595
60	1.50806	0.71679	0.23621	-0.52773	-0.14214	0.18038	0.49827	0.19436	0.58759
59	1.79801	1.10824	0.51056	-0.18036	0.06623	0.32736	0.58305	0.27501	0.70706
58	2.42831	1.53303	0.69433	0.00567	0.09519	0.09481	0.12569	-0.29117	0.12673
57	3.02354	2.09205	1.26048	0.34616	0.45662	0.55057	0.16062	-0.47724	-0.03340
56	2.34306	1.81270	1.24650	0.42217	0.68242	1.07314	0.73167	-0.08389	0.35518
55	2.50949	2.02232	1.65171	1.21197	1.18585	1.26363	0.76985	0.13378	0.76183
54	2.75447	2.43546	2.10724	1.79362	1.55808	1.31232	0.72466	0.02588	0.39338
53	3.46096	3.27998	2.57531	2.24344	1.95657	1.74856	1.08449	0.25214	0.30461
52	3.69562	3.65654	2.98799	2.50992	2.16370	1.89087	1.26260	0.52472	0.73532
51	3.00337	2.64282	2.34579	1.96704	1.84246	1.81252	1.22470	0.62954	0.68040
50	3.00507	2.94375	2.60654	2.14498	2.15827	2.18182	1.43836	0.66709	0.63940
49	1.70523	1.67566	1.62726	1.45013	1.69430	1.70148	1.17811	0.31192	0.43451
48	1.68675	1.78673	1.76595	1.60299	1.73943	1.78929	1.34745	0.47071	0.74647
47	2.67460	2.56503	2.46890	2.06729	2.15870	2.14017	1.59979	0.65438	0.65833
46	3.06811	3.06252	2.69164	2.19285	2.39290	2.45360	1.93041	1.05721	1.18961
45	2.69193	2.60815	2.10464	1.71754	1.70621	1.65559	1.19957	0.55017	0.71337
44	2.55673	2.45486	2.05023	1.73534	1.74908	1.67257	1.17971	0.56361	0.66622
43	2.79650	2.72283	2.44268	1.95518	1.99930	1.83205	1.26792	0.65623	0.72156
42	2.34324	2.30566	1.97692	1.52713	1.58125	1.44497	1.02286	0.55458	0.67791
41	2.32674	2.31740	1.88887	1.48805	1.47088	1.26799	0.97132	0.61484	0.62445
40	2.10313	2.01097	1.60323	1.05764	1.00949	0.81051	0.63869	0.46267	0.49095
39	2.33564	2.20191	1.70995	1.15583	1.14213	0.88087	0.71664	0.38391	0.33471
38	2.67444	2.50843	2.00499	1.34106	1.22505	0.93140	0.66651	0.24726	0.10949
37	2.94115	2.66446	2.08962	1.31021	1.20805	1.18943	0.85376	0.42482	0.24950
36	3.11142	2.81924	2.25652	1.46027	1.31036	1.20177	0.86247	0.47230	0.33259
35	3.42706	3.15964	2.62209	1.94880	1.63683	1.51610	1.06753	0.70529	0.61708
34	3.15964	3.22326	2.83028	2.23749	1.91945	1.74461	1.28009	0.66212	0.74255
33	2.62209	2.63028	2.96041	2.35355	2.11666	1.90735	1.38039	0.91665	0.67891
32	1.94680	2.23449	2.39385	2.46439	2.17529	1.81514	1.30521	0.73130	0.77445
31	1.63683	1.91945	2.11666	2.17529	2.21121	2.05467	1.62006	1.21363	1.03234
30	1.51610	1.74461	1.90735	1.91514	2.05467	2.30910	1.94062	1.54733	1.42635
29	1.06753	1.28009	1.38039	1.30021	1.62006	1.94862	1.69022	1.64729	1.60516
28	0.70529	0.86212	0.91665	0.93130	1.21363	1.54733	1.64729	1.80269	1.96894
27	0.61708	0.74255	0.67891	0.77445	1.03234	1.42635	1.60516	1.96894	2.47274
26	0.42097	0.50737	0.52559	0.74193	0.95068	1.40004	1.53845	1.68052	2.44723
25	-0.07442	-0.12524	-0.13377	0.25838	0.50102	0.85792	1.05501	1.31998	1.74774
24	-0.25635	-0.28502	-0.19738	0.17168	0.53242	0.89413	1.12750	1.31672	1.60408
23	0.03094	0.08795	0.28795	0.69791	1.13824	1.56245	1.71159	1.77917	1.92122
22	0.01509	0.07381	0.29565	0.77681	1.11582	1.49624	1.57019	1.65558	1.81659
21	-0.26156	-0.14502	0.08464	0.51075	0.79552	1.16565	1.30995	1.44354	1.61577
20	-0.47162	-0.22103	0.04030	0.42491	0.49220	0.71013	0.87563	1.04442	1.13755
19	-0.08104	0.19029	0.24308	0.43908	0.22251	0.24664	0.37405	0.57575	0.55709
18	0.08491	0.18185	-0.13122	-0.09942	-0.32072	-0.41371	-0.16637	0.16656	0.17820
17	-0.05686	-0.02314	-0.42710	-0.47951	-0.68563	-0.75167	-0.50482	-0.21272	-0.27036
16	0.00557	-0.09110	-0.36952	-0.46032	-0.60166	-0.63212	-0.62244	-0.55392	-0.70324
15	0.45409	0.25912	0.05925	-0.26703	-0.41795	-0.57786	-0.74531	-0.86850	-1.05649
14	0.65195	0.67653	0.41664	-0.13539	-0.41038	-0.54190	-0.83873	-1.10187	-1.30660
13	0.76485	0.64981	0.37685	-0.07982	-0.38477	-0.63008	-0.95730	-1.18563	-1.30442
12	0.78743	0.71972	0.44229	0.01515	-0.31499	-0.64439	-0.98481	-1.21111	-1.31353
11	1.03431	0.69604	0.63021	0.09916	-0.24354	-0.56928	-0.88696	-1.12940	-1.25579
10	1.28691	1.07348	0.61863	0.18361	-0.16781	-0.49403	-0.78900	-1.03762	-1.20437
9	1.41060	1.14864	0.92697	0.22122	-0.12757	-0.44040	-0.72340	-1.04909	-1.26321
8	1.49141	1.22140	1.04335	0.34754	-0.00203	-0.32774	-0.61246	-1.02903	-1.32748
7	1.61110	1.32826	1.17050	0.48023	0.11463	-0.23185	-0.51912	-1.02508	-1.40414
6	1.73106	1.37909	1.16319	0.41028	-0.00531	-0.35655	-0.63048	-1.20939	-1.58566
5	1.84232	1.42239	1.03002	0.33518	-0.12869	-0.48284	-0.74327	-1.39455	-1.76823
4	1.94417	1.44388	0.92475	0.24646	-0.28439	-0.62153	-0.93696	-1.62914	-2.00705
3	2.25555	1.62786	0.92234	0.05737	-0.54262	-0.97404	-1.32026	-2.09376	-2.50980
2	2.64151	1.65712	0.94520	-0.19061	-0.63055	-1.26039	-1.69770	-2.54440	-2.97779
1	2.99209	1.76675	1.17238	0.36734	-0.15906	-0.57293	-1.12326	-1.61931	-2.14807
0	2.25780	1.96476	1.71922	0.89368	0.16431	-0.15475	-0.67719	-0.92814	-0.69020



	26	25	24	23	22	21	20	19	18
71	-0.84984	-0.12344	0.59666	1.03440	0.40433	-0.42913	-1.31337	-1.99835	-0.15493
70	-1.81512	-0.83853	0.40217	1.04752	0.26561	-0.72988	-1.53817	-2.14887	-0.31371
69	-2.75980	-2.01763	-0.91823	-0.83088	-1.67988	-2.47063	-2.54849	-2.15413	-0.39538
68	-2.92152	-2.18749	-1.16671	-1.48600	-2.12333	-2.43468	-1.95200	-1.17261	0.30609
67	-2.63741	-2.22182	-1.38198	-1.78565	-2.29067	-2.40178	-1.94968	-1.19045	0.03311
66	-2.93878	-2.40610	-1.80032	-2.01254	-2.36449	-2.24853	-2.00071	-1.38352	-0.27532
65	-2.67815	-2.40381	-2.02168	-2.31184	-2.40826	-2.23939	-1.97813	-1.42531	-0.71762
64	-1.17117	-1.18326	-0.96244	-1.07934	-1.10167	-1.13715	-1.37999	-1.49313	-1.77685
63	-0.84863	-1.06856	-0.80275	-0.51962	-0.69761	-0.76179	-1.42947	-1.86146	-2.12716
62	-0.72725	-1.20672	-0.87430	-0.82976	-0.90381	-0.88166	-1.51153	-2.39881	-2.33667
61	-0.71601	-1.37871	-0.85559	-0.84093	-1.04416	-1.16193	-1.80796	-3.02570	-2.47912
60	-0.51453	-1.36043	-1.30044	-1.20190	-1.50101	-1.57559	-1.14912	-3.22504	-2.36253
59	-0.11815	-0.48976	-0.77234	-0.52536	-0.61077	-0.45766	-1.01988	-2.20704	-2.53961
58	-0.23078	-0.24256	-0.30331	0.07356	0.27732	0.56827	0.25009	-0.54408	-1.12689
57	0.45829	0.70049	0.43161	0.25154	0.73420	1.27498	1.33975	1.05309	0.57122
56	0.72169	0.93631	0.91910	0.58570	0.67737	1.05079	0.74676	0.06531	0.01350
55	0.96366	1.18900	1.15482	0.95869	1.14625	1.16413	0.67310	-0.04568	-0.34106
54	0.66360	0.82006	0.92952	1.01124	1.31288	1.37029	1.14683	0.60350	-0.24733
53	0.08369	-0.08161	0.01649	0.13963	0.10669	-0.03002	-0.33842	-0.41167	-0.24605
52	0.26393	-0.07414	0.04040	0.04653	-0.03396	-0.21109	-0.43159	-0.53757	-0.07685
51	0.37321	0.03969	0.10630	-0.15635	-0.17033	-0.21351	-0.46379	-0.52032	-0.13363
50	0.21841	-0.06227	0.31987	0.40824	0.40126	0.15202	-0.36638	-0.80047	-0.84249
49	0.10241	0.18911	0.58522	0.73404	0.77951	0.61443	0.11754	-0.69427	-1.06665
48	0.61289	1.04625	1.35622	1.46647	1.57602	1.31992	0.72902	-0.38318	-1.43442
47	0.69832	1.00772	1.23271	1.10402	1.12557	0.72363	0.20470	-0.67107	-1.23750
46	1.12640	0.84953	1.15161	1.32306	1.01621	0.39175	-0.40091	-1.31822	-1.60522
45	0.63368	0.67350	0.98865	1.03441	0.80094	0.28924	-0.32230	-1.02413	-1.41880
44	0.54546	0.65861	0.94569	0.92454	0.77767	0.41665	-0.00533	-0.55526	-0.84900
43	0.42899	0.02124	0.22366	0.38562	0.27796	0.01210	-0.34722	-0.90114	-1.10443
42	0.20412	-0.38946	-0.29468	-0.05335	-0.20482	-0.47204	-0.87926	-1.40523	-1.40701
41	0.01867	-0.76912	-0.67416	-0.43788	-0.66340	-1.01109	-1.49354	-1.91722	-1.54293
40	-0.30128	-0.93316	-0.95035	-0.86113	-1.00760	-1.22539	-1.52025	-1.69247	-1.11878
39	-0.44962	-0.92631	-0.82299	-0.77183	-0.90795	-1.11570	-1.37958	-1.43716	-0.81995
38	-0.49647	-1.00496	-1.04007	-0.93117	-0.99692	-1.04616	-1.10089	-0.87248	-0.34673
37	-0.33957	-0.89642	-0.95902	-0.71962	-0.86142	-0.96401	-1.14986	-0.89431	-0.36738
36	-0.21325	-0.71102	-0.79559	-0.59334	-0.79576	-1.04025	-1.27438	-0.90613	-0.25660
35	0.42097	-0.07462	-0.25635	0.03094	0.01509	-0.26156	-0.47162	-0.08104	0.08491
34	0.50737	-0.12526	0.08755	0.08755	0.07381	-0.14502	-0.22103	0.19029	0.16185
33	0.52559	-0.12377	-0.19738	0.20795	0.29506	0.04464	0.04620	0.24308	-0.13122
32	0.74193	0.25838	0.17148	0.69701	-0.77641	0.51075	0.42491	0.43708	-0.69942
31	0.95068	0.50102	0.53242	1.13024	1.11582	0.79552	0.49220	0.22251	-0.32672
30	1.40004	0.85792	0.89413	1.56245	1.49624	1.16565	0.71913	0.24664	-0.41371
29	1.53865	1.05501	1.12750	1.71159	1.57019	1.39905	0.87563	0.37465	-0.16637
28	1.88052	1.31998	1.31672	1.77917	1.65558	1.44354	1.04442	0.57575	0.16656
27	2.44723	1.74774	1.60508	1.92122	1.81859	1.61507	1.13755	0.55709	0.17920
26	3.38012	2.94293	2.71857	3.02068	3.13703	3.14238	2.85182	2.19166	1.00756
25	2.94278	3.58213	3.63421	3.65186	3.79316	3.79385	3.49644	2.80795	1.60285
24	2.71657	3.68421	4.26644	4.26399	4.30784	4.19137	3.68951	2.73031	1.42739
23	3.02880	3.65184	4.26399	5.52256	5.49740	5.16422	4.48730	3.29944	1.38112
22	3.13703	3.79316	4.30754	5.49340	5.87963	5.79122	5.36207	4.23429	1.81695
21	3.14238	3.79385	4.19137	5.16422	5.79122	6.19294	6.25713	5.47379	2.68760
20	2.85182	3.49644	3.65951	4.48730	5.36207	6.25713	7.15401	7.20449	4.26772
19	2.19166	2.60795	2.73031	3.20944	4.23429	5.49379	7.20449	8.37005	5.93440
18	1.00706	1.60293	1.42739	1.38312	1.81085	2.68760	4.26772	5.93440	6.49466
17	0.00516	0.40253	0.19400	-0.24247	-0.08594	0.52120	1.79481	3.41081	5.49608
16	-0.71876	-0.36737	-0.49286	-1.31134	-1.24564	-0.63385	0.04652	1.25314	3.27943
15	-1.30733	-1.05994	-1.14717	-2.29295	-2.22551	-2.04511	-1.40958	-0.33415	1.48671
14	-1.72435	-1.61612	-1.71826	-3.09614	-3.19527	-3.04952	-2.66715	-1.77840	0.00341
13	-2.01465	-2.22610	-2.45587	-3.89098	-4.14374	-4.10594	-3.86484	-3.04459	-1.08031
12	-2.29834	-2.78694	-3.09928	-4.53339	-4.94755	-5.07090	-4.94374	-4.17539	-1.96035
11	-2.36676	-2.94142	-3.24693	-4.51720	-4.97350	-5.17379	-5.10147	-4.36363	-2.08440
10	-2.43423	-3.09451	-3.39476	-4.50210	-4.99951	-5.27770	-5.26043	-4.56308	-2.21047
9	-2.49310	-3.17060	-3.47961	-4.39960	-4.90687	-5.24686	-5.32356	-4.74502	-2.46735
8	-2.31712	-2.90588	-3.28864	-3.98635	-4.36191	-4.64559	-4.69347	-4.15253	-2.20755
7	-2.16530	-2.65878	-3.11980	-3.61845	-3.85521	-4.07352	-4.06009	-3.51233	-1.87816
6	-2.22778	-2.49131	-2.91738	-3.50973	-3.62763	-3.77379	-3.67852	-3.02476	-1.55685
5	-2.26967	-2.32109	-2.81379	-3.39972	-3.39852	-3.47235	-3.28777	-2.52199	-1.20984
4	-2.43005	-2.25514	-2.76174	-3.36079	-3.21921	-3.15118	-2.78138	-1.79002	-0.65480
3	-3.29938	-3.02157	-3.50801	-4.42465	-4.21278	-4.03048	-3.53181	-2.23229	-0.90128
2	-4.26642	-3.92077	-4.40915	-5.78107	-5.58131	-5.29046	-4.74420	-3.17066	-1.54491
1	-3.35331	-3.43441	-4.08178	-5.15127	-4.62866	-4.31594	-3.80415	-2.51542	-1.39141
0	-1.62275	-2.32229	-3.28600	-4.10698	-3.43774	-3.20905	-2.50315	-1.49934	-0.95278

	17	16	15	14	13	12	11	10	9
71	0.18086	-0.10153	-0.03791	0.13168	0.35475	0.98231	1.52482	2.06744	2.13450
70	-0.29524	-0.66209	-0.45279	-0.15872	0.21461	1.06315	1.66046	2.25686	2.41459
69	-0.68138	-0.86870	0.05315	0.79921	1.36784	2.39655	3.03824	3.67915	3.85604
68	-0.30918	-0.52096	0.20343	0.53234	0.71922	1.31899	1.89211	2.46500	2.68588
67	-0.47545	-0.40145	0.35279	0.58315	0.37735	0.44411	0.99473	1.54625	1.91377
66	-0.75299	-0.56806	-0.09473	-0.01218	-0.32970	-0.45450	0.03598	0.52754	1.10724
65	-1.19166	-0.53672	0.02542	-0.04700	-0.68285	-1.00447	-0.53803	-0.07078	0.66534
64	-2.62463	-1.44996	-0.57148	-0.56044	-0.67641	-0.57272	-0.16396	0.24535	0.97364
63	-2.90442	-1.74042	-0.85024	-0.67900	-0.63737	-0.36229	0.12301	0.60961	1.32014
62	-2.49775	-1.27445	-0.39026	0.08061	0.25819	0.85363	1.27630	1.69773	2.24037
61	-2.49115	-1.27698	-0.30447	0.41155	0.81793	1.72601	2.25711	2.78713	3.15560
60	-2.30420	-1.56444	-0.54424	0.53201	1.17215	2.12171	2.64962	3.27688	3.69047
59	-3.36338	-2.63814	-1.64920	-0.69202	0.04712	0.74931	1.33716	1.92675	2.39774
58	-2.41846	-2.08471	-1.53901	-1.02210	-0.45063	0.09467	0.72069	1.34723	1.91564
57	-0.76231	-0.57716	-0.36806	-0.14231	-0.10516	-0.02008	0.34465	0.70260	1.16723
56	-0.52322	-0.10101	0.27729	0.58929	0.71641	0.84445	1.05995	1.27493	1.63573
55	-0.97391	-0.43833	0.07725	0.38981	0.50227	0.57099	0.79968	1.02928	1.24789
54	-1.26264	-0.64727	-0.11175	0.04755	0.02646	0.10093	0.42432	0.74785	1.06126
53	-0.54740	0.02138	0.47811	0.62414	0.60467	0.83270	1.24515	1.65640	1.97438
52	-0.20903	0.07570	0.53135	0.74557	0.71873	1.07248	1.53729	2.05145	2.43919
51	-0.10279	0.37678	0.67984	0.72477	0.45005	0.54622	0.87495	1.20252	1.55207
50	-0.69964	-0.26258	0.14219	0.28736	-0.04463	-0.09310	0.25539	0.60276	1.03120
49	-1.52108	-0.80813	-0.38464	-0.26847	-0.29767	-0.22423	0.09385	0.41066	0.75594
48	-2.30013	-1.88741	-1.26888	-0.83133	-0.60071	-0.35733	-0.03919	0.28670	0.69342
47	-1.98391	-1.52628	-0.72042	-0.01218	0.42076	0.93366	1.25826	1.57648	1.90930
46	-2.12824	-1.43296	-0.57199	0.19092	0.71366	1.25950	1.46852	1.67665	1.77091
45	-1.85649	-1.02930	-0.07581	0.64355	1.12151	1.67670	1.87873	2.07941	2.13945
44	-1.31809	-0.44290	0.39551	0.95550	1.25205	1.62673	1.85054	2.07295	2.05982
43	-1.48301	-0.77183	0.04729	0.70169	1.03351	1.40866	1.67136	1.93369	1.95582
42	-1.15032	-0.97363	-0.24998	0.33215	0.63995	0.99529	1.25552	1.51622	1.63097
41	-1.32578	-0.69758	0.02084	0.58892	1.03952	1.54731	1.87482	2.20248	2.26115
40	-0.61046	-0.21339	0.41873	0.99980	1.12993	1.38049	1.67199	1.96403	2.10307
39	-0.39141	-0.10118	0.57625	1.21159	1.31973	1.53711	1.82071	2.10527	2.26810
38	-0.10290	0.18454	0.85750	1.47648	1.45305	1.52071	1.79347	2.06704	2.18390
37	-0.13497	0.22375	0.88997	1.47815	1.46333	1.52320	1.80844	2.09431	2.22530
36	-0.69081	0.17155	0.75318	1.26730	1.28151	1.37441	1.64799	1.91963	2.05124
35	-0.60386	0.00557	0.45469	0.85195	0.76435	0.78243	1.05431	1.29691	1.41060
34	-0.02314	-0.09110	0.29912	0.67853	0.64981	0.71922	0.89694	1.07348	1.14444
33	-0.42710	-0.36952	0.05925	0.41664	0.37685	0.44229	0.63021	0.81863	0.92697
32	-0.47951	-0.46032	-0.26703	-0.13539	-0.07982	0.01515	0.05916	0.16561	0.22122
31	-0.68563	-0.60166	-0.48795	-0.41038	-0.38477	-0.31499	-0.24354	-0.16981	-0.12257
30	-0.75167	-0.63212	-0.57706	-0.54190	-0.63608	-0.64439	-0.56928	-0.49403	-0.44040
29	-0.50482	-0.62244	-0.74531	-0.63873	-0.95730	-0.98481	-0.88696	-0.78900	-0.72340
28	-0.21272	-0.55892	-0.86850	-1.10187	-1.18563	-1.22111	-1.12940	-1.03762	-1.04909
27	-0.27036	-0.70324	-1.05669	-1.30060	-1.30462	-1.31353	-1.25899	-1.20437	-1.26321
26	-0.00516	-0.71876	-1.30733	-1.72435	-2.01465	-2.29934	-2.36676	-2.43423	-2.45310
25	0.40253	-0.36737	-1.05954	-1.61612	-2.22610	-2.78454	-2.94142	-3.09451	-3.17060
24	0.19408	-0.49286	-1.14717	-1.71826	-2.45087	-3.09528	-3.24693	-3.39476	-3.47961
23	-0.24247	-1.31134	-2.29295	-3.09614	-3.89098	-4.53239	-4.51720	-4.50210	-4.39760
22	-0.08594	-1.24564	-2.32451	-3.19927	-4.14374	-4.94755	-4.97350	-4.99954	-4.90689
21	0.52120	-0.83385	-2.04511	-3.04952	-4.10594	-5.07000	-5.17377	-5.27770	-5.24686
20	1.79481	0.04652	-1.40958	-2.66715	-3.86484	-4.94324	-5.10149	-5.26043	-5.32356
19	3.41081	1.29314	-0.33415	-1.77848	-3.04459	-4.17539	-4.36863	-4.56368	-4.74502
18	5.79008	3.27743	1.48671	0.00341	-1.08031	-1.96035	-2.08440	-2.21047	-2.46725
17	6.38265	4.75197	3.21995	2.06328	1.03728	0.29931	0.07966	-0.14050	-0.45154
16	4.75197	4.64955	4.08073	3.47678	2.69768	2.12301	1.91695	1.69127	1.33585
15	3.21995	4.06073	4.64683	4.73537	4.27714	4.00026	3.76526	3.56834	3.19990
14	2.06328	3.47678	4.73037	5.75408	6.67304	5.66309	5.39755	5.13067	4.69442
13	1.03728	2.69768	4.29734	5.67304	6.38798	7.00768	6.76486	6.57073	6.05515
12	0.27931	2.12601	4.00026	5.66309	7.00768	8.24618	8.07666	7.90568	7.44874
11	0.07066	1.91095	3.76526	5.39755	6.76486	8.07666	8.09367	8.10719	7.75133
10	-0.14050	1.69127	3.56834	5.13087	6.52073	7.90968	8.10719	8.30320	6.05247
9	-0.45154	1.33585	3.17990	4.69442	6.05515	7.44874	7.75133	8.05247	7.99956
8	-0.48324	0.87520	2.47471	3.85858	5.01350	6.18066	6.45461	6.72766	6.52744
7	-0.42083	0.53673	1.69976	3.16982	4.10520	5.04652	5.28283	5.51878	5.93109
6	-0.24639	0.77548	2.11200	3.40500	4.10400	4.85879	5.07532	5.29165	5.68753
5	-0.04444	1.05690	2.46491	3.65412	4.11612	4.68945	4.88059	5.08260	5.46142
4	0.28514	1.43066	2.61710	3.91640	4.17807	4.52773	4.69070	4.85158	5.15556
3	0.08612	1.50777	3.15640	4.46093	4.62174	4.81179	4.98607	5.16074	5.38758
2	-0.55226	1.24845	3.32434	5.00620	5.12784	5.18702	5.40208	5.61859	5.76369
1	-0.56774	1.15304	2.58741	4.42034	4.21415	3.86019	4.38815	4.29813	4.42919
0	-0.39125	0.99865	2.78123	4.02098	3.66055	3.13377	3.46588	3.60060	3.67734

	8	7	6	5	4	3	2	1	0
71	1.67594	1.29193	1.19589	1.09822	1.02405	0.77138	0.29930	-1.23538	-1.76023
70	2.08172	1.80127	1.68010	1.58558	1.51739	1.34455	0.89592	-1.29774	-3.03858
69	3.60639	3.42759	3.39775	3.37687	3.36769	3.64788	3.97114	1.41846	0.73800
68	2.74909	2.85958	3.01992	3.18297	3.34761	3.94398	4.73272	2.52946	1.91129
67	2.35196	2.77935	2.99672	3.20284	3.41396	4.35210	5.65236	3.86863	3.19455
66	1.95521	2.75403	3.20391	3.64080	4.02531	5.27891	6.94844	5.35078	4.08562
65	1.75165	2.77943	3.46974	4.15085	4.68091	6.16209	8.00044	7.13440	6.23425
64	1.83082	2.59712	3.27589	3.94857	4.33917	4.68398	5.10553	4.66761	5.03058
63	1.60449	2.25604	2.89463	3.51549	3.73945	4.44709	5.62165	5.26972	4.38698
62	2.49839	2.76079	3.24163	3.70903	3.71480	4.71462	6.37100	6.05625	5.14240
61	3.04805	2.98382	3.24248	3.48963	3.36363	4.64562	6.56974	6.13672	5.44493
60	3.71103	3.70775	3.55693	3.39019	3.08468	4.79264	7.29093	6.50365	5.75375
59	2.55301	2.72846	2.78089	2.81434	2.02026	4.29969	6.34502	5.50017	5.12188
58	2.25550	2.51684	2.69684	2.67115	3.04884	4.39308	6.14739	4.65502	3.61033
57	1.65540	2.08124	2.37517	2.67928	2.93934	4.61329	5.36835	4.00812	2.82797
56	1.95167	2.14825	1.96854	1.79542	1.49737	1.82153	2.46651	1.46365	0.55338
55	1.25404	1.22077	1.28715	1.34738	1.36861	1.46251	1.58469	0.80468	0.68589
54	1.24608	1.33383	1.20983	1.08430	0.87287	1.24346	1.87311	1.30132	0.27228
53	1.99156	1.91197	1.67106	1.43246	0.98297	1.46571	2.44260	2.10487	0.04854
52	2.47560	2.39710	1.99366	1.59851	0.90263	1.67655	3.16245	3.21268	2.50283
51	1.77782	1.86727	1.55373	1.24865	0.59595	1.49378	3.11138	3.56055	2.54708
50	1.33209	1.46437	1.04122	0.62933	-0.07228	0.78387	2.36810	2.73078	1.39131
49	0.86651	0.82099	0.67084	0.53399	0.19938	0.69621	1.63926	2.01537	1.01721
48	0.98928	1.19191	1.06805	0.94699	0.71576	1.09561	1.82070	1.36223	1.05649
47	2.06222	2.16034	1.97319	1.80260	1.54103	1.97433	2.72359	2.03264	2.24638
46	1.59073	1.37994	1.03214	0.69499	0.35675	0.75715	1.40765	0.84155	1.12712
45	1.79630	1.44146	1.16880	0.91264	0.61355	0.95859	1.50003	0.84139	1.56621
44	1.65857	1.27666	1.11818	0.97706	0.89247	1.49901	2.26878	1.67504	1.94975
43	1.62299	1.30592	1.11327	0.92525	0.80615	1.47813	2.35017	1.96114	2.34165
42	1.50593	1.36484	1.13278	0.89486	0.65992	1.20377	2.00575	1.67594	2.01672
41	1.64998	1.42646	1.07734	0.72640	0.38346	0.89138	1.63691	1.47239	2.04120
40	2.00191	1.90782	1.66993	1.42545	1.17364	1.44206	2.06050	1.91197	2.32266
39	2.12105	2.06021	1.87287	1.67374	1.47027	1.92970	2.66092	2.55587	2.55587
38	2.16645	2.18287	2.17743	2.16228	2.15286	2.96662	3.94468	3.68516	3.79611
37	2.16674	2.13989	2.16335	2.17919	2.21025	2.97772	4.00217	3.53470	2.67509
36	2.01621	2.01396	2.05279	2.06064	2.12782	2.77080	3.61099	2.95458	2.12499
35	1.49141	1.61110	1.73106	1.84232	1.94417	2.26555	2.64151	2.29209	2.15980
34	1.22140	1.32626	1.37909	1.42239	1.44388	1.62186	1.65912	1.76675	1.96476
33	1.04335	1.17050	1.10329	1.03002	0.92475	0.92234	0.94520	1.17238	1.71922
32	0.34754	0.48023	0.41028	0.33518	0.24646	0.05737	-0.19061	0.36734	0.89368
31	-0.00203	0.11463	-0.00531	-0.12869	-0.28439	-0.54262	-0.83055	-0.15906	0.16431
30	-0.32776	-0.23185	-0.35655	-0.48284	-0.66953	-0.97404	-1.26039	-0.57293	-0.15475
29	-0.61246	-0.51912	-0.63048	-0.74327	-0.92696	-1.37026	-1.69770	-1.12326	-0.67719
28	-1.02903	-1.02508	-1.20939	-1.39455	-1.62914	-2.09376	-2.54440	-1.81531	-0.92014
27	-1.32748	-1.40414	-1.58566	-1.76823	-2.00705	-2.50950	-2.97779	-2.14307	-0.60620
26	-2.31712	-2.16530	-2.22778	-2.28967	-2.43005	-3.29938	-4.26642	-3.35331	-1.62575
25	-2.90503	-2.65876	-2.49131	-2.32109	-2.25514	-3.02157	-3.92077	-3.43441	-2.32229
24	-3.28864	-3.11980	-2.96788	-2.81377	-2.76174	-3.50801	-4.40915	-4.08178	-3.28600
23	-3.98635	-3.61845	-3.50973	-3.39972	-3.38079	-4.42465	-5.78107	-5.15127	-4.10678
22	-4.36191	-3.65521	-3.62763	-3.39652	-3.21921	-4.21278	-5.58131	-4.72866	-3.43774
21	-4.64549	-4.07352	-3.77379	-3.47235	-3.15228	-4.03048	-5.29046	-4.31594	-3.26905
20	-4.69347	-4.06009	-3.67852	-3.28777	-2.78138	-3.53181	-4.74420	-3.80415	-2.56315
19	-4.15253	-3.51233	-3.02496	-2.52189	-1.79002	-2.23229	-3.17066	-2.51542	-1.49934
18	-2.20755	-1.87816	-1.55685	-1.20984	-0.65480	-0.90128	-1.54491	-1.39141	-0.95278
17	-0.48324	-0.42003	-0.24839	-0.04444	0.28514	0.06812	-0.55226	-0.56726	-0.39125
16	0.87520	0.52673	0.77548	1.05650	1.43066	1.50777	1.24545	1.15304	0.99865
15	2.47471	1.89926	2.17020	2.46491	2.81710	3.15640	3.32434	2.98441	2.76123
14	3.85859	3.16902	3.40500	3.65412	3.91840	4.46093	5.00620	4.42034	4.02698
13	5.01350	4.10520	4.10400	4.11612	4.1807	4.62174	5.12784	4.21415	3.66055
12	6.18066	5.04652	4.85879	4.68845	4.52973	4.81179	5.18702	3.86019	3.13377
11	6.45461	5.28283	5.07532	4.88559	4.69070	4.98407	5.40208	4.03815	3.46588
10	6.72766	5.51878	5.29165	5.08260	4.85158	5.16074	5.61157	4.29813	3.65060
9	6.92744	5.93109	5.66753	5.46142	5.15556	5.38758	5.78369	4.42919	3.87734
8	6.66436	6.39315	6.08417	5.78599	5.36131	5.47290	5.79782	4.53641	3.75762
7	6.39315	6.78556	6.47337	6.16538	5.70422	5.70568	5.95584	4.85790	3.63866
6	6.08417	6.47337	6.66514	6.85928	6.85362	6.93823	7.13830	5.82864	5.04375
5	5.78599	6.16538	6.35928	7.05485	8.01472	8.16614	8.29904	7.09515	6.22537
4	5.36931	5.70422	6.85882	8.01472	9.01438	9.36487	9.50402	8.21268	7.37628
3	5.47290	5.70568	6.93823	8.16614	9.36487	11.07715	12.93869	11.18852	9.10774
2	5.79762	5.95984	7.13830	8.29904	9.50402	12.93869	17.22347	15.05168	11.35778
1	4.58641	4.65790	5.96864	7.09515	8.21268	11.18852	15.05168	15.56279	14.27486
0	3.78762	3.83866	5.04375	6.22537	7.37628	9.10774	11.35778	14.27486	19.45529





	53	52	51	50	49	48	47	46	45
71	4.11046	4.58933	3.24383	1.93893	1.93383	2.52188	3.31473	4.19785	5.34501
70	4.08290	4.58594	3.26268	2.39859	2.681052	3.39861	4.66410	4.70640	5.42671
69	4.11537	4.96228	2.64452	2.13861	2.29241	3.03323	4.81906	5.15160	5.61990
68	4.12798	4.78851	2.34950	2.31159	2.65025	2.73344	4.48836	4.53525	4.78325
67	5.18925	5.64028	3.39811	3.62112	3.21936	2.56065	4.05913	3.90541	4.25468
66	5.75775	6.46393	4.68672	5.19909	4.41198	2.65952	4.05282	3.85551	4.30940
65	4.16270	5.52310	6.04342	5.73265	4.08780	1.97300	3.31095	2.40736	2.74758
64	3.82762	4.33815	4.96355	4.35813	3.70232	1.91595	3.14333	2.10331	2.48844
63	3.72331	4.59766	5.35936	5.19630	4.93315	2.82220	3.91990	2.95429	3.67252
62	3.81166	5.51368	6.61591	5.52449	5.15311	3.34312	4.97463	3.50936	3.25244
61	3.94163	6.20166	6.93833	4.38367	3.99729	0.30303	5.22819	4.30168	3.86025
60	4.49321	6.20503	6.49117	3.87237	3.26527	2.39343	5.21580	5.01728	4.26091
59	4.93759	6.14793	5.95029	3.74689	3.81266	4.50675	5.70377	5.71234	5.15240
58	7.29135	6.16049	5.52456	5.95227	6.04382	6.34365	7.24267	6.65322	6.62732
57	6.54815	8.91523	8.57463	7.34462	7.26010	7.21038	6.12482	7.52737	7.69617
56	9.41450	9.83895	8.71967	8.14799	8.13554	7.97731	8.29134	8.03188	7.43425
55	8.79127	8.34126	6.91401	6.80250	6.46188	7.70465	7.35953	6.83613	6.17251
54	11.69657	11.21264	6.89279	8.81899	8.16435	7.95401	7.54805	7.49924	7.04980
53	13.93256	13.58927	10.69735	10.53639	8.32783	6.90023	6.99433	7.08802	6.41460
52	15.58927	15.25108	12.86869	12.32847	9.27499	7.82047	8.35990	7.92245	7.54751
51	10.69735	12.86869	13.67522	12.33018	8.66513	6.32461	6.82122	5.73410	5.62658
50	10.53639	12.32847	12.33018	12.99939	9.60711	7.44555	7.59789	6.42899	5.96958
49	0.32783	9.27499	6.66513	9.80711	9.65159	8.05937	7.66457	6.07658	5.31552
48	6.90023	7.82047	6.32461	7.64595	6.05937	9.53217	9.32070	7.18813	6.60553
47	6.99433	8.35990	6.62122	7.96767	7.66457	9.32070	10.63017	8.89551	7.62511
46	7.05802	7.92245	5.73410	6.42899	6.07658	7.18813	6.89551	9.93749	8.67711
45	6.41460	7.54751	5.68688	5.96958	5.31552	6.06053	7.62511	8.67911	8.6452
44	5.94264	7.00817	5.62357	5.75895	5.15433	5.87351	7.36589	7.90304	7.76229
43	5.27176	6.27535	5.13715	5.62405	5.02791	5.63996	6.97436	7.33357	6.65115
42	4.40748	5.36494	4.50472	4.93887	4.23610	4.53467	5.26376	5.58265	5.07371
41	4.09425	5.29021	4.50486	4.76182	4.14271	4.01779	4.73379	5.25433	4.65916
40	2.63140	3.37732	2.87887	3.05692	2.51278	2.31151	2.62432	3.21604	2.64151
39	2.66050	3.60176	2.95704	3.27063	2.75189	2.53444	2.95717	3.36740	3.11895
38	3.36217	3.86914	3.15077	3.44605	2.75431	2.31179	2.80336	3.15261	2.73258
37	3.40821	3.80052	3.28489	3.54913	2.64955	2.16038	2.66025	3.09290	2.63474
36	3.34176	3.47117	2.89853	3.14321	2.21474	1.85619	2.46088	2.97770	2.51942
35	3.45558	3.41768	2.72119	2.85054	1.59254	1.74971	2.42552	2.94324	2.51642
34	3.27509	3.40570	2.58613	2.80353	1.57315	1.68076	2.36144	2.94893	2.45931
33	2.57193	2.76675	2.12117	2.46384	1.53756	1.67278	2.27062	2.59225	1.96651
32	2.24122	2.39491	1.65028	2.08120	1.40350	1.55456	1.96423	2.14118	1.64575
31	1.95616	2.14255	1.62100	2.14655	1.68573	1.73073	2.13975	2.38340	1.65351
30	1.74895	1.91978	1.83274	2.17667	1.70955	1.79748	2.15801	2.44255	1.66512
29	1.08817	1.34975	1.31317	1.46669	1.21344	1.38414	1.67789	1.96956	1.25397
28	0.25445	0.64416	0.75079	0.67332	0.36034	0.52101	0.76142	1.11087	0.66473
27	0.30661	0.83629	0.98495	0.69651	0.47626	0.78983	0.95061	1.23567	0.77765
26	0.05773	0.42275	0.58522	0.33422	0.16708	0.90082	1.08547	1.22922	0.76434
25	-0.07587	0.22471	0.34309	0.10346	0.31028	1.17210	1.27554	0.97979	0.66606
24	0.02487	0.46326	0.53611	0.25437	0.75667	1.53429	1.61168	1.34158	1.25243
23	0.14855	0.57504	0.38022	0.71133	0.94833	1.62903	1.57767	1.56050	1.36435
22	0.11525	0.40842	0.27831	0.64660	0.95888	1.76231	1.52203	1.21496	1.07714
21	-0.02203	0.20187	0.20574	0.38104	0.78186	1.49381	1.09372	0.57728	0.54794
20	-0.33218	-0.10647	-0.13676	-0.16774	0.24814	0.85567	0.45438	-0.25530	-0.12121
19	-0.40794	-0.34462	-0.32442	-0.63347	-0.61604	-0.30193	-0.49816	-0.123154	-0.39348
18	-0.24368	0.05176	-0.00915	-0.77449	-1.03293	-1.38279	-1.12762	-1.54714	-1.34226
17	-0.54643	-0.15869	-0.05167	-0.87172	-1.50067	-2.27873	-1.93879	-2.10262	-1.82525
16	0.01890	-0.05281	0.26631	-0.35385	-0.84024	-1.94153	-1.64145	-1.49069	-1.10552
15	0.47119	0.17344	0.31648	-0.05630	-0.12575	-1.04117	-1.04117	-0.73279	-0.29925
14	0.61413	0.22813	0.20144	0.00040	-0.47624	-1.04922	-0.47591	-0.04155	0.32052
13	0.59556	0.24767	-0.02819	-0.30586	-0.48866	-0.79927	-0.00140	0.59033	0.65274
12	0.82590	0.61921	0.13680	-0.31674	-0.38773	-0.52715	0.57721	1.07833	1.42494
11	1.23652	1.09128	0.42214	0.09804	-0.06698	-0.22601	0.65855	1.26814	1.66029
10	1.64694	1.56244	0.70606	0.33178	0.12157	0.07478	1.13824	1.45666	1.77433
9	1.94473	1.94023	1.04551	0.75049	0.59364	0.48231	1.45313	1.54565	1.87791
8	1.98713	1.58919	1.28298	0.61479	0.66589	0.78403	1.62541	1.37176	1.49202
7	1.90241	1.90311	1.58576	1.19035	0.62070	0.98389	1.71764	1.15802	1.13303
6	1.65850	1.34460	0.89178	0.68128	0.40770	0.79473	1.39151	0.74054	0.76360
5	1.41696	0.79740	0.43532	0.18506	0.20918	0.60763	1.06464	0.33508	0.41252
4	0.95461	-0.04639	-0.36475	-0.59586	-0.18549	-0.31606	0.69035	-0.06971	0.02097
3	1.44304	0.50452	0.30387	0.13390	0.22100	0.60206	0.92397	0.23057	0.22690
2	2.41425	1.69701	1.62359	1.55541	1.04509	1.20360	1.11028	0.74928	0.58516
1	2.08933	1.75571	1.69557	1.71206	1.27056	0.59467	0.38937	0.01627	-0.30546
0	0.00000	0.00000	0.00000	0.00000	0.00000	0.00000	0.00000	0.00000	0.00000











	8	7	6	5	4	3	2	1	0
71	2.01792	1.63852	1.65128	1.66029	1.69003	1.59369	1.32748	0.05347	0.00000
70	2.67206	2.39956	2.47421	2.55585	2.66704	2.76407	2.67080	0.92691	0.00000
69	3.46301	3.28228	3.20683	3.14121	3.08847	3.30311	3.54007	0.67809	0.00000
68	2.37774	2.48325	2.57265	2.57265	2.62647	3.05109	3.61630	1.13001	0.00000
67	1.73308	2.14990	2.16944	2.18202	2.20443	2.85065	3.78504	1.52769	0.00000
66	1.16146	1.94950	2.14692	2.33619	2.47950	3.37026	4.58196	2.35928	0.00000
65	0.46276	1.47317	1.75339	2.03241	2.17082	3.06281	4.12528	2.27678	0.00000
64	0.65348	1.80661	1.97443	2.34221	2.43583	2.33387	2.16709	0.98420	0.00000
63	0.95220	1.39425	1.75967	2.11464	2.07963	2.39765	3.05715	2.05757	0.00000
62	1.49753	1.75326	1.91124	2.06596	1.74916	2.31227	3.36425	2.29097	0.00000
61	1.99022	1.91173	1.83382	1.75116	1.30353	2.10195	1.36977	2.15014	0.00000
60	2.59223	2.57387	2.06708	1.55131	0.89585	2.10235	3.93516	2.28708	0.00000
59	1.59794	1.71797	1.45581	1.17883	0.89239	1.90693	3.35325	1.74992	0.00000
58	1.55409	1.80598	1.76281	1.71831	1.68287	2.70646	4.03895	1.92633	0.00000
57	1.10598	1.52442	1.64355	1.77626	1.86937	2.69216	3.71649	1.93747	0.00000
56	1.84436	2.03949	1.82544	1.61903	1.28836	1.56348	2.14386	1.05920	0.00000
55	1.12609	1.09110	1.11677	1.13709	1.11943	1.15484	1.20600	0.32246	0.00000
54	1.19318	1.26022	1.13939	0.99736	0.76985	1.11626	1.71467	1.10195	0.00000
53	1.98213	1.90241	1.65650	1.41696	0.96461	1.44304	2.14125	2.06733	0.00000
52	1.98919	1.90311	1.34440	0.79740	-0.04639	0.50452	1.69761	1.35751	0.00000
51	1.26298	1.36576	0.89178	0.43532	-0.36475	0.30387	1.62359	1.69557	0.00000
50	1.06179	1.19033	0.68128	0.18506	-0.59868	0.13390	1.55541	1.71266	0.00000
49	0.64689	0.62070	0.40770	0.20918	-0.18549	0.22100	1.04509	1.27656	0.00000
48	0.78403	0.68369	0.79473	0.60963	0.31606	0.60206	1.20360	0.59467	0.00000
47	1.62541	1.71764	1.39151	1.08464	0.69035	0.92397	1.41028	0.30937	0.00000
46	1.37176	1.15802	0.74654	0.33508	-0.04671	0.23057	0.74928	0.01627	0.00000
45	1.45262	1.13508	0.76340	0.41252	0.20797	0.27690	0.58618	0.30540	0.00000
44	1.27977	0.69276	0.61374	0.35447	0.15478	0.58615	1.12491	0.24743	0.00000
43	1.16817	0.84497	0.50762	0.17771	-0.07959	0.38447	0.99073	0.24702	0.00000
42	1.11412	0.67775	0.61103	0.25069	-0.10312	0.26163	0.62775	0.19930	0.00000
41	1.45342	1.02456	0.54927	0.07481	-0.30664	-0.06220	0.44462	-0.02218	0.00000
40	1.55067	1.45049	1.06904	0.68378	0.29485	0.04699	0.72380	0.21131	0.00000
39	1.62450	1.55697	1.21164	0.85760	0.50625	0.73569	1.11300	0.51678	0.00000
38	1.52725	1.53505	1.32624	1.11169	0.90804	1.36760	2.02308	1.27113	0.00000
37	1.64703	1.61317	1.47126	1.32498	1.19812	1.72501	2.43961	1.57599	0.00000
36	1.60298	1.59518	1.50252	1.40685	1.32307	1.77715	2.36648	1.39920	0.00000
35	1.07181	1.18584	1.12730	1.15265	1.12700	1.24656	1.37994	0.71068	0.00000
34	0.83969	0.94141	0.67079	0.79500	0.70051	0.70460	0.71147	0.32815	0.00000
33	0.70954	0.83199	0.65951	0.48104	0.27428	0.11918	-0.05902	-0.06643	0.00000
32	0.17391	0.30426	0.17907	0.04981	-0.09167	-0.36013	-0.71262	-0.28701	0.00000
31	-0.03395	0.08228	-0.04762	-0.18116	-0.34656	-0.61938	-0.92653	-0.27937	0.00000
30	-0.29770	-0.20138	-0.31652	-0.43343	-0.60998	-0.90175	-1.19900	-0.45962	0.00000
29	-0.45090	-0.36578	-0.45528	-0.52703	-0.68074	-1.00390	-1.30214	-0.62741	0.00000
28	-0.84672	-0.64233	-0.74927	-1.09818	-1.27798	-1.66016	-2.00226	-1.13973	0.00000
27	-1.17202	-1.24659	-1.37864	-1.51271	-1.70429	-2.13597	-2.51039	-1.56216	0.00000
26	-2.00185	-1.84579	-1.80776	-1.77130	-1.81648	-2.55129	-3.31855	-2.16513	0.00000
25	-2.45471	-2.20153	-1.89051	-1.57954	-1.37650	-1.93660	-2.84428	-1.73402	0.00000
24	-2.65024	-2.47279	-2.11776	-1.76451	-1.51848	-1.97291	-2.48975	-1.67577	0.00000
23	-3.16846	-2.60980	-2.44722	-2.08628	-1.62691	-2.50602	-3.28213	-2.14413	0.00000
22	-3.69403	-3.17833	-2.73825	-2.30079	-1.91854	-2.60679	-3.57328	-2.11154	0.00000
21	-4.02214	-3.44167	-2.94357	-2.44764	-1.93813	-2.53133	-3.41601	-1.96626	0.00000
20	-4.20716	-3.56723	-3.03093	-2.48847	-1.83430	-2.36243	-3.26207	-1.97714	0.00000
19	-3.66124	-3.21712	-2.63707	-2.04322	-1.22274	-1.53185	-2.29487	-1.41760	0.00000
18	-2.02244	-1.69056	-1.31036	-0.90560	-0.29431	-0.45618	-0.99636	-0.69379	0.00000
17	-0.40723	-0.34580	-0.14717	0.00049	0.43317	0.12089	-0.32373	-0.27677	0.00000
16	0.68119	0.35010	0.51712	0.73802	1.05782	1.04124	0.66213	0.42183	0.00000
15	1.93438	1.33615	1.45067	1.57681	1.76481	1.85711	1.69978	0.95099	0.00000
14	3.07739	2.37810	2.36473	2.37015	2.39706	2.58247	2.65749	1.47618	0.00000
13	4.30233	3.58445	3.15696	2.94724	2.79310	2.91166	2.96967	1.53389	0.00000
12	5.57163	4.42949	4.04805	3.68778	3.34406	3.34780	3.35654	1.58564	0.00000
11	5.78127	4.60041	4.17866	3.77687	3.37937	3.36693	3.37761	1.55043	0.00000
10	5.93940	4.77057	4.30855	3.86917	3.41384	3.38551	3.39895	1.51576	0.00000
9	6.17415	5.16765	4.68442	4.23331	3.66856	3.57422	3.51888	1.59019	0.00000
8	5.92851	5.64738	5.10427	4.57653	3.93625	3.70346	3.56541	1.81311	0.00000
7	5.64738	6.02974	5.41627	4.93962	4.25166	3.91239	3.71762	2.04723	0.00000
6	5.10427	5.48027	5.36027	5.24871	4.95050	4.58197	4.19217	2.29560	0.00000
5	4.57653	4.93662	5.24871	5.56697	5.65934	5.25787	4.66271	2.53692	0.00000
4	3.93625	4.25166	4.95050	5.65934	6.22355	5.91894	5.11543	2.81175	0.00000
3	3.70346	3.91239	4.58197	5.25787	5.91894	6.02234	7.61873	4.51981	0.00000
2	3.58541	3.71762	4.66271	5.19543	5.9543	7.61873	10.57170	6.71353	0.00000
1	1.81311	2.04723	2.29560	2.53692	2.81175	4.51894	6.71353	5.11071	0.00000
0	0.00000	0.00000	0.00000	0.00000	0.00000	0.00000	0.00000	0.00000	0.00000

REFERENCES

- ABEL P.G., ELLIS P.J., HOUGHTON J.T., PECKHAM G., RODGERS C.D., SMITH S.D., WILLIAMSON E.J. 1970 : Remote sounding of atmospheric temperatures from satellites II. The selective chopper radiometer for Nimbus D. Proc.Roy.Soc. Lond. A320, 35.
- BACKUS G.E., GILBERT J.F. 1967 : Numerical Applications of a formalism for Geophysical inverse problems. Geophys. J.R.astr.Soc. 13, 247.
- BACKUS G.E., GILBERT J.F. 1968 : The resolving power of Gross Earth data. Geophys.J.R. astr. Soc. 16, 169.
- BACKUS G.E., GILBERT J.F. 1969 : Uniqueness in the inversion of inaccurate Gross Earth data. Phil. Trans. Roy. Soc. London, A266, 123.
- BARNETT J.J., CROSS M.J., HARWOOD R.S., HOUGHTON J.T., MORGAN C.G., PECKHAM G.E., RODGERS C.D., SMITH S.D., WILLIAMSON E.J. 1972 : The first year of the selective chopper radiometer on Nimbus 4. Quart. J.R. Met. Soc. 98, 17.
- BECK J.V., ARNOLD K.J. 1977 : Parameter Estimation in engineering and science. John Wiley and Sons, New York, 1977.
- BISHOP W., BOLIN B. 1966 : Space and Time variations of the CO<sub>2</sub> content of the troposphere and lower stratosphere. Tellus 18, 155.

- CHANDRASEKHAR S. 1950 : Radiative Transfer. Oxford, The Clarendon Press, 1950, 9.
- ELSASSER W.M. 1938 : Mean absorption coefficients of a Band Spectrum. The Physical Review, 54, No.2, Series 2, 126.
- FRANKLIN J.N. 1968 : Matrix Theory. Prentice-Hall Inc. 1968.
- GEORGII H.W., JOST D. 1969 : Concentration of CO<sub>2</sub> in the upper troposphere and lower stratosphere. Nature, Lond. 221, 1040.
- HAYS P.B., OLIVERO J.J. 1970 : Carbon dioxide and monoxide above the tropopause. Planet Space Sci. 18, 1729.
- HOUGHTON J.T. 1969 : Absorption and emission by carbon dioxide in the mesosphere. Q.J.R. Met. Soc. 95, 1.
- HOUGHTON J.T., SMITH S.D. 1970 : Remote sounding of atmospheric temperature from satellites I. Proc. Roy. Soc. Lond. A320, 23.
- HOUGHTON J.T., TAYLOR F.W. 1973 : Remote sounding from artificial satellites and space probes of the atmospheres of the Earth and the planets. Rep. Prog. Phys. 36, 827.
- KAPLAN L.D. 1959 : Inference of atmospheric structure from remote radiation measurements. J. Opt. Soc. Am. 49, 1004.
- PECKHAM G. 1974 : The information content of remote measurements of atmospheric temperature by satellite infrared radiometry and optimum radiometer configurations. Quart. J.R. Met. Soc. 100, 406.

- RODGERS C.D. 1970 : Remote sounding of the atmospheric temperature profile in the presence of cloud. Quart. J.R. Met. Soc. 96, 654.
- RODGERS C.D. 1971 : Some theoretical aspects of remote sounding in the Earth's atmosphere. J. Quant. Spectrosc. Radiat. Transfer, 11, 767.
- RODGERS C.D. 1976 : Retrieval of Atmospheric temperature and composition from remote measurements of Thermal radiation. Reviews of Geophysics and Space Physics. 14, 607.
- RODGERS C.D. 1975 : The vertical resolution of remotely sounded temperature profiles with a priori statistics. J. Atmos. Sci. 33, 707.

ACKNOWLEDGEMENTS

I have received help from a number of people in the work described in this report. I wish to thank the following people in particular.

Dr. Grahame Fraser, my supervisor, who suggested this project and has given much encouragement.

Mrs. Beverley Bristowe for the typing of this report.